IJARAI

International Journal of
Advanced Research in Artificial Intelligence

Volume 4 Issue 7

www.ijarai.thesai.org

IJARAI

INTERNATIONAL JOURNAL OF
ADVANCED RESEARCH IN ARTIFICIAL INTELLIGENCE

THE SCIENCE AND INFORMATION ORGANIZATION

OAlster   getCITED   Google Scholar BETA   BASE Bielefeld Academic Search Engine   ULRICHSWEB GLOBAL SERIALS DIRECTORY   arXiv.org

DOAJ DIRECTORY OF OPEN ACCESS JOURNALS   IET InspecDirect   INDEX COPERNICUS INTERNATIONAL   WorldCat Window to the world's libraries   Microsoft Academic Search Beta   EBSCO HOST Research Databases

Editorial Preface

From the Desk of Managing Editor...

Artificial Intelligence is hardly a new idea. Human likenesses, with the ability to act as human, dates back to Geek mythology with Pygmalion's ivory statue or the bronze robot of Hephaestus. However, with innovations in the technological world, AI is undergoing a renaissance that is giving way to new channels of creativity.

The study and pursuit of creating artificial intelligence is more than designing a system that can beat grand masters at chess or win endless rounds of Jeopardy!. Instead, the journey of discovery has more real-life applications than could be expected. While it may seem like it is out of a science fiction novel, work in the field of AI can be used to perfect face recognition software or be used to design a fully functioning neural network.

At the International Journal of Advanced Research in Artificial Intelligence, we strive to disseminate proposals for new ways of looking at problems related to AI. This includes being able to provide demonstrations of effectiveness in this field. We also look for papers that have real-life applications complete with descriptions of scenarios, solutions, and in-depth evaluations of the techniques being utilized.

Our mission is to be one of the most respected publications in the field and engage in the ubiquitous spread of knowledge with effectiveness to a wide audience. It is why all of articles are open access and available view at any time.

IJARAI strives to include articles of both research and innovative applications of AI from all over the world. It is our goal to bring together researchers, professors, and students to share ideas, problems, and solution relating to artificial intelligence and application with its convergence strategies. We would like to express our gratitude to all authors, whose research results have been published in our journal, as well as our referees for their in-depth evaluations.

We hope that this journal will inspire and educate. For those who may be enticed to submit papers, thank you for sharing your wisdom.

Editorial Board

Reviewer Board Members

(iii)

CONTENTS

A Minimal Spiking Neural Network to Rapidly Train and Classify Handwritten Digits in Binary and 10-Digit Tasks

Amirhossein Tavanaei

The Center for Advanced Computer Studies
University of Louisiana at Lafayette
Lafayette, LA, USA

Anthony S. Maida

The Center for Advanced Computer Studies
University of Louisiana at Lafayette
Lafayette, LA, USA

Abstract—**This paper reports the results of experiments to develop a minimal neural network for pattern classification. The network uses biologically plausible neural and learning mechanisms and is applied to a subset of the MNIST dataset of handwritten digits. The research goal is to assess the classification power of a very simple biologically motivated mechanism. The network architecture is primarily a feedforward spiking neural network (SNN) composed of Izhikevich regular spiking (RS) neurons and conductance-based synapses. The weights are trained with the spike timing-dependent plasticity (STDP) learning rule. The proposed SNN architecture contains three neuron layers which are connected by both static and adaptive synapses. Visual input signals are processed by the first layer to generate input spike trains. The second and third layers contribute to spike train segmentation and STDP learning, respectively. The network is evaluated by classification accuracy on the handwritten digit images from the MNIST dataset. The simulation results show that although the proposed SNN is trained quickly without error-feedbacks in a few number of iterations, it results in desirable performance (97.6%) in the binary classification (0 and 1). In addition, the proposed SNN gives acceptable recognition accuracy in 10-digit (0-9) classification in comparison with statistical methods such as support vector machine (SVM) and multi-perceptron neural network.**

Keywords—Spiking neural networks; STDP learning; digit recognition; adaptive synapse; classification

I. INTRODUCTION

Neural networks that use biologically plausible neurons and learning mechanisms have become the focus of a number of recent pattern recognition studies [1, 2, 3]. Spiking neurons and adaptive synapses between neurons contribute to a new approach in cognition, decision making, and learning [4-8].

Recent examples include the combination of rank order coding (ROC) and spike timing-dependent plasticity (STDP) learning [9], the calculation of temporal radial basis functions (RBFs) in the hidden layer of spiking neural network [10], and linear and non-linear pattern recognition by spiking neurons and firing rate distributions [11]. The studies mentioned utilize spiking neurons, adaptive synapses, and biologically plausible learning for classification.

Learning in the present paper combines STDP with competitive learning. STDP is a learning rule which modifies the synaptic strength (weight) between two neurons as a function of the relative pre- and postsynaptic spike occurrence times [12]. Competitive learning takes the form of a winner-take-all (WTA) policy. This is a computational principle in neural networks which specifies the competition between the neurons in a layer for activation [13]. Learning and competition can be viewed as two building blocks for solving classification problems such as handwritten digit recognition. Nessler et al. (2009) utilized the STDP learning rule in conjunction with a stochastic soft WTA circuit to generate internal models for subclasses of spike patterns [14]. Also, Masquelier and Thorpe (2007) developed a 5-layer spiking neural network (SNN) consisting of edge detectors, subsample mapping, intermediate-complexity visual feature extraction, object scaling and position adjustment, and categorization layers using STDP and WTA for image classification [15].

Auditory and visual signals have special authentication processes in the human brain. Thus, one or more neuron layers are required to model the signal sequences in one and two-dimensional feature vectors in addition to the learning phase. Wysoski et al. (2008 and 2010) proposed a multilayer SNN architecture to classify audiovisual input data using an adaptive online learning procedure [16, 17]. The combination of Izhikevich's neuron firing model, the use of conductance-based synaptic dynamics, and the STDP learning rule can be used for a convenient SNN for pattern recognition. As an example, Beyeler et al. (2013) developed a decision making system using this combination in a large-scale model of a hierarchical SNN to categorize handwritten digits [18]. Their SNN architecture consists of 3136 plastic synapses which are trained and simulated in 500 (ms). They trained the system by 10/100/1000/2000 samples of the MNIST dataset in 100 iterations and achieved a 92% average accuracy rate. In another study, Nessler et al. (2013) showed that Bayesian computation is induced in their proposed neural network through STDP learning [2]. They evaluated the method, which is an unsupervised method for learning a generative model, by MNIST digit classification and achieved an error rate of 19.86% (80.14% correctness). Their proposed neural network for this experiment includes 708 input spike trains and 100 output neurons in a complete-connected feedforward network.

Some previous studies (c.f. [18], [2]) have attempted to develop an autonomous and strong artificial intelligence based on human brain anatomy in a large network of neurons and

synapses. However, two inevitable and important aspects of the brain simulation are 1) the size of the network that is, number of the neurons and synapses, and 2) rapid learning and decision making. In some cases, a concise network is needed to be tuned and make a decision quickly in a special environment such as binary classification in the real time robot vision. Although large networks provide convenient circumstances for handling the details and consequently desirable performance, they are resource intensive. Our goal is to develop a fast and small neural network to extract useful features, learn their statistical structure, and make accurate classification decisions quickly.

This paper presents an efficient 3-layer SNN with a small number of neurons and synapses. It learns to classify handwritten MNIST digits. The training and testing algorithms perform weight adaptation and pattern recognition in a time and memory efficient manner while achieving good performance. The proposed SNN provides a robust solution for the mentioned challenge in three steps. First, the digit image is converted to spike trains so that each spike is a discriminative candidate of a row pixel in the image. Second, to reduce the network size and mimic human perception of the image, the spike trains are integrated to a few sections. In this part, each output spike train specifies a special part of the image in the row order. Third, training layer which involves STDP learning, output spike firing, and WTA competition by inhibitory neuron modifies a fast pattern detection strategy. The remarkably simple SNN is implemented for binary ("0, 1" c.f. Fig. 1) and 10-digit task (0-9) handwritten digit recognition problem to illustrate efficiency of the proposed strategy in primitive classifications. Furthermore, the obtained results are compared with statistical machine learning models in the same circumstances (same training/testing data without feature mapping) to depict the trustworthy of our model in similar situations.

II. SPIKING NEURAL NETWORK ARCHITECTURE

The proposed SNN architecture is shown in Fig. 2. It includes three components: 1) a neural spike generator, 2) image segmentation, and 3) learning session and output pattern creator. Theory and implementation of each component will be explained.

A. First layer: Presynaptic spike train generator

Each row in the 28×28 binary image (c.f. Fig. 3) is transcribed into a spike train in a left-to-right fashion. Fig. 3 shows an example digit "0" with $N \times M$ binary pixels. Rows are converted to spike trains where a pixel value of "1" represents a spike occurrence. To apply the discriminative features of the image in a small network architecture, the digit image is recoded to N presynaptic spike trains with $A \times M$ discrete time points. A controls the interspike spacing and is interpreted as the refractory period of the neuron. In summary, the first layer converts the binary digit image into N rows of spike trains according to the white pixels of the digit foreground.

Fig. 1. Sample of handwritten digit images "0" and "1"
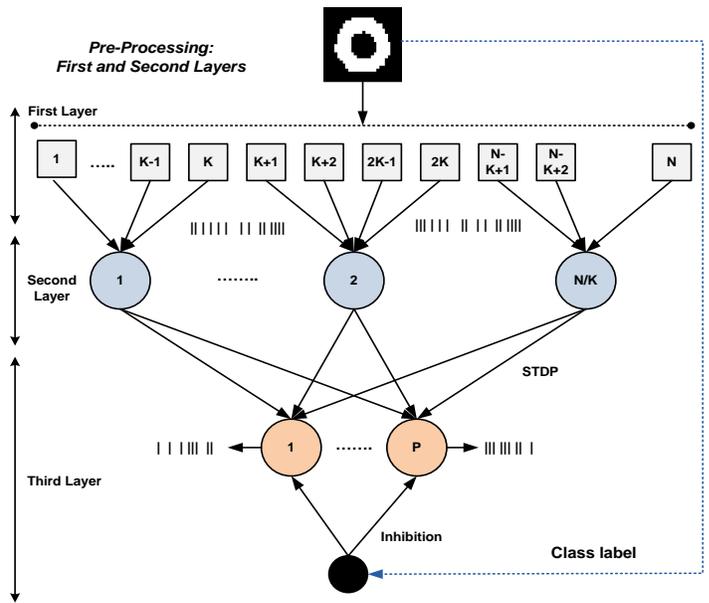
Fig. 2. Supervised SNN architecture containing spike transcription layer, spike train segmentation, STDP learning, output pattern firing, and inhibitory neuron. N: number of rows. K: number of adjacent rows connected to one neuron. P: number of classes. Black circle inhibits all output neurons except the one designated by the class label
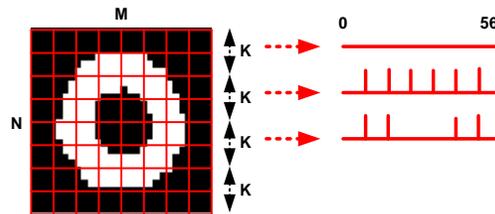
Fig. 3. A digit image with $N \times M$ pixels divided into N/K segments, consisting of k rows per segment

B. Second Layer: Image segmentation

The first layer generates N spike trains, where N is the number of the rows, encoding the image features row by row. However, it does not consider the slight change in orientation and thickness of the digit foreground in comparison with its background. To address this, the second layer illustrated in Fig. 2 merges every K spike trains (rows) onto one neuron. Then the digit image is segmented into N/K parts while preserving the spike train order. This preprocessing layer reduces the number of trainable parameters. Fig. 4 shows three instances of digit "1" (from the MNIST). The second layer converts these different shapes to similar N/K rows of spike trains. In addition, combining the sequential rows increases the network flexibility in pattern classification by decreasing its size. In summary, without the second layer, spike trains are sensitive to noise, outlier data, and diverse writing styles.

Fig. 4. Three instances of the handwritten digit "1"

To simulate the conductance of the postsynaptic membrane of the second layer units upon receipt of a presynaptic spike, the α-function is used. Equation (1) and Fig. 5 show the formula and graph of the postsynaptic conductance based on the α-function.

$$G_{\text{syn}}(t) = K_{\text{syn}} \, t \, e^{-t/\tau} \tag{1}$$

K_{syn} controls the peak conductance value and τ controls the time at which the peak conductance is reached.

Additionally, the total conductance of N input synapses with $N_{\text{rec},k\,(k=1:N)}$ spikes is calculated by (2)

$$G^{\text{tot}}(t) = \sum_{k=1}^{N} \sum_{j=1}^{N_{\text{rec},k}} K_{\text{syn},k} \, (t - t_{k,j}^{\text{f}}) \, e^{-(t-t_{k,j}^{\text{f}})/\tau} \tag{2}$$

where t^{f} is spike firing time. This formula performs linear spatio-temporal summation across the received spike train. The total postsynaptic current is obtained by (3)

$$I_{\text{syn}}(t) = \sum_{k=1}^{N} E_{\text{syn},k} G^{\text{tot}}_{\text{syn},k}(t) - V(t) \sum_{k=1}^{N} G^{\text{tot}}_{\text{syn},k}(t) \tag{3}$$

In this investigation, spike generation in the second and third layer is controlled by Izhikevich's model [19] (4) specified by two coupled differential equations.

$$C\frac{dV}{dt} = k(V - V_{\text{rest}})(V - V_{\text{th}}) - U + I_{\text{inj}}$$
$$\frac{dU}{dt} = a\big[b(V - V_{\text{rest}}) - U\big] \tag{4}$$

There is also a reset condition after a spike is generated, given in (5).

$$\textit{if } V \geq V_{\text{peak}} : V = c, \, U = U + d$$
$$\textit{an AP is emitted} \tag{5}$$

Where, V denotes membrane potential and U specifies the recovery factor preventing the action potential (AP) and keeping the membrane potential close to the resting point. *"a"*, *"b"*, *"k"*, *"c"*, *"d"*, and *"V_{peak}"* are predefined constants controlling the spike shapes. The time of spike events is taken to occur at reset.
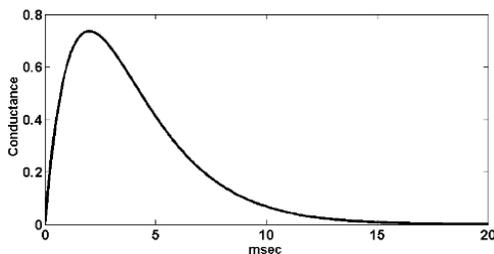
Fig. 5. Conductance graph with $K_{\text{syn}}=1$ (α-function) and $\tau=2$ (msec)

C. Third layer: Learning and output neurons

Third layer of the SNN shown in Fig. 2 learns the input spike patterns and generates output spikes based on the evolving synaptic weights. STDP is controlled by relative pre- and postsynaptic spike times. Equation (6) specifies that postsynaptic spikes which follow presynaptic spikes cause the synaptic weight to be increased (LTP) and in contrast, synapses are weakened when presynaptic spike occurs after postsynaptic spike generation time (LTD).

$$\Delta K_{ji} = \begin{cases} 0.01 A_{\text{ltp}} \exp(-(|\,t_j^f - t_i^f\,|)/_{\tau+}) \,, & t_j^f - t_i^f > 0 \\ 0.01 A_{\text{ltd}} \exp(-(|\,t_j^f - t_i^f\,|)/_{\tau-}) \,, & t_j^f - t_i^f < 0 \end{cases} \tag{6}$$

In (6), A_{ltp} and $\tau+$ (A_{ltd} and $\tau-$) are maximum and time constant strengthening (weakening) constants respectively. In addition, the change in synaptic weights contributes to change in conductance amplitude, K_{syn}, in α-function derivation. The learning strategy used in this investigation is basically derived from the STDP concept. The proposed network in the first layer emits spike trains with maximum M spikes, where M is the number of columns in the image matrix. The second layer presents new information of spike trains at which spikes depict explicit foreground pixel information. In addition, the membrane potential is accumulated based on the received action potentials. Therefore, in the proposed minimal network architecture which models the patterns by exact object coordinates, a modified STDP learning is defined in (7).

$$\Delta K_{ji} = \begin{cases} \dfrac{A_{\text{ltp}}}{K_{ji}} \exp(-(|\,t_j^f - t_i^f\,|)/_{\tau+}) \,, & \begin{pmatrix} P_j = 1, \\ t_i^f \in [\min(t_j^{f-1}, t_j^f - \sigma), t_j^f] \end{pmatrix} \\ -A_{\text{ltd}} \exp(-\beta) \,, & \begin{pmatrix} P_j = 1, \\ t_i^f \notin [\min(t_j^{f-1}, t_j^f - \sigma), t_j^f] \end{pmatrix} \end{cases} \tag{7}$$

where A_{ltp}, A_{ltd}, $\beta > 1$, and σ are constant parameters. In (7), if output neuron P_j fires, the synaptic weights can be either increased or decreased. Presence of the presynaptic spikes in the σ time interval before current time strengthens the synaptic conductance. In contrast, absence of the presynaptic spikes reduces the synaptic conductance. To prevent aliasing between σ time interval and previous output spike, presynaptic spikes after the last emitted postsynaptic spike are counted. Also, the inverse value of the conductance amplitude (K_{ji}) controls rate of the LTP in the high conductance conditions.

In addition, output neurons in the third layer receive N/K spike trains and generate P (as number of the output patterns) output spike trains based on the current synaptic weights, presynaptic spike trains, and Izhikevich's model for the spike generation mechanism. Furthermore, each output neuron specifies one class. The learning strategy in the output layer is supervised. This is implemented by using an inhibitory neuron that imposes a WTA discipline across the output units. Specifically, the inhibitory unit uses the category label for the current training stimulus to inhibit all the output neurons that do not match the label. The net learning effect is that the nonmatching units undergo LTD, while the single matching unit undergoes LTP. Equation (8) specifies the LTD rule for inactive neurons. The synaptic conductance reduction in this formula depends on the presynaptic spikes "y_i" conveyed to the neuron in the time interval [$\min(t_j^{f-1}, t_j^f - \sigma), t_j^f$].

$$C = \frac{-\gamma}{\sum\limits_{i=\min(t_j^{f-1}, t_j^f - \sigma)}^{t_j^f} y_i} \quad , \quad \Delta K'_{ji} = -0.01e^C \qquad (8)$$

Where, γ is rate of the inhibition. In the last step, conductance magnitude of the synapses (which can be interpreted as synaptic weights) are updated by (9)

$$K_{ji}^t = K_{ji}^{t-1} + \mu \Delta K_{ji}^t \qquad (9)$$

where, μ is learning rate. Finally, the result will be an array of synaptic weights and output spike patterns. Fig. 6 shows pseudocode for the SNN architecture and learning strategy.

D. Justification

Digits belonging to the same categories are not entirely similar due to different handwriting styles, variations in orientation, and variations in line thickness. The second layer converts the various images of one digit into a small number of similar patterns. It combines K spike trains to adjust the thickness and presents the image in N/K row segments. The slight diversity of the images in a digit category can be manipulated by foreground adjustment in height and width which is implemented by row segmentation and regular spiking (RS) neurons respectively. In addition, N input spike trains are mapped to N/K spike trains to minimize the network size.

To explain the learning procedure and justify its function in classification, an example consisting of the digits 2, 4, 1, and 9 is described step by step. Fig. 7 shows the digits. They are divided into 4 horizontal segments which are mapped into 4 adaptive synapses. If an output spike occurs, the synapses carrying more frequent and closer presynaptic spikes (white pixels) before the output spike have more casual effects. Thus, their weights are increased based on the LTP rule. For example, the synapses {1,4}, {3}, and {1,2} in digits 2, 4, 9 respectively carry frequent presynaptic spikes, so their weights are increased more than the other synapses in each digit. In digit "1", all of the synapses have analogous influences onto the output neuron firing. So, the synaptic weights should be almost unbiased. After the first training period including weight augmentation and reduction, in the next iteration, the synaptic weights are tuned better according to the input digit patterns. Additionally, synaptic weights, which are connected to the same neurons in the second layer and different output neurons, are adapted in a competition due to the inhibitory neuron. Therefore, the synaptic weights demonstrate discriminative weight vectors for different digit patterns. In Fig. 7, some nominal synaptic weights (Ex. {0.20, 0.20, 0.45, 0.15} for digit 4) have been shown.

In the test session, if the digit spike trains are matched to the synaptic weights, the target output neuron releases a spike train close to the target pattern. Otherwise, due to discriminative synaptic weights, if the input spike trains are not compatible with the synaptic weights and target pattern, the output neuron might release a spike train either with 0 frequency or arbitrary pattern. Finally, the digit having maximum correlation with training data will be recognized in a small and fast neural network.

III. Experiments and Results

A subset of the MNIST machine learning data set consisting of handwritten digit images was used for evaluation of the proposed method [20]. Digital images in the dataset are 28 pixels in height and 28 pixels in width for a total of 784 pixels composing each grayscale image.

A. Binary classification

In the first experiment, 750 images of the digits "0" and "1" were sampled. Each grayscale image was converted to a binary image by applying the middle point threshold (threshold pixel=128). The 750 digit samples were divided into training and testing sets by 3-fold cross validation to guarantee the generality of the method.

The first layer scans the rows pixel by pixel and generates spikes where the digit points occur. Pixel values equal to 1 denote spike occurrences. In addition, a refractory period, A, is assumed to be 2 (ms). Therefore, the spike trains represent a row fall into a 28×2=56 (ms) temporal window. Fig. 3 gives an example of spike train generation for a sample digit "0". Finally, 28 spike trains with 56 (ms) discrete time points are obtained as presynaptic spikes conveyed to the second layer.

To segment the image into groups of rows, presynaptic spikes are collected to the N/K layer-2 neurons where N=28 and K=4. That is, every 4 consecutive sequential spike trains are connected to one neuron in the second layer. Spike generation of the neuron in this layer is computed by Izhikevich's RS model with parameters given in Table 1. Spike trains from seven layer-2 neurons submit information to the output neurons in the layer 3.

```
Function OneDataPassTraining(image, &
weights):OutputSpike
{
    [N,M]=size(image);
    r=2; % refractory period
    % Layer 1
    for each row of the B/W image
        spikes=generate spikes in r*M time points (1: spike
occurrence)
    %Layer 2
    for i=1:N/K
    {
        for j=1:K
            preSpikes{i}.append(spikes{(i-1)*K+j})
        middleSpikes{i}=Izhikevich's model (preSpikes{i});
    }
    %Layer 3
    for p=1:#classes
    {
        OutputSpike=Izhikevich's model (middleSpikes);
        STDP learning for target output
        Inhibition for non-target output based on STDP
        weights=update Synaptic weights
    }
```

Fig. 6. SNN pseudocode for handwritten digit classification
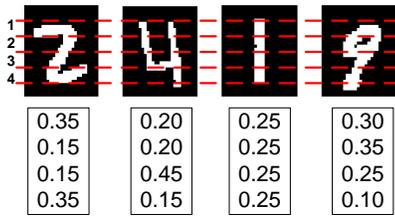
Fig. 7. Synaptic weights for digits 2, 4, 1, and 9. The intervals between dashed lines specify synapses. The numbers below each digit denote the synaptic weights

The output neurons use the same parameters in Izhikevich's model of the second layer to generate the spikes. In the third layer, synaptic weights projecting to the output neurons are initialized uniformly and updated by the STDP rule with parameters of LTP and LTD in Table 2. Furthermore, the inhibition neuron prevents the non-target (0 or 1) neuron to fire while receiving the presynaptic spikes. Hence, synaptic weights are changed according to the relative pre- and postsynaptic spike times.

After one batch of training (500 training samples), 14 synaptic weights (7 synapses for output "0" and 7 synapses for output "1") and a set of output spike patterns for "0" and "1" are obtained. Fig. 8 shows the simulation results (with *ΔT*=0.1 (msec)) of output spike trains of some handwritten digit images in "0" and "1" categories (each row shows a spike train). The illustrated spike trains in Fig. 8 show 1) specific first spike times and 2) discriminative spike time patterns for class "1" and class "0". Therefore, extracted target patterns are appropriate sources for pattern recognition. The output patterns of the testing samples are compared with the average target patterns for each class. Finally, the similarity measure denotes the objective function for the classification that is shown in (10).

$$Similarity^{\text{pattern}} = \cfrac{1}{\sqrt{\cfrac{1}{T} \sum_{i \in \text{spike train}} (Target_i^{\text{pattern}} - Output_i)^2}} \quad (10)$$

Where *T* is size of the target pattern.

Five different simulation step sizes (*ΔT*=0.05, 0.1, 0.2, 0.5, 1 (msec)) were studied. Table 3 specifies scaled synaptic weights connected to the output neurons "0" and "1" in the five temporal resolutions. Synaptic weights in Table 3 claim that *ΔT* in range of 0.05 to 0.5 (msec) give discriminative weight vectors for different classes. On the other hand, in *ΔT*=1 (msec), the training is biased to "0" because the simulation step size is so large and the learning procedure is not converged.

A subset of disjoint training and testing data was applied to the trained SNN to evaluate the accuracy rate of the proposed method. The results are shown in Table 4. The average accuracy rate is 97.6 for the testing sets. In addition, values of *ΔT* in the range of 0.05 to 0.5 (msec) give acceptable performance. *ΔT*=1 (msec), as explained, is not applicable. According to the results in Table 4, *ΔT*=0.2 (msec) has the best performance. It is also a fast neuron simulation for training and testing sessions.

TABLE I. REGULAR SPIKING NEURON PARAMETERS

Parameter	Value	Parameter	Value
V_{rest}	-60 (mv)	a	0.03
$V_{\text{threshold}}$	-40 (mv)	b	-2
V_{peak}	35 (mv)	c	-50
C	100	d	100
K	0.7	U_0	0
ΔT	0.05, 0.1, 0.2, 0.5, 1	I_{inj}	0

TABLE II. STDP PARAMETERS

Parameter	value
A	103
B	-40
$\tau+$	14
$\tau-$	34
K Default	10
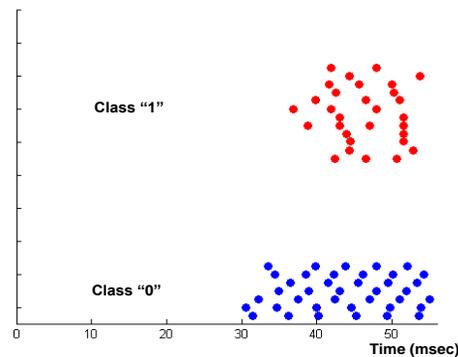
Fig. 8. Example output spike trains for the digits "0" (Blue) and "1" (Red) after learning. *ΔT*=0.1 (msec)

TABLE III. SYNAPTIC WEIGHTS (AFTER TRAINING) PROJECTING TO THE OUTPUT NEURONS REPRESENTING CATEGORIES "0" AND "1" IN DIFFERENT SIMULATION STEP SIZES (*ΔT*). EACH COLUMN INDICATES THE IMPORTANCE OF ONE OF THE *N/K*=7 IMAGE SEGMENTS TO EACH CATEGORY. THE BOLD WEIGHTS SHOW ACCEPTABLE LEARNING. *ΔT* IMPACTS ON MEMBRANE POTENTIAL COMPUTATION AND SYNAPTIC WEIGHT ALTERNATIONS. THEREFORE, EACH COLUMN SHOWS SOME SLIGHT VARIATIONS IN THE SYNAPTIC WEIGHTS. HOWEVER, THE SYNAPTIC WEIGHTS FOR EACH SIMULATION SHOW SEPARATE CATEGORIES

ΔT	Digit	Syn1	Syn2	Syn3	Syn4	Syn5	Syn6	Syn7
0.05	0	**0.00**	**1.30**	**6.60**	**5.24**	**0.26**	**6.60**	**0.00**
	1	**0.00**	**0.00**	**0.00**	**10.19**	**4.29**	**5.52**	**0.00**
0.1	0	**0.00**	**2.98**	**5.66**	**4.17**	**1.55**	**5.66**	**0.00**
	1	**0.00**	**0.00**	**0.00**	**10.43**	**4.20**	**5.37**	**0.00**
0.2	0	**0.00**	**3.69**	**5.94**	**4.16**	**0.26**	**5.94**	**0.00**
	1	**0.00**	**0.00**	**0.00**	**9.83**	**7.36**	**2.81**	**0.00**
0.5	0	**0.00**	**2.42**	**7.24**	**1.05**	**1.27**	**8.03**	**0.00**
	1	**0.00**	**0.00**	**0.00**	**17.40**	**2.25**	**0.36**	**0.00**
1	0	0.00	5.06	5.06	4.59	0.24	5.06	0.00
	1	0.03	0.00	0.00	0.00	0.00	0.00	19.97

TABLE IV. ACCURACY RATE OF THE PROPOSED SNN FOR HANDWRITTEN DIGIT CLASSIFICATION OF HANDWRITTEN DIGITS "0" AND "1"

ΔT	Accuracy Rate (Testing Data) %	Accuracy Rate (Training Data) %
0.05	**97.20**	---
0.1	**97.60**	---
0.2	**98.00**	**99.00**
0.5	**97.60**	---
1	56.00	---

B. 10-digit classification task

In the second experiment, 320 image samples of the MNIST handwritten digits were randomly selected and converted to binary images. The first and second layers of the SNN are the same as in the binary classification experiment except the segmentation factor, *K*, is set to 2. Therefore, the learning component consists of 28/2=14 adaptive synapses connected to 10 output neurons representing the digits 0 to 9 (140 adaptive synapses total and 24 layer-2 neurons). According to the mentioned theory, the second layer should generate candidate spike trains for a large variety of the input patterns. Fig. 9b illustrates 14 spike trains in the second layer which show a schematic of the input digits in Fig. 9a.

These discriminative spike trains invoke STDP learning in the next layer to adapt the synaptic weights and generate distinguishable spike patterns for digit categories (0-9). Fig. 10 shows the convergence scenario of the training process in 1000 iterations. This chart determines total distance between synaptic weights in sequential trials that is calculated by (11). It is concluded that, the training algorithm converges in 84 iterations and more training trials will not change the synaptic weights considerably. The synaptic weight matrix after 84 training iterations is shown in Table 5.

$$\Delta W_{Total}^{t} = \sum_{i=0}^{9} \left(\sum_{j=1}^{N/K=14} (w_{ij}^{t} - w_{ij}^{t-1})^2 \right)^{\frac{1}{2}} \qquad (11)$$

The adjusted synaptic weights and input digits provide 10 patterns of output spike trains shown in Fig. 11. The membrane potential and spike times in Fig. 11 illustrates discriminative patterns for different digits. For example, spikes in time stream of the digit "1" are close together in the center of the time window because all of the presynaptic spikes are gathered in a small range of simulation time (30-40 (ms)).

However, the proposed method as a minimal SNN architecture with 10×14 adaptive synapses (14-D weight vector) is designed for small classification problems such as binary categorization, not optimized for 10 categories, the performance of 10-digit task is 75.93% in average.
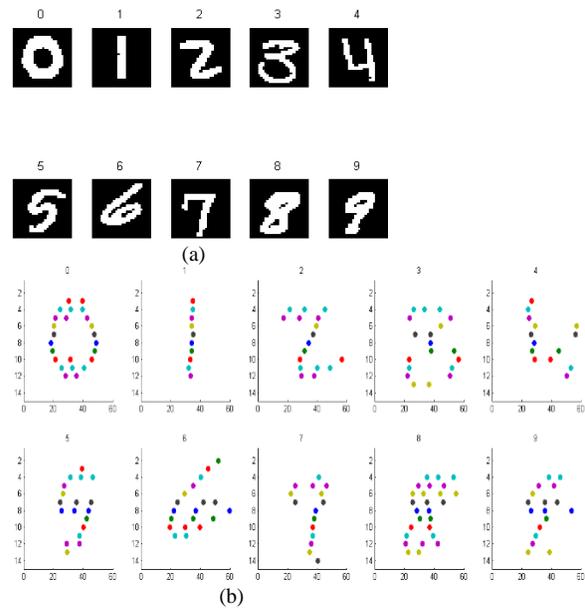
Fig. 9. a) Handwritten digits 0-9. b) 14 spike patterns emitted from RS neurons of the second layer
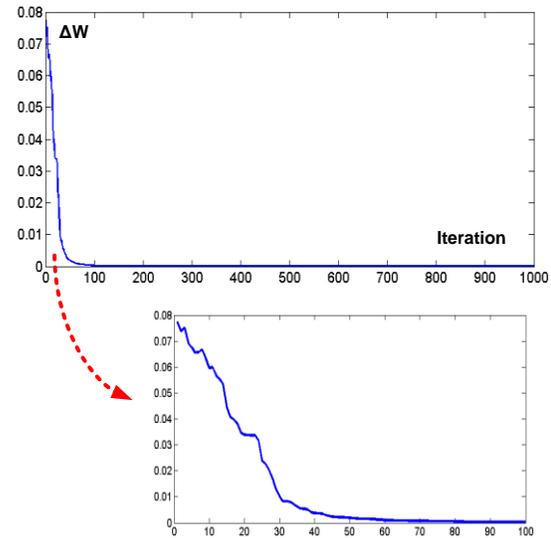
Fig. 10. Convergence plot obtained from 1000 iterations

TABLE V. SYNAPTIC WEIGHTS OF 14 SYNAPSES OF 10 DIGITS 0-9. THE FIRST TWO SYNAPTIC WEIGHTS AND THE LAST ONE ARE SMALLER THAN OTHER SYNAPSES BECAUSE THEY MOSTLY CONVEY BACKGROUND INFORMATION. THUS, RELATIVELY MUCH WEAK SYNAPSES PROVIDE A FAST METHOD OF BACKGROUND ELIMINATION IN THE ROW ORDER

Syn \ Digit	1	2	3	4	5	6	7	8	9	10	11	12	13	14
1	0.008	0.008	0.041	0.028	0.033	0.070	0.109	0.137	0.158	0.155	0.132	0.105	0.008	0.008
2	0.009	0.010	0.062	0.147	0.100	0.034	0.026	0.051	0.147	0.190	0.142	0.063	0.009	0.009
3	0.009	0.009	0.130	0.190	0.083	0.045	0.076	0.062	0.018	0.026	0.122	0.186	0.033	0.010
4	0.010	0.010	0.010	0.028	0.082	0.138	0.187	0.208	0.159	0.055	0.036	0.038	0.029	0.010
5	0.008	0.008	0.020	0.065	0.092	0.117	0.137	0.152	0.051	0.105	0.144	0.088	0.008	0.008
6	0.009	0.033	0.051	0.043	0.051	0.071	0.132	0.165	0.171	0.151	0.097	0.011	0.009	0.009
7	0.010	0.010	0.010	0.079	0.199	0.114	0.069	0.045	0.051	0.044	0.066	0.091	0.151	0.063
8	0.006	0.006	0.032	0.084	0.114	0.127	0.113	0.055	0.089	0.113	0.113	0.112	0.029	0.006
9	0.008	0.008	0.008	0.059	0.133	0.154	0.152	0.155	0.052	0.027	0.041	0.072	0.124	0.008
0	0.008	0.008	0.021	0.047	0.083	0.092	0.122	0.126	0.114	0.146	0.156	0.061	0.008	0.008
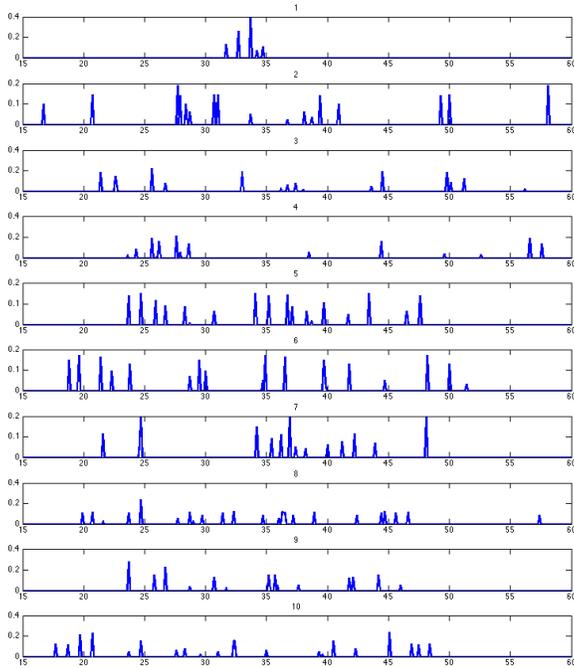
Fig. 11. Membrane potential and spike patterns for digits 0-9 after training

C. Comparison with other models

To compare our model with statistical machine learning strategies, the same training and testing datasets were applied to 1) a support vector machine (SVM) which maximizes the border distances between the classes [21]; and 2) a back propagation multi perceptron artificial neural network (BP-ANN) which learns the synaptic weights using error-feedback adjustment [22]. The obtained results are shown in Table 6. They have been implemented by the R software package [23, 24]. If more data are used in statistical models (with modified parameters) and some preprocessing algorithms such as principle components analysis (PCA) are applied, the performance should be higher than the rates reported in Table 6. However, based on the same situations at which the SNN performs, the SVM and ANN methods show accuracy rates that are slightly lower than the proposed SNN. We claim that the minimal SNN in this investigation has sufficient capacity to be improved more by the required preprocessing and experiments while using the biologically plausible principles.

IV. CONCLUSION AND DISCUSSION

A minimal time and memory efficient SNN architecture for classification was presented. This research shows that phenomenological STDP in a minimal model can support pattern recognition learning. The algorithms and neuron models were chosen to be biologically plausible. The proposed method represented an architecture which specifies a remarkably simple and fast network in comparison with previous investigations.

TABLE VI. ACCURACY OF 10-DIGIT RECOGNITION USING STATISTICAL MACHINE LEARNING MODELS. 200 TRAINING DATA WITHOUT PREPROCESSING

Method	Acc. %	Description
SVM	73.44	Polynomial kernel n=3.
ANN	70.87	40 hidden neurons, Decay=0.0001, 550 iterations.

Our SNN was applied to handwritten digit classification for a subset of images in the MNIST dataset. First, the initial layer interpreted the image logically based on the exact foreground pixel locations. Therefore, digit image was scanned row by row to generate the spikes as impulse reaction to the object perception. Also, this layer extracted the feature spikes directly from the image and represented a quick and natural image perception without complex computations. Second, every *K* (Ex. 2 or 4) spike trains were accumulated in a sequential order to provide the segmentation aspect of object detection in order to reduce the working space using Izhikevich's neuron model. This part of the network guaranteed to reduce number of the computational neurons and kept the order of the image segments from top to bottom. This layer provided a structure to produce set of spike trains invariant to diverse handwriting styles, outlier points, and slight changes in foreground orientation and thickness. The extracted sections mimicked digital scanning methods in a fast and implementable manner. Third, STDP learning and inhibitory neuron prepared the required environment for training the network and competition among dissimilar categories. The third layer's algorithm focused on supervised learning of the summarized input patterns. Additionally, the STDP rule was applied in two different sets of the synapses (connected to the target and non-target neurons) simultaneously and the training process converged after a small number of iterations. Thus, The SNN was tuned to categorize the input spike patterns quickly and it did not need many feature spike trains.

In summary, the introduced strategy was implemented in a simple and fast way due to the small number of the neurons and adaptive synapses (totally, {10 and 25} computational neurons and {14 and 140} adaptive synapses for binary and 10-digit classifications respectively). Finally, evaluation of the presented model demonstrated admirable performance of 98.0% maximum and 97.6% average accuracy rates for binary ("0" and "1") handwritten digit recognition. Furthermore, in spite of the minimal architecture of the presented SNN, acceptable performance of 75.93% was obtained in 10-digit recognition. The comparison between accuracy rate of the proposed method and statistical machine learning approaches (basic models without preprocessing and a small number of training data) determined slightly better performance of our SNN in the same and basic situations as well as incremental learning ability of the SNN. The minimal SNN worked much better for binary classification than 10-digit task. However, the reported results showed the potential capability of the SNN to be shrunk and work fast in training and prediction phases.

Therefore, the proposed SNN architecture and learning procedure can be a trustworthy model for classification due to its simple structure, quick feature extraction and learning, robust synaptic adaptation, and feasible implementation on VLSI chips in the future experiments.

REFERENCES

[1] Maass, Wolfgang. "Networks of spiking neurons: the third generation of neural network models." Neural networks 10.9 (1997): 1659-1671.

[2] Nessler, Bernhard, et al. "Bayesian computation emerges in generic cortical microcircuits through spike-timing-dependent plasticity." PLoS computational biology 9.4 (2013): e1003037.

[3] Kappel, David, Bernhard Nessler, and Wolfgang Maass. "STDP installs in winner-take-all circuits an online approximation to hidden markov model learning." PLoS computational biology 10.3 (2014): e1003511.

[4] Gerstner, Wulfram, and Werner M. Kistler. "Spiking neuron models: Single neurons, populations, plasticity". Cambridge University Press, 2002.

[5] Rozenberg, Grzegorz, Thomas Back, and Joost N. Kok. "Handbook of natural computing". Springer Publishing Company, Incorporated, 2011.

[6] Wade, John J., et al. "SWAT: a spiking neural network training algorithm for classification problems." Neural Networks, IEEE Transactions on 21.11 (2010): 1817-1830.

[7] Yousefi, Ali, Alireza A. Dibazar, and Theodore W. Berger. "Synaptic dynamics: Linear model and adaptation algorithm." Neural Networks 56 (2014): 49-68.

[8] Chrol-Cannon, Joseph, and Yaochu Jin. "Computational modeling of neural plasticity for self-organization of neural networks" BioSystems 125 (2014): 43-54.

[9] Kasabov, Nikola, et al. "Dynamic evolving spiking neural networks for on-line spatio-and spectro-temporal pattern recognition." Neural Networks 41 (2013): 188-201.

[10] Wang, Jinling, et al. "An Online Supervised Learning Method for Spiking Neural Networks with Adaptive Structure." Neurocomputing (2014).

[11] Vázquez, Roberto A. "Pattern recognition using spiking neurons and firing rates." Advances in Artificial Intelligence–IBERAMIA 2010. Springer Berlin Heidelberg, 2010. 423-432.

[12] Caporale, Natalia, and Yang Dan. "Spike timing-dependent plasticity: a Hebbian learning rule." Annu. Rev. Neurosci. 31 (2008): 25-46.

[13] Maass, Wolfgang. "On the computational power of winner-take-all." Neural computation 12.11 (2000): 2519-2535.

[14] Nessler Bernhard, Michael Pfeiffer, and Wolfgang Maass. "STDP enables spiking neurons to detect hidden causes of their inputs." Advances in neural information processing systems. 2009.

[15] Masquelier, Timothée, and Simon J. Thorpe. "Unsupervised learning of visual features through spike timing dependent plasticity." PLoS computational biology 3.2 (2007): e31.

[16] Wysoski, Simei Gomes, Lubica Benuskova, and Nikola Kasabov. "Fast and adaptive network of spiking neurons for multi-view visual pattern recognition." Neurocomputing 71.13 (2008): 2563-2575.

[17] Wysoski, Simei Gomes, Lubica Benuskova, and Nikola Kasabov. "Evolving spiking neural networks for audiovisual information processing." Neural Networks 23.7 (2010): 819-835.

[18] Beyeler, Michael, Nikil D. Dutt, and Jeffrey L. Krichmar. "Categorization and decision-making in a neurobiologically plausible spiking network using a STDP-like learning rule." Neural Networks 48 (2013): 109-124.

[19] Izhikevich, Eugene M. "Simple model of spiking neurons." IEEE Transactions on neural networks 14.6 (2003): 1569-1572.

[20] LeCun, Y., Bottou, L., Bengio, Y., and Haffner, P. (1998). "Gradient-based learning applied to document recognition". Proceedings of the IEEE, 86, 2278–2324.

[21] Bishop, Christopher M. "Pattern recognition and machine learning". New York: Springer, 2006.

[22] Cross, Simon S., Robert F. Harrison, and R. Lee Kennedy. "Introduction to neural networks." The Lancet 346.8982, pp. 1075-1079, 1995.

[23] Karatzoglou, Alexandros, David Meyer, and Kurt Hornik. "Support vector machines in R." 2005.

[24] Günther, Frauke, and Stefan Fritsch. "Neuralnet: Training of neural networks." The R Journal 2.1, pp.30-38, 2010.

An Arabic Natural Language Interface System for a Database of the Holy Quran

Khaled Nasser ElSayed

Computer Science Department, Umm AlQura University

Abstract—In the time being, the need for searching in the words, objects, subjects, and statistics of words and parts of the Holy Quran has grown rapidly concurrently with the grow of number of Moslems and the huge usage of smart mobiles, tablets and lab tops. Because, databases are used almost in all activities of our life, some DBs have been built to store information about words and surah of Quran. The need for accessing Quran DBs became very important and wide uses, which could be done through database applications or using SQL commands, directly from database site or indirectly by a special format through LAN or even through the WEB. Most of peoples are not experienced in SQL language, but they need to build SQL commands for their retrievals. The proposed system will translate their natural Arabic requests such as questions or imperative sentences into SQL commands to retrieve answers from a Quran DB. It will perform parsing and little morphological processes according to a sub set of Arabic context-free grammar rules to work as an interface layer between users and Database.

Keywords—Natural Language Processing (NLP); Arabic Question Answering System; Morphology; Arabic Grammar; Database; SQL

I. INTRODUCTION

Language obeys regularities and exhibits useful properties at a number of somewhat separable "levels". Suppose that a database user has some requests that he wishes to convey to database. His requests impose linearity on the signal. All you can play with is the properties of a sequence of tokens. A meaning gets encoded as a sequence of tokens, each of which has some set of distinguishable properties, and is then interpreted by figuring out what meaning corresponds to those tokens in that order.

The properties of the tokens and their sequence somehow "elicit" an understanding of the meaning. Language is a set of resources to enable us to share meanings, but isn't best thought of as a means for *encoding* meanings. This is a sort of philosophical issue perhaps, but if this point of view is true, it makes much of the AI approach to NLP somewhat suspect, as it is really based on the "encoded meanings" view of language.

The expression "natural" language refers to the spoken languages, such as English, Arabic, and French as opposed to artificial languages like languages of programming. NLP systems are programs perform some processes on natural language in some way or another .NLP is considered as one of the most important subfields of AI. It draws on techniques of logical and probabilistic knowledge representation and reasoning, as well as on ideas from philosophy and linguistics.

It requires an empirical investigation of actual human behavior, so it is complex and interesting [1].

The main function of NLP is to extract information from the natural input sentences with no care of method of inputting sentences to the computer. It could be used in many applications like: User interfaces (just tell the computer what to do in a textual interface), Knowledge-Acquisition (programs that could read books and manuals or the newspaper, with no need to explicitly encode all of the knowledge), Information Retrieval (find articles about a given topic and to determine whether the articles match a given query), and Translation (machines could automatically translate from one language to another) [2].

Because most of persons have no knowledge of database language, they find it difficult to access database. Recently, there is a rising demand for non-expert users to query relational database in a more natural language. Therefore the idea of using natural language instead of SQL triggered the development of new method of processing named: Natural Language Interface to Database (NLIDB) [3]. The advantages of NLIDB over formal query language and form based interfaces are ; No need to know the physical data structure, No need to learn AI, and Easy to use. In the other side, the disadvantages of NLIDB are; Difficult to decide success or failure of a query, Limited dealing with natural language, and Wrong assumption by users [4].

Mobile applications of the Arabic language are going to grow in the time being and near future. There is an increasing of the need of enriching the Arabic digital content. Almost, there is no study have had its focus on identifying the challenging aspects of developing mobile applications in mobile applications in Arabic. Many studies emphasized that there is a need of considering the identified challenges by interaction designers, developers, and other stakeholders in the early stages of the software life cycle [5]. Arabic Language understanding is an important field of AI. This field can be used to build an intelligent system for translating the natural Arabic request to SQL commands.

The proposed system performs parsing and interpreting of the natural Arabic input such as a question or an imperative sentence. It applied morphology and context-free parsing techniques on context-free grammar of Arabic Language. Then, the system produces an SQL command, which could retrieve the suitable answer from the database of Quran statistics. It uses an approach that lets the computer accepts natural language sentences, but extract only the essential

information from that command. Also, it enables users to learn how to build their SQL commands.

II.   RELATED WORK

Daoud introduced in [6] a SMS system named CATS, for posting and searching through free Arabic text using a technology of information extraction. This system can handle structured data stored in relational database and unstructured free Arabic SMS text. He used Arabic interaction language between sellers and buyers through SMS in a classified domain.

Al-Johar and McGregor proposed in [7] developing an Arabic natural language interface to database systems in prolog. They used the approach of intermediate meaning representation in building LMRA notation as a representative for this approach for the Arabic language. This notation divides common nouns into two classes: A mammal common noun (more than one possible gender), and a non-mammal common noun (one possible gender). It has logical formulas to represent a number of Arabic words and phrases.

Mohammad, Nasser, and Harb produced in [8] a Knowledge Based Arabic Question Answering System (AQAS) in prolog. Their system has a knowledge base of a radiation diseases domain. It divided the Arabic query into two parts: the required part (the information requested) and the known part (the thing asked about). Its parser converts the input query into internal meaning representation (IMR), and then it is processed to locate and retrieve the answer for the user. Its IMR is looking for certain words in the query to specify the required information about certain thing.

El-Mouadib, Zubi, Almagrous, and El-Feghi introduced in [9] the design and implementation of an English natural language interface to a database system. Its name is Generic Interactive Natural Language Interface to Databases (GINLIDB). It has two types of semantic grammars parser to supports a wide range of natural language statements: The first is a single lexicon semantic grammar which consists of individual words and some of their synonyms that are used in the English language grammar. While the second is a composite lexicon semantic grammar which is a combination of terminal words (terminals that exist only in the lexicon) that form phrases or sentences in a specific structure. It is designed using of UML and developed using Visual Basic.

Kanaan, Hammouri, Al-Shalabi, and Swalha presented in [10] the architecture of a question answering system. Their system depends on data redundancy rather than complicated linguistic analyses of either questions or contender answers. So, it is different from the other similar system, because a wrong answer is often worse than no answer. It receives Arabic natural language questions, and then it attempts to generate short answers. They used an existing tagger to identify proper names and other crucial lexical items and build lexical entries. They provided an analysis of Arabic question forms and attempted to formulate better kinds of more appropriated answers.

Abu Shawar introduced in [11] a method to access Arabic Web Question Answering (QA) corpus using a chatbot. This method was used properly with English and other European

languages. With this method, there is no need for sophisticated NLP or logical inference. Any NLP interface to QA system is constrained to reply with the given answers, so there is no need for NLP generation to recreate well-formed answers, or for deep analysis or logical inference to map user input questions onto this logical ontology. There is simple (but large) set of pattern-template matching rules. This paper used the same chatbot to react in terms of Arabic Web QA corpus.

III.   SYSTEM STRUCTURE

The system receives simple requests in natural Arabic language questions as inputs from users. It is responsible of generating a final SQL command and executing it to retrieve the available answer from the database of the holy Quran. To perform that, the input sentence passes through multiple processing operations. Figure 1 presents the structure of the system.
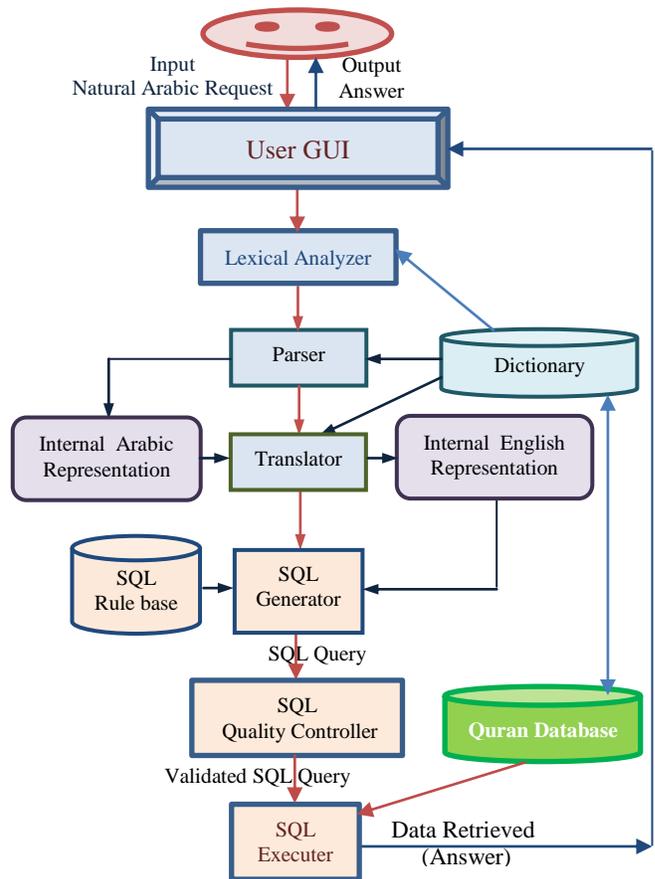
Fig. 1.   Structure of the system

User GUI: the system provides an easy Graphical User Interface for easy **interaction** with its users. It is user friendly for none experts of computer or database and even for children. This is done through a menu driven and easy visual forms.

Lexical Analyzer : this stage includes performing four functions; splitting step (scan the user input character by character until recognizing a word to divide natural input into the lowest level of lexemes or words), spelling (checks the spelling of words using the dictionary, if word is not found

correction is done or a new word is added to it), tokenizing (produces a token -the category or meaning – for each word), and abstracting (removes non important words that has no effect in the meaning of request and could be considered as noisy or excessive words).

Parser: The parser performs parsing according to context-free parsing techniques. The syntax of input sentences is represented in context-free grammar rules. It produces the internal Arabic representation of the input sentence according to the suitable grammar rule, using the dictionary. Its syntactic analysis is based on Augmented Transition Network (ATN), which checks if the structure of input tokens is allowed according to grammar rules.

Translator: Early research speculated that computers could be used for Machine Translation "Translation from one language to another". The translator in the proposed system uses the internal Arabic representation of the input sentence produced by the parser and uses the information stored in the dictionary to produce the corresponding internal English representation. It brings the English word corresponding to name of column or table in the applied database.

SQL Generator: The generator uses internal English representation produced by the translator and the SQL rule base to produce the SQL command. It uses the format of SQL rules stored in the SQL rule base as format or a frame and fill slots from the internal English representation.

SQL Quality Controller: The task of the SQL quality controller is to verify the generated SQL query. The query should be verified for valid names of tables, columns and format before applying to the Quran database.

SQL executor: The task of the SQL executor is to retrieve the suitable answer from the database of the holy Quran. Then, the system will consult the answer (the retrieved data) as output to the user.

IV. DATABASE OF THE HOLY QURAN

The database used by the system was prepared to hold data about the Quran, to enable executing SQL queries retrieving its statistics data. Mainly, it keeps data about word(s), ayah(s), surah(s), and 30 Jozaa (chapter). Each Jozaa has with two Hezb (section), while each section has four quarters. Figure 2 present the Entity-Relationship diagram for the database of this system.

The entity DICTIONARY has the attributes: WordCode, WordNum, Word_Text, WordNumOfChar, Word_Meaning, Word_Root. While the entity AYAH has the attributes: AyahCode, AyahNum, Ayah_Text, AyaPageNo, and Ayah_meaning. The entity SORAH has the attributes: SurahCode, SurahNum, SurahName, Surah_Area, RevelationOrder, SurahPageNum, Quarter#, Hezb#, Jozaa#. Also there some attributes in the relationship between entities WORD and AYAH, like Word#InAyah.

Most of statistics of the words, ayah, and surah of the Holy Quran for the presented system is transferred from the database of TANZIL resources [12].
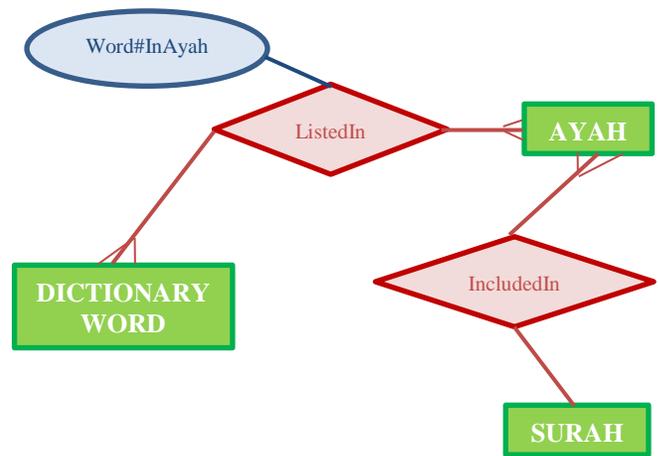
Fig. 2. Entity-Relationship Diagram of Quran Database

V. PARSING AND MORPHOLGY

A. Parsing Process

Parsing (syntactic analysis) is the core of the proposed system where the input utterance is being checked to ensure that its syntax is correct and structured representations of the possible parses are generated. In parsing, a grammar is used to determine what sentences are legal [2].

Grammar is being applied using a parsing algorithm to produce a structure representation, or parse tree. Parser reads every input sentence, character by character, to decide what is what. It can recognize the underlying structure of a source text and checks that a token is a part of a legal pattern specified by the language grammar. It also gets some attributes of tokens from the dictionary [8].

Context-free grammar is used in parsing the Arabic request inputted to the proposed system, as will as in parsing of most of programming language because it has several advantages. It can deal with the word level and the phrase level. Also, it knows where it is in the sentence at all times. Its main disadvantage is that, it can't handle the numerous valid ways that a language can construct, due to the limitations of size and speed [8].

Context-free grammars are simply grammars consisting entirely of rules with a single symbol on the left-hand side of the BNF rules. The obvious advantage of BNF is that it is simple to define. Many of the grammars used for NLP systems are BNF, as such they have been widely studied and understood and hence highly efficient parsing mechanisms have been developed to apply them to their input.

The system uses context-free parsing technique. It begins by looking at the rules for the sentence, then it looks up the rules for the constituents of the sentence and progresses until a complete sentence structure is build up. If a sentence rule match the input sentence then the parsing process is ended, otherwise, the parser restarts again at the top level with the next rule. It performs syntax analysis recursively until firing certain rule structure or fail.

The parse tree breaks down the sentence into structured parts so that the computer can easily understand and process it. For the parsing algorithm to construct this parse tree, a set of BNF rules, which describes what tree structures are legal, must be available. These rules say that a certain symbol may be expanded in the tree by a sequence of other symbols.

Also, the system used noise disposal parsing for our application, because it is suitable for those application that concern only with a few keywords that a sentence contains, not with all associative words that make up a language. In essence, these types of applications are interested only in the information included in the sentence. This task is done by considering all unknown and un-required words as noise and discarding them. Simply, all sentences must follow a rigid format that resembles natural language.

Its main advantages are the easier implementation of extracting information from sentences, while it is not useful outside restricted situations such as the database queries. This is because it is based on two assumptions: the first is that the sentence follows a strict format, the second is that, only a few keywords or symbols are important. While in normal conversation, most words are important in some way or another.

B. Morphology and Dictionary

Morphology: NLP system doesn't always include morphological analysis. The alternative is to put all possible forms of each word into the dictionary, however storing all possible variants is inefficient and unnecessary. The terms: noun, verb, etc. are morphological but the nominal and verbal which are defined by the distribution of the forms in the sentences are syntactic analysis. Morphology process depends mainly on the dictionary entries and language grammar inflection [13]. This system will discard the prefix and postfix additional characters from a word. It is always one of those listed in Table 1.

Dictionary: a dictionary for NLP system contains the vocabularies known by that system. Its main function is to assist the parser in translating the input sentence into an internal meaning representation (IMR) to be processed.

Any word in the input sentence must be located in the dictionary, taking in consideration the necessary morphological process done by the system. It determines the capabilities of the system. The problem of the format and structure of the dictionary are closely related to the problems of the text storing. If the text is compressed to optimize storage size, the processing time is increased to compress and expand the data.

The format of each dictionary entry depends on the information stored in that entry. The most important data item within each entry is the morpheme itself called the head. Each entry has its appropriate information. The morphological algorithm is responsible of isolating the heads of the dictionary entries from the stream of the input words. Each entry contains the corresponding English meaning of each Arabic word stored in it. Actually, it has the English meaning of imperative verbs or interrogatives and the names of columns and tables of the applied database.

TABLE I. A LIST OF ADDITIONAL PREFIXES AND POSTFIXES

Addition Type		Examples and Meaning	
Pronoun	ضمير	هو, هي, هما, هم, هـ, هن	Its, his, her, their, he, she, they
Preposition	حرف جر	لـ, بـ, كـ,	for, with, as
Preposition and Pronoun	ضمير مع حرف جر	له, لها, لهما, لهم, لهن, به, ..	for him, with him, as him, ….
Definition character	أداة تعريف	ال	the
Preposition and Definition character	حرف جر مع أداة التعريف	لل, بال, كال	for the, with the, as the

VI. SQL QUERIES, INPUTS AND OUTPUTS

First of all, we should take in consideration the already exist SQL queries and their format. Then we should find out how to map between the expected inputs and the generated SQL queries, to finally generate the suitable answer.

A. SQL Queries

This system is run over MySQL database. So, it should generate complete SQL Query as usual in MySQL. Any SQL Query consists of SQL command beside names of attributes (columns) from certain tables and tables themselves and given values of some attributes as conditions if there is.

SQL commands are classified into two categories: Data Definition Language (DDL) commands like: CREATE, ALTER, DROP, DESCRIBE, etc. Data Manipulation Language (DML) commands like: SELECT UPDATE, DELETE, INSERT, etc. [14]. This system will generate SQL queries with the command SELECT only. Dependent on the natural input request, it translates the predicted request to this command. No way to generate another command.

B. Inputs and SQL Queries

The proposed system is expected to process the input sentence in the some of the following two modes [15]:

1) Imperative Mode: This sentence starts with imperative verb like:

استخرج الآيات التي بها كلمة الجنة

Retrieve the Ayah that include the word Paradise.

Table 2 shows list of some examples of imperative verbs beside their meanings and objects. As example, the first five imperative verbs (green color) are allowed from the user. But the last four imperative verbs (red color) are disallowed.

2) Question Mode: This sentence starts with interrogative question like:

ما اسم السورة التي تتضمن أحكام الصوم؟

Retrieve name of Sora include fasting rules?

Table 3 shows some examples of Questions beside their meanings and goals.

TABLE II.   LIST OF SOME IMPERATIVE REQUESTS AND SQL QUERIES

Imperative Verb فعل أمر باللغة العربية	English meaning	Corresponding SQL Command
استخرج	Retrieve	SELECT
اعرض	Show	SELECT
أعطني	give me	SELECT
أذكر	List	SELECT
وضّح	illustrate	SELECT
عدّل	change	UPDATE
احذف	Erase	DELETE
صف	describe	DESCRIBE
أدخل أو خزن	add/store	INSERT

3) Imperative and Question Mode: This sentence starts with imperative verb followed by interrogative question like:

وضح لي أين توجد آيات الحج؟

Tell me, Where is the Ayah of Pilgrim?

Similarly, the user can mix any of the allowed imperative verbs, like shown in table 2 with question like those listed in table 3.

TABLE III.   LIST OF SOME QUESTIONS AND CORRESPONDING SQL

Interrogative	English meaning	Corresponding SQL Command
ما	Which	SELECT
ماذا	What	SELECT
من	Who	SELECT
كم	how many/much	SELECT
أين	Where	SELECT

C. The Output Answer

It is predicted the output retrieved from the database of the holy Quran, to be statistics about word (s), Sora (s), and subject(s).

VII. PROCESSING ARABIC REQUEST

All Arabic requests received from users have a common part and parcel. This common part contains all necessary information needed to build an output SQL command, and was given the name REQUEST. The REQUEST part has several forms. Each form represents certain one of the three expected input requests listed above, and were represented by some BNF grammar rules.

The REQUEST part might consists mainly from four components beside some noise data. The first part is the mode itself which included explicitly with the imperative or interrogative or declarative sentence. The second part is the TABLES component, which consists of SQL table names. The third part is the REQUIRED component, which has the names of the items of information actually needed to be retrieved (needed values of attributes of database table). The fourth part

is the CONDITION component, which implies the condition to be applied on certain SQL query.

The main task of the SQL generator is to map the elements of the natural query to the elements of the SQL commands of the used databases. There is a general SQL command generated for all queries which is SELECT. So, the SQL generator should finds out the columns (attributes) to be in front of the SELECT command, table(s) to be in front of FROM clause, conditions for WHERE clause and a the method or displaying resulted data in certain order if needed.

VIII. CONCLUSIONS & FUTURE WORK

The presented system satisfies the need for accessing Quran DBs through LAN or WEB for all users, especially with no knowledge of database. It could accept natural Arabic requests such as imperative statements or questions. Then, it generated the suitable SQL command to be verified and executed. Finally it presents the answer from a database of Quran data to the user in an easy manner.

It performed parsing and little morphological processes according to a sub set of Arabic context-free grammar rules to work as an interface layer between users and Database.

In future, the database will be extended to include more tables and attributes. Also, the system will be extended to accept more complex search request and link answer with explanation of meaning of surah and ayah of the holy Quran.

REFERENCES

[1] S. J. Russell and P. Norvig, "Artificial Intelligence – A Modern Approach", 3th edition, Pearson, 2010.

[2] E. V. Provider, "Talking with Computer in Natural Language", Springer-Verlog, NY, 1986.

[3] M. Tyagi, " Natural Language Interface to Databases: A Survey", International Journal of Science and Research (IJSR), Volume 3 Issue 5, pp. 1443-1445, May, 2014. http://www.ijsr.net/archive/v3i5/MDIwMTMyMTU3.pdf

[4] A. Popescu, O. Etzioni, H. Kautz, "Towards a theory of natural language interfaces to databases", In: 8th Intl. Conf. on Intelligent User Interfaces, Miami, FL, pp. 149–157, USA, 2003. http://dl.acm.org/citation.cfm?id=604070

[5] S. N. Zawati and M. A. Muhanna, "Arabic mobile applications: Challenges of interaction design and development", 2014 International Conference (IWCMC) of Wireless Communications and Mobile Computing, Nicosia, pp 134-139, 2-8 Aug 2014. http://ieeexplore.ieee.org/xpl/login.jsp?tp=&arnumber=6906345&url

[6] D. Daoud, "Building an Arabic Application employing information extraction technology", In Proceedings of the Second International Conference on Information Technology (ICIT05), Amman, Jordan, pp. 1-9., 2005. http://icit.zuj.edu.jo/icit05/2005/Information%20Systems/193.pdf

[7] B. Al-Johar and J. McGregor, "A Logical Meaning Representation for Arabic Representation (LMRA)", . In: Proceedings of the 15th National Computer Conference, Riyadh, Saudi Arabia, pp 31-40, 1997. http://www.ccse.kfupm.edu.sa/~sadiq/proceedings/NCC1997/Pap24.doc

[8] F. Mohammad, Kh .Nasser and H. Harb "A Knowledge Based Arabic Question Answering System (AQAS)." In SIGART Bulletin, A Quarterly Publication of the ACM, Special Interest Group on Artificial Intelligence, Vol. 4, No. 4, October, 1993. dl.acm.org/citation.cfm?id=165488

[9] F. A. El-Mouadib, Z. S. Zubi, A. A. Almagrous, I. El-Feghi, "Interactive Natural Language Interface", Journal WSEAS TRANSACTIONS on COMPUTERS, Issue 4, Volume 8, pp 661-680, April 2009. http://dl.acm.org/citation.cfm?id=1558765

[10] G. Kanaan, A. Hammouri, R. Al-Shalabi, M. Swalha, "A New Question Answering System for the Arabic Language", American Journal of Applied Sciences 6: pp. 797-805, 2009. http://thescipub.com/PDF/ajassp.2009.797.805.pdf

[11] B. Abu Shawar, "A Chatbot as a Natural Web Interface to Arabic Web QA", iJET – Volume 6, Issue 1, pp. 37-43, March 2011. http://www.editlib.org/p/44956/article_44956.pdf

[12] Tanzil, "Tanzil Quran Navigator", 1/3/2015 http://tanzil.net/

[13] A. Walker, "Knowledge Systems and Prolog", IBM T.J. Watson Research Center, Addison-Wesley, 1997.

[14] R. Elmasri, and S. Navathe, "Fundamentals of Database Systems", 6th edition, Addison Wesley, 2010.

[15] F. Noama, "Summary of Arabic Grammar", Scientific Center for translation, Cairo, 1988.

AUTHOR PROFILE

The Author is Dr. Eng. Khaled Nasser. ElSayed. He was born in Cairo, Egypt 9 Oct. 1963. He have got his PhD of computers and systems from Faculty of Engineering, Ain Shams University, Cairo, Egypt, 1996.

He has worked as an associate professor of computer science, in Umm-AlQura Uni. in Makkah, Saudi Arabia since 2008. Artificial Intelligence is his major. His interest research is Distant Education, E-Learning, and Agent. Dr. Khaled Nasser ElSayed translated the 4th edition of "Fundamentals of Database Systems", Ramez Elmasei and Shamkant B. Navathe, Addison Wesley, fourth edition, 2004, published by King Saud University, Riyadh, Saudi Arabia, 2009. He is also the author several books in programming in C & C++, Data Structures in C& C++, Computer and E-Society, Database Design and Artificial Intelligence.

Trend Analysis of Relatively Large Diatoms Which Appear in the Intensive Study Area of the Ariake Sea, Japan in Winter (2011-2015) based on Remote Sensing Satellite Data

Kohei Arai 1

1Graduate School of Science and Engineering
Saga University, Saga City, Japan

Toshiya Katano 2

2Tokyo University of Marine Science and Technology
Tokyo Japan

Abstract—**Behavior of relatively large size of diatoms which appear in the Ariake Sea areas, Japan in winter based on remote sensing satellite data is clarified. Through experiments with Terra and AQUA MODIS data derived chlorophyll-a concentration and truth data of chlorophyll-a concentration together with meteorological data and tidal data which are acquired for 5 years (winter 2011 to winter 2015), it is found that strong correlation between the chlorophyll-a concentration and tidal height changes. Also it is found that the relations between ocean wind speed and chlorophyll-a concentration. Meanwhile, there is a relatively high correlation between sunshine duration a day and chlorophyll-a concentration.**

Keywords—chlorophyl-a concentration; red tide; diatom; sunshine duration; ocean winds; tidal effect

I. INTRODUCTION

The Ariake Sea is the largest productive area of Nori (Porphyra yezoensis1) in Japan. In winters of 2012 and 2013, a massive diatom bloom occurred in the Ariake Sea, Japan [1]. In case of above red tides, bloom causative was Eucampia zodiacus 2 . This bloom has being occurred several coastal areas in Japan and is well reported by Nishikawa et al. for Harimanada sea areas [2]-[10]. Diatom blooms have recurrently occurred from late autumn to early spring in the coastal waters of western Japan, such as the Ariake Sea [11] and the Seto Inland Sea [12], where large scale "Nori" aquaculture occurs. Diatom blooms have caused the exhaustion of nutrients in the water column during the "Nori" harvest season. The resultant lack of nutrients has suppressed the growth of "Nori" and lowered the quality of "Nori" products due to bleaching with the damage of the order of billions of yen [3].

This bloom had been firstly developed at the eastern part of the Ariake Sea. However, as the field observation is time-consuming, information on the developing process of the red tide, and horizontal distribution of the red tide has not yet been clarified in detail. To clarify the horizontal distribution of red tide, and its temporal change, remote sensing using satellite data is quite useful.

In particular in winter, almost every year, relatively large size of diatoms of *Eucampia zodiacus* appears in Ariake Sea areas. That is one of the causes for damage of *Porphyra yezoensis*. There is, therefore, a strong demand to prevent the damage from Nori farmers. Since 2007, *Asteroplanus karianus* appears in the Ariake Sea almost every year. In addition, *Eucampia zodiacus* appears in Ariake Sea since 2012. There is a strong demand on estimation of relatively large size of diatoms appearance, size and appearance mechanism).

In this paper, the chlorophyll-a concentration algorithm developed for MODIS [3] is firstly validated. Then apply the algorithm to MODIS data which are acquired at the Ariake Sea areas, Japan specifically. Then a trend analysis of chlorophyll-a concentration in winter in 2011 to 2015 is made. The major influencing factor of *Eucampia zodiacus* appearance is chlorophyll-a concentration. The other environmental factors, such as sea water temperature, northern wind for convection of sea water have to be considered. Also, the relations between tidal effects and chlorophyll-a concentration as well as between ocean wind speed and chlorophyll-a concentration together with between sunshine duration a day and chlorophyll-a concentration.

In the next section, the method and procedure of the experimental study is described followed by experimental data and estimated results. Then conclusion is described with some discussions.

II. METHOD AND PROCEDURE

A. The Procedure
The procedure of the experimental study is as follows,

1) Gather the truth data of chlorophyll-a concentration measured at the observation towers in the Ariake Sea areas together with the corresponding areas of MODIS derived chlorophyll-a concentration,

2) Gather the meteorological data which includes sunshine duration a day, ocean wind speed and direction, tidal heights,

---

[1] http://en.wikipedia.org/wiki/Porphyra

[2] http://www.eos.ubc.ca/research/phytoplankton/diatoms/centric/eucampia/e_zodiacus.html

[3] http://modis.gsfc.nasa.gov/

3) Correlation analysis between the truth data and MODIS derived chlorophyll-a concentration as well as between geophysical parameters, ocean wind speed, sunshine duration a day, tidal heights and chlorophyll-a concentration is made.

B. The Intensive Study Areas

Fig.1 shows the intensive study areas in the Ariake Sea area, Kyushu, Japan.

There are three observation tower points, TW, S, and A. TW is closely situated to the Saga Ariake Airport and is situated near the river mouth. On the other hand, A is situated most closely to the coastal area while S is situated in the middle point of the Ariake Sea width and is situated most far from the coastal areas and river mouths.
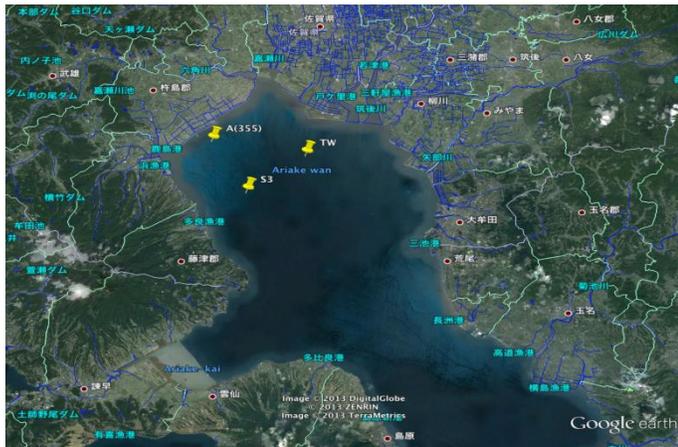

Fig. 1.   Intensive study areas (Yellow pins shows the areas)

III.   EXPERIMENTS

A. The Data Used

The truth data of chlorophyll-a concentration measured at the observation towers in the intensive study areas in the Ariake Sea areas together with the corresponding areas of MODIS derived chlorophyll-a concentration which area acquired for the observation period of one month during from January 1 to February 1 in 2011 to 2015 are used for the experiments. Also, the meteorological data which includes sunshine duration, ocean wind speed and direction, tidal heights which are acquired for the same time periods as MODIS acquisitions mentioned above. In particular for 2015, two months data are used for trend analysis.

Fig.2 shows an example of the chlorophyll-a concentration image which is derived from MODIS data which is acquired on 2 March 2015. The chlorophyll-a concentration is measured at the tower, TW. This is red tide (Phytoplankton) blooming period. Such this MODIS derived chlorophyll-a concentration data are available almost every day except cloudy and rainy conditions.

Blooming is used to be occurred when the seawater becomes nutrient rich water, calm ocean winds, long sunshine duration after convection of seawater (vertical seawater current from the bottom to sea surface).
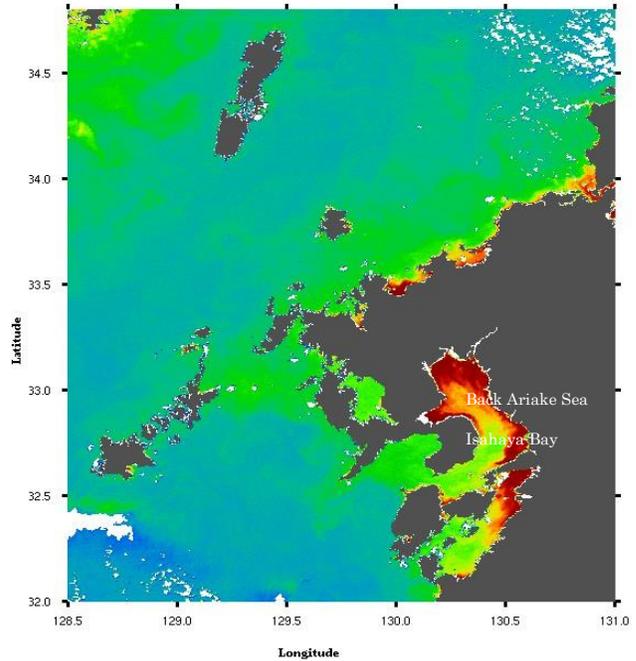
Fig. 2.   Example of the chlorophyll-a concentration image which is derived from MODIS data which is acquired on 2 March 2015

Therefore, there must are relations between the geophysical parameters, ocean wind speed, sunshine duration, tidal heights and chlorophyll-a concentration. As shown in Fig.2, it is clear that the diatom appeared at the back in the Ariake Sea and is not flown from somewhere else. Also, there is relatively low chlorophyll-a concentration sea areas between Isahaya bay area and the back in the Ariake Sea area. Therefore, chlorophyll-a concentration variations are isolated each other (Isahaya bay area and the back in the Ariake Sea area).

B. The Relation Between Truth Data and MODIS Derived Colorophyl-a Concentrations (Validation of the Algorithm for Chlorophyl-a Concentration Estimation)

In order to validate the chlorophyll-a concentration estimation algorithm, the relation between truth data of Shipment data as well as Tower data and MODIS derived chlorophyll-a concentration is investigated. Before that, Tower data of chlorophyll-a concentration is compared to Shipment data. Fig.3 shows the relation between these for intensive study area of TW. Also, Fig.4 shows relation of chlorophyll-a concentration between tower data and the other two of shipment data as well as MODIS data derived chlorophyll-a concentration. The time for data collection by ship is different from MODIS data acquisition time and tower data acquisition. Spatial resolutions of MODIS data derived Chlorophyll-a Concentration is 500 m^2 while that of the shipment data and the tower data is just one point of data. Tower data is acquired every one hour. In the validation, averaged chlorophyll-a concentration a day is used because the shipment data acquisition time is varied and also MODIS data acquisition time is different by day by day. Therefore, relation between truth data and MODIS derived Chlorophyll-a Concentration is so scattered.
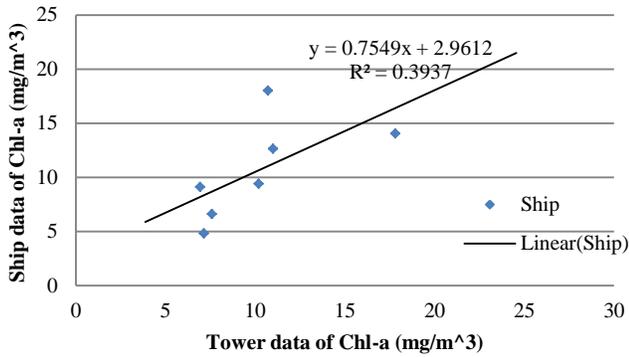
Fig. 3.   Relation of the measured chlorophyll-a concentration between Tower data and Shipment data

Fig. 4.   Validation of Chlorophyll-a Concentration estimation algorithm

C. Trend Analysis

Fig.5 shows the trends of shipment data, tower data and MODIS derived chlorophyll-a concentrations measured in January to February in 2015. It seems that trends of MODIS, Tower, and Ship data derived chlorophyll-a concentration are similar. Also, it is found that high chlorophyll-a concentration is occurred on Spring tide while low chlorophyll-a concentration appears on neap time frames. Namely, the dates of neap of this time period are January 15, January 29, February 14 and February 28.

Meanwhile those of spring tide are January 7, January 23, February 7, February 21, and March 7. Chlorophyll-a concentration get up and down repeatedly on spring tides and neaps.

Fig. 5.   Chlorophyll-a trend in January and February in 2015

On the other hand, Fig.6 (a) to (d) shows the results from trend analysis of chlorophyll-a concentrations in 2014, 2013, 2012, and 2011, respectively.
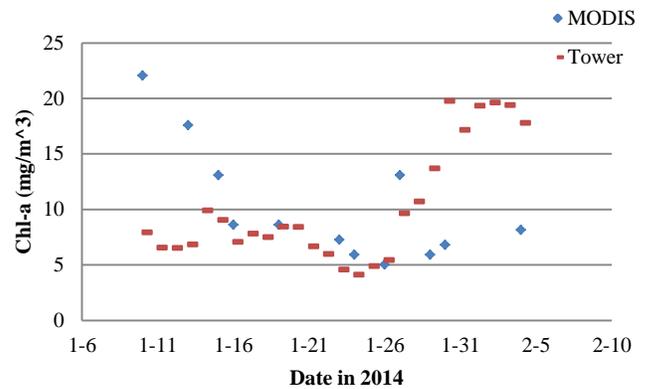
(a)January 2014
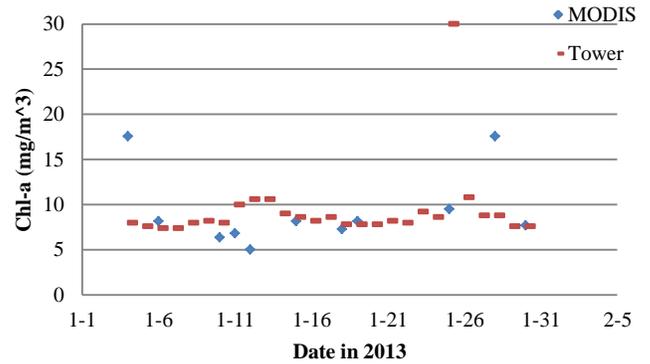
(b)January 2013
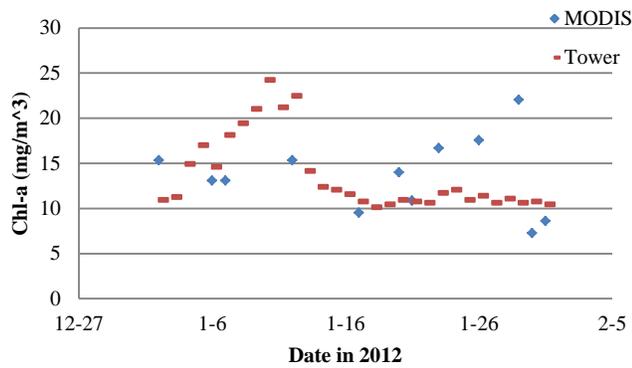
(c)January 2012
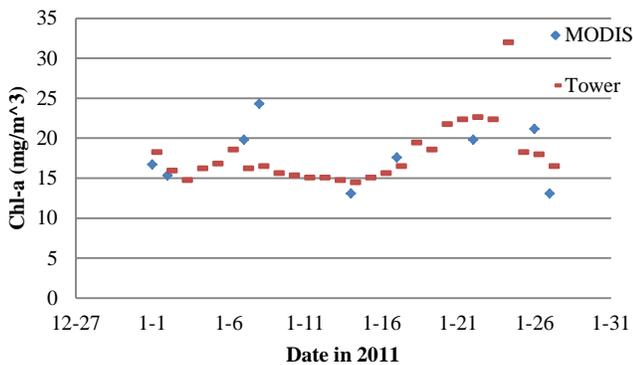
(d)January 2011

Fig. 6.   Chlorophyll-a concentration trends in 2011 to 2014

Spring tides occurred on January 3, January 19 and February 2 while neaps appeared on January 10, and January 26 in 2014. Namely, chlorophyll-a concentration raised from January 26 and reached at the maximum on February 2.

It, however, is not always true. There is no peak at the spring tide on January 19 in the tower data derived chlorophyll-a concentration.

In 2013, the spring tides occurred on January 14 and January 30 while neaps appeared on January 7 and January 22, respectively. Tower data derived chlorophyll-a concentration shows the trend of the up and down of the concentration on sprig tides and neaps slightly. Meanwhile, the spring tides occurred on January 11, and January 25 while the neaps appeared on January 3, January 19 and February 2 in 2012, respectively. Although the tower data derived chlorophyll-a concentration shows the peak on January 11, there is no such peak on January 25 while the MODIS data derived chlorophyll-a concentration shows two peaks on January 11 and January 25. On the other hand, the spring tides occurred on January 6 and January 22 while the neaps appeared on January 14 and January 22, respectively. For both of the spring tide periods, both of MODIS data and tower data derived chlorophyll-a concentrations show the peaks and also show the valleys on the neaps. Therefore, it may conclude that there is strong relation between tide and chlorophyll-a concentration, it is not always true though.

In the neap period, vertical direction of sea water mixing due to tidal effect is not so large. Therefore, relatively large scale of diatoms moves to the sea bottom. Meantime, turbidity is getting down in neap period. Then the moved diatoms may be survived when transparency of sea water is getting up. After that, vertical direction of seawater mixing is occurred in spring tide period. Then the survived diatoms are getting up to sea surface. Thus blooming would occur if nutrition rich seawater is there.

D. Relation Among Chlorophyll-a Concentration and Tidal Height Difference a Day, Sun Shine Duration a Day, and Wind Speed from North

Relation among chlorophyll-a concentration (Chl-a), tidal height difference a day, sun shine duration a day and wind speed from the north is clarified. Fig.7 shows the result.
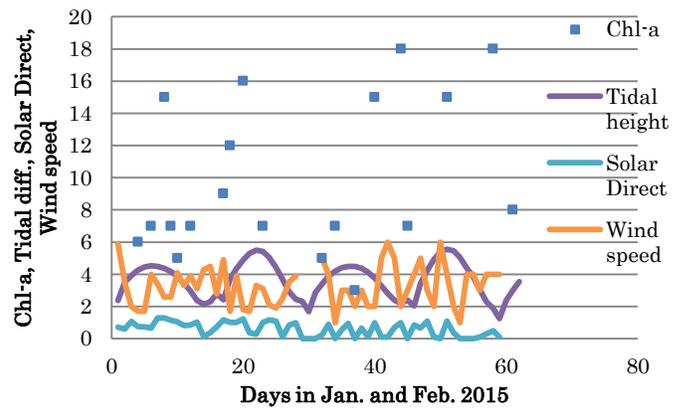
Fig. 7.   Relation among chlorophyll-a, tidal height difference a day, sun shine duration a day and wind speed from the north

As shown in Fig.6, there is strong relation between tides and chlorophyll-a concentration. It, however, is not always true. Other factors, sun shine time duration a day is one of those as well as wind speed, in particular, north wind. In accordance with the other measured data of three dimensional chlorophyll-a as well as seawater temperature, salinity, Dissolved Oxygen: DO, turbidity, ph ratio, etc., it shows that poor oxygen water mass appears at the bottom of the sea and then it raised up to the sea surface (accordingly, chlorophyll-a rich seawater raised from the bottom of the sea and raised up to the sea surface). Wind speed helps to convection of the sea surface water while sun shine time duration helps to increase chlorophyll-a concentration in conjunction of warm up of the sea surface temperature.

These relations are almost same for the other year of chlorophyll-a concentration. Correlation coefficients are calculated between chlorophyll-a concentration and the other data of tidal difference a day, sun shine time duration a day and wind speed from the north. The result shows that there is a strong relation between chlorophyll-a concentration and tidal difference a day, obviously followed by wind speed from the north as shown in Fig.8.

It is not always true. The situation may change by year by year. In particular, there is clear difference between year of 2011 and the other years, 2012 to 2015. One of the specific reasons for this is due to the fact that chlorophyll-a

concentration in 2011 is clearly greater than those of the other years. Therefore, clear relation between chlorophyll-a concentration and the other data of tidal difference a day, sun shine time duration a day and wind speed from the north cannot be seen. That is because of the fact that there is time delay of chlorophyll-a increasing after the nutrient rich bottom seawater is flown to the sea surface.
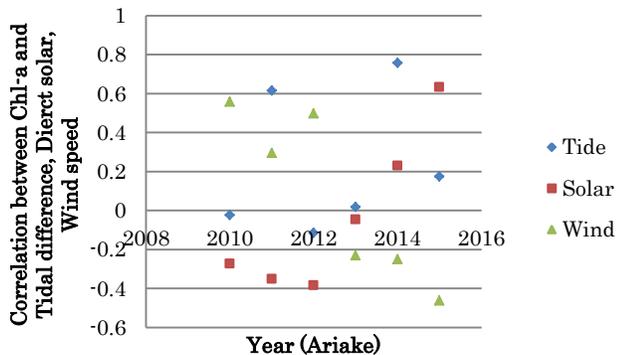
Fig. 8. Correlation coefficients between chlorophyll-a concentration and the other data of tidal difference a day, sun shine time duration a day and wind speed from the north

IV. CONCLUSION

Behavior of relatively large size of diatoms which appear in the Ariake Sea areas, Japan in winter based on remote sensing satellite data is clarified. Through experiments with Terra and AQUA MODIS data derived chlorophyll-a concentration and truth data of chlorophyll-a concentration together with meteorological data and tidal data which are acquired for 5 years (winter 2011 to winter 2015), it is found that strong correlation between the chlorophyll-a concentration and tidal height changes. Also it is found that the relations between ocean wind speed and chlorophyll-a concentration. Meanwhile, there is a relatively high correlation between sunshine duration a day and chlorophyll-a concentration.

An analysis on phytoplankton distribution changes monitoring for the intensive study area of the Ariake Sea, Japan based on remote sensing satellite data is conducted. Phytoplankton distribution changes in the Ariake Sea areas, Japan based on remote sensing satellite data is studied. Through experiments with Terra and AQUA MODIS data derived chlorophyll-a concentration and truth data of chlorophyll-a concentration together with meteorological data and tidal data which are acquired in January in 2011 to 2015, it is found that strong correlation between the truth data of chlorophyll-a and MODIS derived chlorophyll-a concentrations with R square value ranges from 0.677 to 0.791. Also it is found that the relations between ocean wind speed and chlorophyll-a concentration as well as between tidal difference a day and chlorophyll-a concentration. Meanwhile, there is a relatively high correlation between sunshine duration a day and chlorophyll-a concentration.

One of the knowledge raised from this study is the diatom appearance mechanism. The diatom appeared at the back in the Ariake Sea and is not flown from somewhere else. Also,

there is relatively low chlorophyll-a concentration sea areas between Isahaya bay area and the back in the Ariake Sea area. Therefore, chlorophyll-a concentration variations are isolated each other (Isahaya bay area and the back in the Ariake Sea area).

Further study is required for clarification of

1) the difference between 2011 and the other years, 2012 to 2015,

2) the reason why it is not always true that chlorophyll-a concentration get high on the spring tide while that get low on the neap,

3) some other mechanism for diatoms appearance is clarified,

4) three dimensional measurements of seawater temperature, salinity, turbidity, DO, ph, and chlorophyll-a concentration have to be made,

5) nutrition rich water current from the river mouths has to be taken into account,

6) interaction between relatively large size of diatoms and the other red tide species has to be clarified and is taken into account on the appearance mechanism studies.

REFERENCES

[1] Yuji Ito, Toshiya Katano, Naoki Fujii, Masumi Koriyama, Kenji Yoshino, and Yuichi Hayami, Decreases in turbidity during neap tides initiate late winter large diatom blooms in a macrotidal embayment, Journal of Oceanography,69: 467-479. 2013.

[2] Nishikawa T (2002) Effects of temperature, salinity and irradiance on the growth of the diatom *Eucampia zodiacus* caused bleaching seaweed *Porphyra* isolated from Harima-Nada, Seto Inland Sea, Japan. Nippon Suisan Gakk 68: 356–361. (in Japanese with English abstract)

[3] Nishikawa T (2007) Occurrence of diatom blooms and damage tocultured *Porphyra* thalli by bleaching. Aquabiology 172: 405–410. (in Japanese with English abstract)

[4] Nishikawa T, Hori Y (2004) Effects of nitrogen, phosphorus and silicon on the growth of the diatom *Eucampia zodiacus* caused bleaching of seaweed *Porphyra* isolated from Harima-Nada, Seto Inland Sea, Japan. Nippon Suisan Gakk 70: 31–38. (in Japanese with English abstract)

[5] Nishikawa T, Hori Y, Nagai S, Miyahara K, Nakamura Y, Harada K, Tanda M, Manabe T, Tada K (2010) Nutrient and phytoplankton dynamics in Harima-Nada, eastern Seto Inland Sea, Japan during a 35-year period from 1973 to 2007. Estuaries Coasts 33: 417–427.

[6] Nishikawa T, Hori Y, Tanida K, Imai I (2007) Population dynamics of the harmful diatom *Eucampia zodiacus* Ehrenberg causing bleachings of *Porphyra* thalli in aquaculture in Harima- Nada, the Seto Inland Sea, Japan. Harmful algae 6: 763–773.

[7] Nishikawa T, Miyahara K, Nagai S (2000) Effects of temperature and salinity on the growth of the giant diatom *Coscinodiscus wailesii* isolated from Harima-Nada, Seto Inland Sea, Japan. Nippon Suisan Gakk 66: 993–998. (in Japanese with English abstract)

[8] Nishikawa T, Tarutani K, Yamamoto T (2009) Nitrate and phosphate uptake kinetics of the harmful diatom *Eucampia zodiacus* Ehrenberg, a causative organism in the bleaching of aquacultured *Porphyra* thalii. Harmful algae 8: 513–517.

[9] Nishikawa T, Yamaguchi M (2006) Effect of temperature on lightlimited growth of the harmful diatom *Eucampia zodiacus* Ehrenberg,

a causative organism in the discoloration of *Porphyra* thalli. Harmful Algae 5: 141–147.

[10] Nishikawa T, Yamaguchi M (2008) Effect of temperature on lightlimited growth of the harmful diatom *Coscinodiscus wailesii*, a causative organism in the bleaching of aquacultured *Porphyra* thalli. Harmful Algae 7: 561–566.

[11] Syutou T, Matsubara T, Kuno K (2009) Nutrient state and nori aquaculture in Ariake Bay. Aquabiology 181: 168–170. (in Japanese with English abstract)

[12] Harada K, Hori Y, Nishikawa T, Fujiwara T (2009) Relationship between cultured *Porphyra* and nutrients in Harima-Nada, eastern part of the Seto Inland Sea. Aquabiology 181: 146–149. (in Japanese with English abstract)

AUTHORS PROFILE

Kohei Arai, He received BS, MS and PhD degrees in 1972, 1974 and 1982, respectively. He was with The Institute for Industrial Science and Technology of the University of Tokyo from April 1974 to December 1978 also was with National Space Development Agency of Japan from January, 1979 to March, 1990. During from 1985 to 1987, he was with Canada Centre for Remote Sensing as a Post Doctoral Fellow of National Science and Engineering Research Council of Canada. He moved to Saga University as a Professor in Department of Information Science on April 1990. He was a councilor for the Aeronautics and Space related to the Technology Committee of the Ministry of Science and Technology during from 1998 to 2000. He was a councilor of Saga University for 2002 and 2003. He also was an executive councilor for the Remote Sensing Society of Japan for 2003 to 2005. He is an Adjunct Professor of University of Arizona, USA since 1998. He also is Vice Chairman of the Commission "A" of ICSU/COSPAR since 2008. He wrote 33 books and published 500 journal papers. He is now the Editor-in-Chief of IJACSA and IJISA.

Realistic Rescue Simulation Method with Consideration of Road Network Restrictions

Kohei Arai 1

Graduate School of Science and Engineering
Saga University
Saga City, Japan

Takashi Eguchi [1]

Graduate School of Science and Engineering
Saga University
Saga City, Japan

Abstract—A realistic rescue simulation method with consideration of road network restrictions is proposed. Decision making and emergency communication system play important roles in rescue process when emergency situations happen. The rescue process will be more effective if we have appropriate decision making method and accessible emergency communication system. In this paper, we propose centralized rescue model for people with disabilities. The decision making method to decide which volunteers should help which disabled persons is proposed by utilizing the auction mechanism. The GIS data are used to present the objects in a large-scale disaster simulation environment such as roads, buildings, and humans. The Gama simulation platform is used to test our proposed rescue simulation model. There are road network restrictions, road disconnections, one way traffic, roads which do not allow U-Turn, etc. These road network restrictions are taken into account in the proposed rescue simulation model. The experimental results show around 10% of additional time is required for evacuation of victims.

Keywords—Rescue Simulation for people with disabilities; GIS MultiAgent-based Rescue Simulation; Auction based Decision Making

I. INTRODUCTION

In an emergency situation, a human tends to perform two main activities: the rescue and the evacuation. It is very difficult and costly if we want to do experiments on human rescue and or evacuation behaviors physically in real scale level. It is found that multi agent-based simulation makes it possible to simulate the human activities in rescue and evacuation process [1, 2]. A multi agent-based model is composed of individual units, situated in an explicit space, and provided with their own attributes and rules [3]. This model is particularly suitable for modeling human behaviors, as human characteristics can be presented as agent behaviors. Therefore, the multi agent-based model is widely used for rescue and evacuation simulation [1-5].

In this study, GIS map is used to model objects such as road, building, human, fire with various properties to describe the objects condition. With the help of GIS data, it enables the disaster space to be closer to a real situation [5-10]. Kisko et al. (1998) employs a flow based model to simulate the physical environment as a network of nodes. The physical structures, such as rooms, stairs, lobbies, and hallways are represented as nodes which are connected to comprise a evacuation space. This approach allows viewing the movement of evacuees as a continuous flow, not as an aggregate of persons varying in

physical abilities, individual dispositions and direction of movement [11]. Gregor et al. (2008) presents a large scale microscopic evacuation simulation. Each evacuee is modeled as an individual agent that optimizes its personal evacuation route. The objective is a Nash equilibrium, where every agent attempts to find a route that is optimal for the agent [12]. Fahy (1996; 1999) proposes an agent based model for evacuation simulation. This model allows taking in account the social interaction and emergent group response. The travel time is a function of density and speed within a constructed network of nodes and arcs [13, 14]. Gobelbecker et al. (2009) presents a method to acquire GIS data to design a large scale disaster simulation environment. The GIS data is retrieved from a public source through the website OpenStreetMap.org. The data is then converted to the Robocup Rescue Simulation system format, enabling a simulation on a real world scenario [15]. Sato et al. (2011) also proposed a method to create realistic maps using the open GIS data. The experiment shows the differences between two types of maps: the map generated from the program and the map created from the real data [2]. Ren et al. (2009) presents an agent-based modeling and simulation using Repast software to construct crowd evacuation for emergency response for an area under a fire. Characteristics of the people are modeled and tested by iterative simulation. The simulation results demonstrate the effect of various parameters of agents [3]. Cole (2005) studied on GIS agent-based technology for emergency simulation. This research discusses about the simulation of crowding, panic and disaster management [6]. Quang et al. (2009) proposes the approach of multi-agent-based simulation based on participatory design and interactive learning with experts' preferences for rescue simulation [9]. Hunsberger et al. (2000), Beatriz et al. (2003) and Chan et al. (2005) apply the auction mechanism to solve the task allocation problem in rescue decision making. Christensen et al. (2008) presents the BUMMPEE model, an agent-based simulation capable of simulating a heterogeneous population according to variation in individual criteria. This method allows simulating the behaviors of people with disabilities in emergency situation [23].

Our study will focus mainly on proposing a rescue model for people with disabilities in large scale environment. This rescue model provides some specific functions to help disabled people effectively when emergency situation occurs. Important components of an evacuation plan are the ability to receive critical information about an emergency, how to respond to an emergency, and where to go to receive assistance. We propose

a wearable device which is attached to body of disabled people. This device measures the condition of the disabled persons such as their heart rate, body temperature and attitude; the device can also be used to trace the location of the disabled persons by GPS. That information will be sent to emergency center automatically. The emergency center will then collect that information together with information from volunteers to assign which volunteer should help which disabled persons.

The rest of the paper is organized as follows. Section 2 describes the centralized rescue model and the rescue decision making method. Section 3 provides the experimental results of different evacuation scenarios. Finally, section 4 summarizes the work of this paper.

II. PROPOSED RESCUE SYSTEM

A. Proposed Rescue Model

Important components of an evacuation plan are the ability to receive critical information about an emergency, how to respond to an emergency, and where to go to receive assistance. We proposes a wearable device which is attached to body of disabled people. This device measures the condition of the disabled persons such as their heart rate, body temperature and attitude; the device can also be used to trace the location of the disabled persons by GPS. Those information will be sent to emergency center automatically. The emergency center will then collect those information together with information from volunteers to assign which volunteer should help which disabled persons. The centralized rescue model presented has three types of agents: volunteers, disabled people and route network. The route network is also considered as an agent because the condition of traffic in a certain route can be changed when a disaster occurs. The general rescue model is shown in Figure 1.
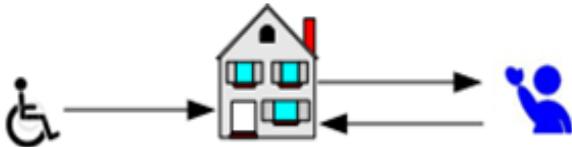
Fig. 1.   Centralized Rescue Model

Before starting the simulation, every agent has to be connected to the emergency center in order to send and receive information. The types of data exchanged between agents and emergency center are listed as below.

Message from agent
A1: To request for connection to the emergency center
A2: To acknowledge the connection
A3: Inform the movement to another position
A4: Inform the rescue action for victim
A5: Inform the load action for victim
A6: Inform the unload action for victim
A7: Inform the inactive status
Message from emergency center
K1: To confirm the success of the connection
K2: To confirm the failure of the connection
K3: To send decisive information

Before starting the simulation, every agent will send the command A1 to request for connection to the emergency center. The emergency center will return the response with a command K1 or K2 corresponding to the success or failure of their connection respectively. If the connection is established, the agent will send the command A2 to acknowledge the connection. The initial process of simulation is shown in Figure 2.
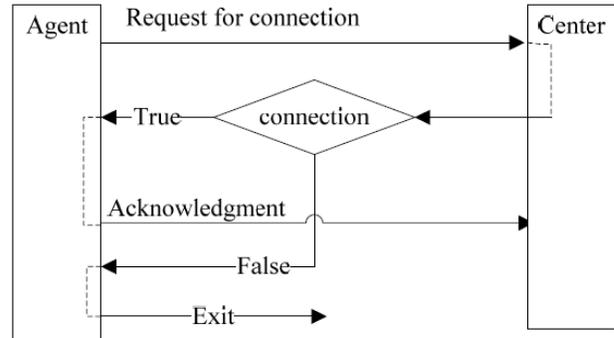
Fig. 2.   Initial Process

After the initial process, all the connected agents will receive the decisive information such as the location of agents and health level via command K3; after that the rescue agents will make a decision of action and submit to the center using one of the commands from A3 to A7. At every cycle in the simulation, each rescue agent receives a command K3 as its own decisive information from the center, and then submits back an action command. The status of disaster space is sent to the viewer for visualization of simulation. The repeating steps of simulation are shown in Figure 3.
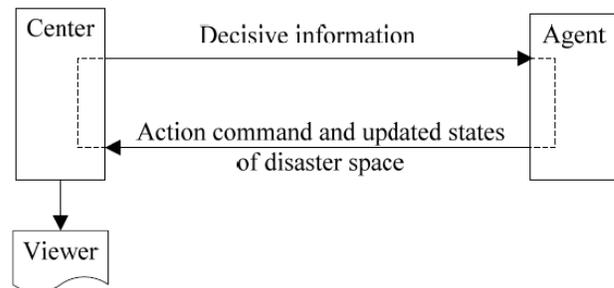
Fig. 3.   Simulation Cycles

B. Disaster Area Model

The disaster area is modeled as a collection of objects: Nodes, Buildings, Roads, and Humans. Each object has properties such as its positions, shape and is identified by a unique ID. Table 1 to Table 7 presents the properties of Nodes,

Buildings, Roads and Humans object respectively. These properties are derived from RoboCup rescue platform with some modifications.

The topographical relations of objects are illustrated from Figure 4 to Figure 7. The representative point is assigned to every object, and the distance between two objects is calculated from their representative points.

TABLE I.   PROPERTIES OF NODE OBJECT

Property	Unit	Description
x,y	–	x-yCordinate
Edges	ID	Connected_road_and_Building

TABLE II.   PROPERTIES OF BUILDING OBJECT

Property	Description
x,y	x-y coordinate of the representative point
Entrance	Node_connecting_building_and_road

TABLE III.   PROPERTIES OF ROAD OBJECT

Property	Unit	Description
Start_Point_and_End_Point	ID	Point_to_enter_the_Road_
Length_and_Width	m	Length_and_width_of_Road
Lane	Lane	Number_of_lanes
Blocked_road	Lane	Number_of_blocked_lanes
Clear_Cost	Cycle	Cost_required_for_clearing_blocks

TABLE IV.   PROPERTIES OF VICTIM AGENT

Property	Unit	Description
Position	ID	Object_where_victim_is_on
Position_in_road	m	Lecgth_from_Start_Point_when_victim_is_on_road,_Otherwise_it_is_zero
Health_Level	Health_Point	Health_level_of_victim
Damage_Point	Health_Point	Health_level_dwindles_by_Damage
Disability_Type	Type(1-7)	Disability_types
Disability_Level	High_or_Low	High_disability_level_means_Highest_Damage_Point

TABLE V.   PROPERTIES OF VOLUNTEER AGENT

Property	Unit	Description
Position_on_road	ID	Object=that_victim_is_on
Position_on_road	m	Length_from_Start_Point
Current_Action	Type(1-3)	See_in_Table_VII
Energy	Level(1-5)	Empty_level_of_vehicle_gasoline
Panic_Level	Level(0-9)	Hesitance_level_of_decision

TABLE VI.   ACTION OF VOLUNTEER AGENT

Action_ID	Action	Description
1	Stationary	Rescue_person_Stays
2	Move_to_Victim	Rescue_person_moves_to_victim
3	Move_to_Shelter	Rescue_person_carry_victim_to_shelter

TABLE VII.   TYPE OF DISABILITY

Type	Description
1	Cognitive_Impaiment
2	Dexterity_Impairment
3	Mobility_Impairment
4	Elderly
5	Hearing_Impairment
6	Speech_and_Language_Impairment
7	Visdual_Impairment
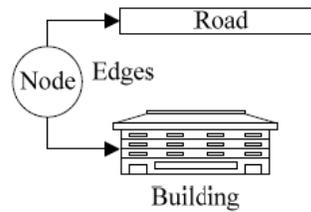
Fig. 4.   Node object
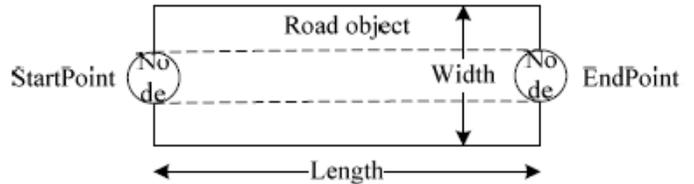
Fig. 5.   Road object
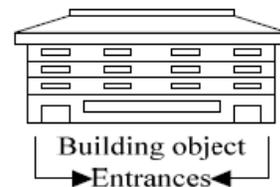
Fig. 6.   Building object
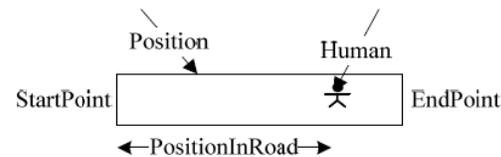
Fig. 7.   Human object

C. Path finding in Gama Simulation Platform

After a volunteer makes the decision to help a certain victim, the path finding algorithm is used to find the route from volunteer agent to victim agent. The GIS data presents roads as a line network in graph type. Figure 8 shows an example of graph computation. The Dijkstra algorithm is implemented for the shortest path computation [8].

In this section, we present experimental studies on different scenarios. We show the experimental results with traditional rescue model which not considering the updated information of victims and volunteers such as health conditions, locations, traffic conditions.
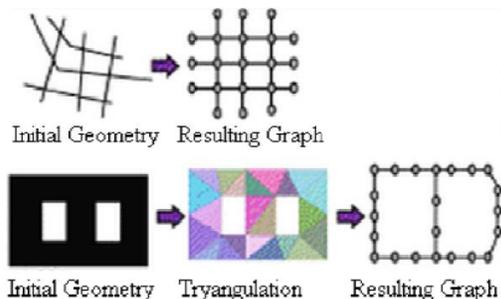
Fig. 8.   Example of Graph Computation [8]

The traditional rescue model provides fixed mission for which volunteers should help which victims. Whereas, our rescue model provides flexible mission for which volunteers should help which victims. The targets of volunteers can be changed dynamically according to current situation. The experimental results of our proposed rescue model are also presented to show the advantages comparing to traditional model.

The evacuation time is evaluated from the time at which the first volunteer started moving till the time at which all saved victims arrive at the shelters. The simulation model is tested using the Gama simulation platform [8, 10].

We consider the number of volunteers, number of disabled persons, panic level of volunteer, disability level of victim and the complexity of traffic as parameters to examine the correlation between these parameters with rescue time. The traffic complexity is function of the number of nodes and links in a road network.

Figure 9 presents the sample GIS map consisting of 4 layers: road, volunteer, disabled person and shelter. The initial health levels of disabled persons are generated randomly between 100 point and 500 point. If the health level is equal or less than zero, the corresponding agent is considered as dead.
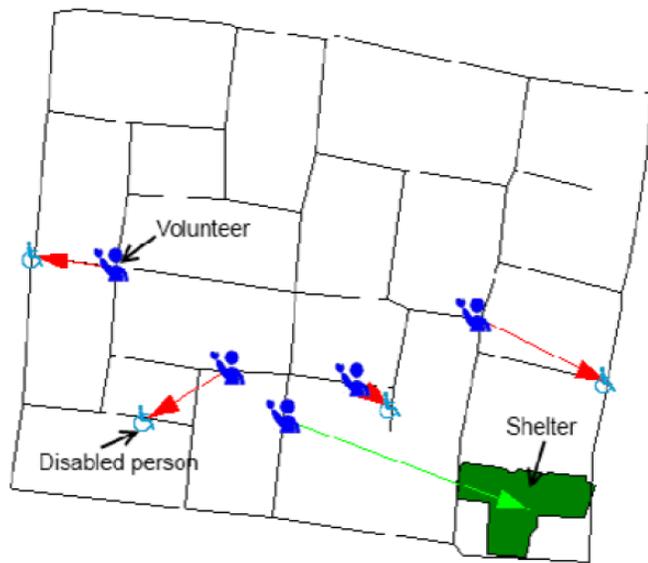
Fig. 9. Sample GIS Map of Disaster Space

D. Realistic Simulation Designating to Saga City, Japan

Figure 10 (a) shows the rescue simulation site which is situated at Saga University and the surrounding areas. The shelter around this site is Saga University. Meanwhile, Figure 10 (b) shows road network and locations of victims and rescue peoples as initial conditions. At the top right corner, entrance gate is situated at the shelter.
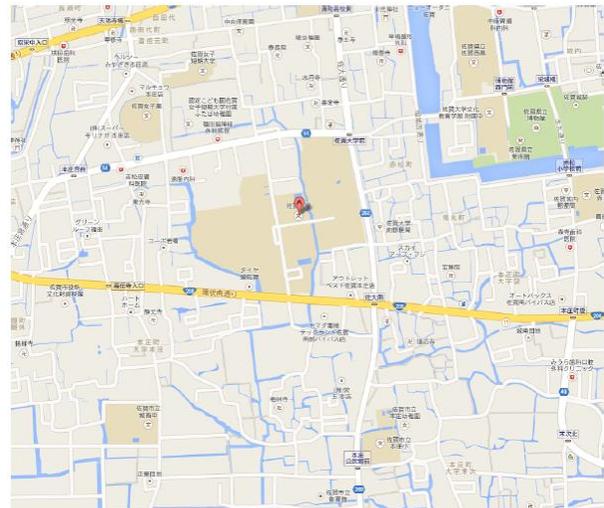
(a)Topographic map of the rescue simulation site
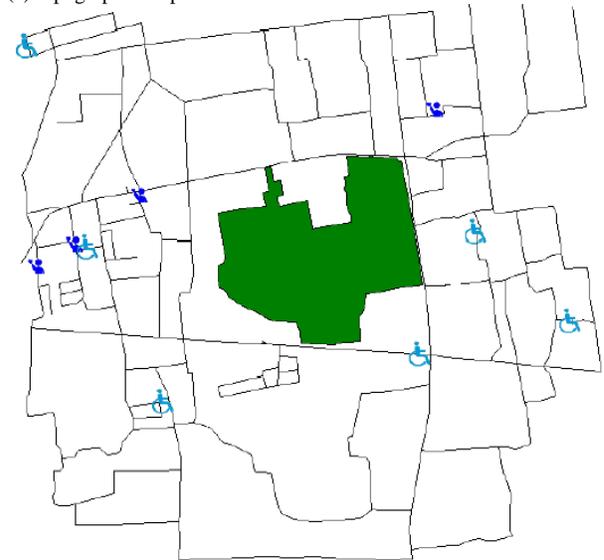
(b)Road network of the rescue simulation site

Fig. 10. Rescue simulation site of Saga University and its surrounding areas

III. EXPERIMENTS

Simulations are conducted with the aforementioned initial conditions on the road network. There are two victims. ①The rescue person goes the victim #1, firstly, and ②,③he goes to the victim #2 after that. Then he goes to the shelter together with the victims #1 and #2. It is expected the rescue route length would be 4.34 km and the expected rescue time would be 10 min. and 40 sec. as shown in Figure 11 (a). Figure 11 (b) shows the route for rescue the victim #3. In this case, the number of rescue victims is just one. Therefore, the route length is 2.66 km and it takes 5 min. and 16 sec. Another possible route for rescue the victim #4 is shown in Figure 11 (c). There is only one victim. Therefore, the route length is 2.36 km and the time required for rescue is 4min. and 18 sec.
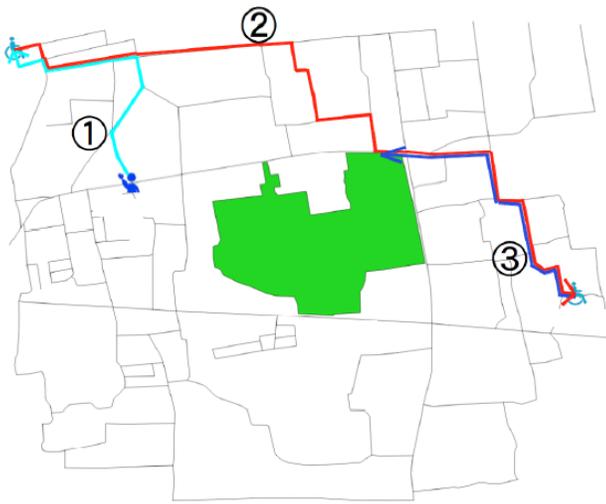
(a)Possible route for rescue the victims #1 and #2
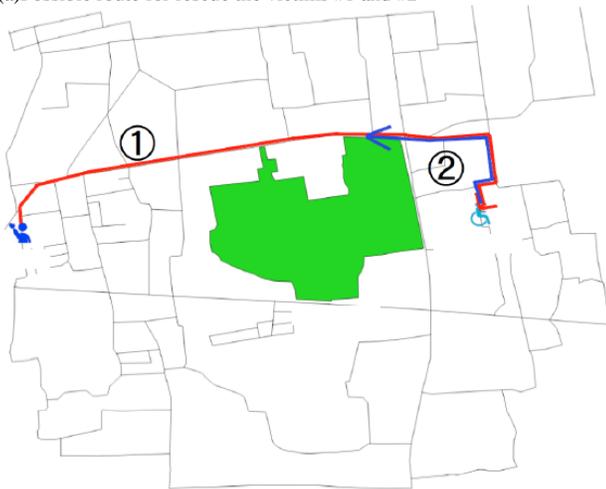
(b)Possible route for rescue the victim #3
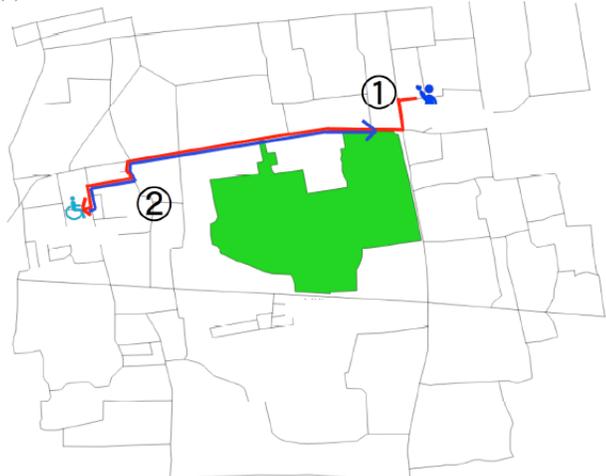
(c)Possible route for rescue the victim #4
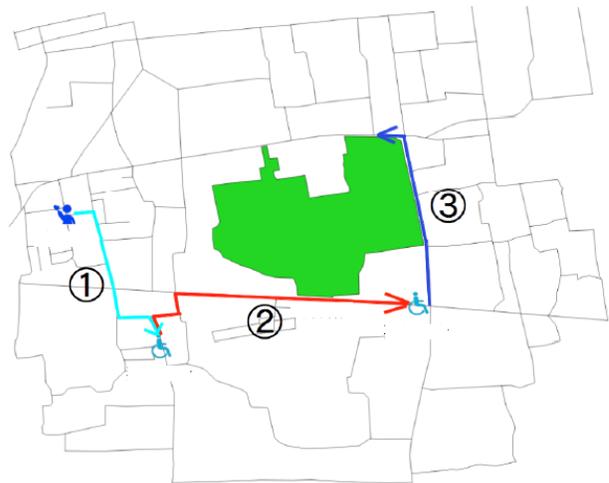
(d)Possible route for rescue the victims #5 and #6

Fig. 11. Possible routes for rescue the victims #1-#6

On the other hand, the possible route for rescue the victim #5 and #6 is shown in Figure 11 (d). In this case, the number of victims is two for the rescue person. The route length is 2.385 km and it takes 6 min. and 20 sec. The time required for rescue for each case is summarized in Table 8. These are simulation results. The experiments are conducted in real world twice. The time required for rescue is shown in Table 9 (the first trial) and 10 (the second trial).

TABLE VIII.   THE TIME REQUIRED FOR RESCUE (SIMULATION)

	Rescue A	Rescue B	Rescue C	Rescue D
First victim	2:26	3:58	2:50	2:10
Second victim	8:00	---	---	4:18
Rescue time	10:40	5:16	4:18	6:20

TABLE IX.   THE TIME REQUIRED FOR RESCUE (REAL WORLD TRIAL #1)

	Rescue A	Rescue B	Rescue C	Rescue D
First victim	2:56	5:36	3:36	2:36
Second victim	11:41	---	---	6:10
Rescue time	16:54	7:47	6:37	8:37

TABLE X.   THE TIME REQUIRED FOR RESCUE (REAL WORLD TRIAL #2)

	Rescue A	Rescue B	Rescue C	Rescue D
First victim	1:45	5:54	4:12	1:49
Second victim	10:22	---	---	4:51
Rescue time	14:57	8:13	6:59	7:13

Most of the rescue simulation software does not care about the one way roads and the roads of which u-turn is impossible. There, however, are one way traffic roads and the u-turn impossible roads in the real world situation. Therefore, it takes much time for rescue when these realistic road conditions are taken into account in comparison to the simulations and the experiments which do not taken into account the conditions.

Figure 12 (a) shows an example of the one way traffic road in Saga city. Black cross mark shows one way traffic road from right to left. Therefore, the rescue person cannot take this one way traffic road (Figure 12 (b)). On behalf of this road, the rescue person takes another alternative road (Second shortest pass shown in Figure 12(c)). On the other hand, there are narrow roads of which u-turn cannot be done as is shown in Figure 13. Figure 13 (a) shows the route for conventional rescue simulation result while Figure 13 (b) shows the route for the proposed rescue simulation. Due to the fact that the road is narrow which does not allow make any u-turn, the rescue person have to take the alternative route of Figure 13 (b). As the results of these considerations on the proposed rescue simulation, the rescue person A, B, C, D takes the rescue time and the route length which are shown in Table 11. Meanwhile, Table 12 shows rescue time in the case of the considerations of one way traffic road and u-turn impossible road in the proposed rescue simulation. On the other hand, Table 13 shows effects of rescue time increasing in the case of the considerations of one way traffic road and u-turn impossible road in the proposed rescue simulation. In case of the consideration of one way traffic road and u-turn impossible road, the alternative route of the second shortest pass has to be taken. Therefore, rescue time is increased.

simulation-

TABLE XI. THE TIME REQUIRED FOR RESCUE AND THE ROUTE LENGTH

	Rescue A	Rescue B	Rescue C	Rescue D
Route length	4.34	2.66	2.36	2.38
Rescue time	2'26"	3'58"	2'50"	2'10"

TABLE XII. RESCUE TIME IN THE CASE OF THE CONSIDERATIONS OF ONE WAY TRAFFIC ROAD AND U-TURN IMPOSSIBLE ROAD IN THE PROPOSED RESCUE SIMULATION

	Rescue A	Rescue B	Rescue C	Rescue D
First Victim	2'35"	4'10"	3'40"	2.10
Second victim	9'14"	---	---	4'30"
Overall Rescue time	12'15"	5'44"	6'1"	6'50"

TABLE XIII. EFFECT OF THE CONSIDERATIONS OF ONE WAY TRAFFIC ROAD AND U-TURN IMPOSSIBLE ROAD IN THE PROPOSED RESCUE SIMULATION

	Rescue A	Rescue B	Rescue C	Rescue D
First Victim	+9"	+12"	+50"	0"
Second victim	+1'14"	---	---	+12"
Overall Rescue time	+1'35"	+28"	+1'43"	+30"

It is much hard to pass the route if the road is much narrow road which is shown in Figure 14. Figure 14 (a) shows the photo of the narrow road while Figure 14 (b) shows the narrow road on the topographic map.

In such case, it is better to take another alternative much wider road than the narrow road from the rescue time point of view. Therefore, it is better to take the route #2 (Figure 15 (b)) rather than the route #1 (Figure 15 (a)).

(a)One way traffic road

(b)Shortest pass   (c)Second shortest pass

Fig. 12. Consideration of one way traffic road in the proposed rescue simulation

(a)U-turn traffic road   (b)Alternative route
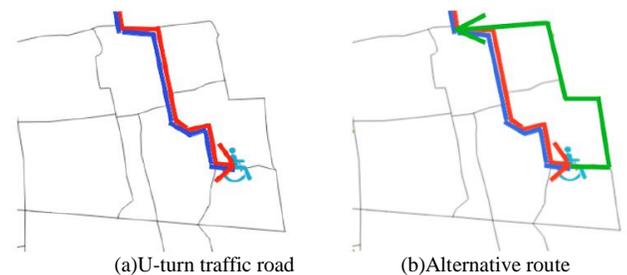
Fig. 13. Consideration of U-turn impossible roads in the proposed rescue

(a)Photo of the narrow road   (b)The narrow road on map
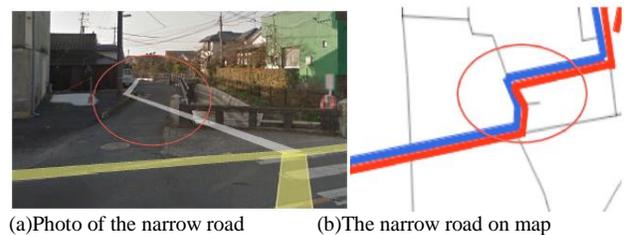
Fig. 14. Consideration of the narrow road in the proposed rescue simulation
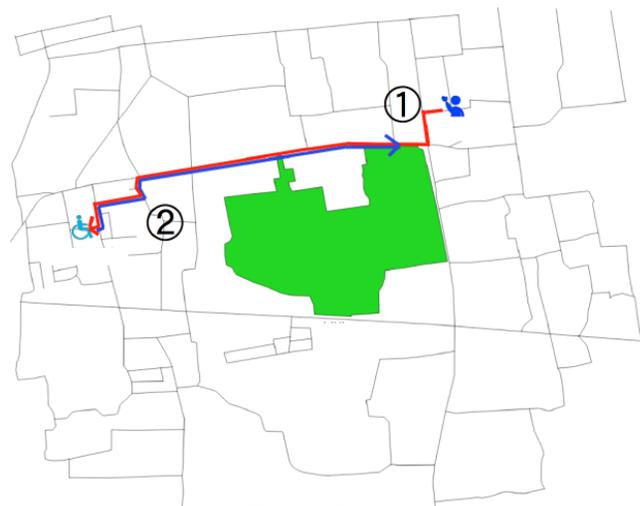
(a)Route #1
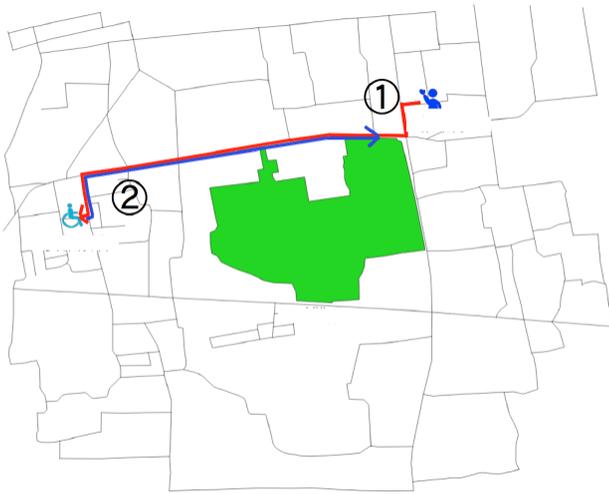
(b)Route #2

Fig. 15. Consideration of priority of wide roads rather than narrow roads in the proposed rescue simulation

Meanwhile, there are the routes which take much longer time for crossing very wide boulevards than narrow roads as shown in Figure 16. Figure 16 (a) shows an example of photo of the route which takes much longer time for crossing very wide boulevard than narrow roads while Figure 16 (b) shows the route which takes much longer time for crossing very wide boulevard than narrow roads on map.
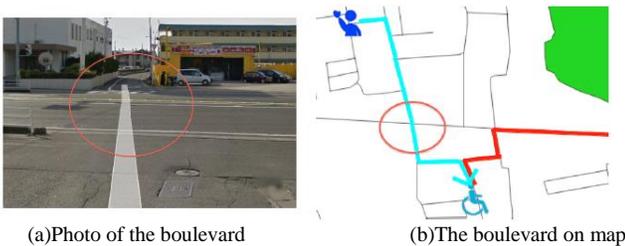
(a)Photo of the boulevard   (b)The boulevard on map

Fig. 16. Routes which take much longer time for crossing very wide boulevards than narrow roads

IV. Conclusion

A realistic rescue simulation method with consideration of road network restrictions is proposed. Decision making and emergency communication system play important roles in rescue process when emergency situations happen. The rescue process will be more effective if we have appropriate decision making method and accessible emergency communication system.

In this paper, we propose centralized rescue model for people with disabilities. The decision making method to decide which volunteers should help which disabled persons is proposed by utilizing the auction mechanism. The GIS data are used to present the objects in a large-scale disaster simulation environment such as roads, buildings, and humans.

The Gama simulation platform is used to test our proposed rescue simulation model. There are road network restrictions, road disconnections, one way traffic, roads which do not allow U-Turn, etc. These road network restrictions are taken into account in the proposed rescue simulation model.

The experimental results show around 10% of additional time is required for evacuation of victims in maximum. In order to reduce rescue time, considerations of priority of wide roads rather than narrow roads in the proposed rescue simulation are taking into account.

References

[1] Obelbecker G., & Dornhege M., "Realistic cities in simulated environments - an Open Street Map to Robocup Rescue converter", Online-Proceedings of the Fourth International Workshop on Synthetic Simulation and Robotics to Mitigate Earthquake Disaster, 2009.

[2] Sato, K., & Takahashi, T., "A study of map data influence on disaster and rescue simulation's results", Computational Intelligence Series, vol. 325. Springer Berlin / Heidelberg, 389–402, 2011.

[3] Ren C., Yang C., & Jin S., "Agent-Based Modeling and Simulation on emergency", Complex 2009, Part II, LNICST 5, 1451 – 1461, 2009.

[4] Zaharia M. H., Leon F., Pal C., & Pagu G., "Agent-Based Simulation of Crowd Evacuation Behavior", International Conference on Automatic Control, Modeling and Simulation, 529-533, 2011.

[5] Quang C. T., & Drogoul A., "Agent-based simulation: definition, applications and perspectives", Invited Talk for the biannual Conference of the Faculty of Computer Science, Mathematics and Mechanics, 2008.

[6] Cole J. W., Sabel C. E., Blumenthal E., Finnis K., Dantas A., Barnard S., & Johnston D. M., "GIS-based emergency and evacuation planning for volcanic hazards in New Zealand", Bulletin of the New Zealand society for earthquake engineering, vol. 38, no. 3, 2005.

[7] Batty M., "Agent-Based Technologies and GIS: simulating crowding, panic, and disaster management", Frontiers of geographic information technology, chapter 4, 81-101, 2005.

[8] Patrick T., & Drogoul A., "From GIS Data to GIS Agents Modeling with the GAMA simulation platform", TF SIM 2010.

[9] Quang C. T., Drogoul A., & Boucher A., "Interactive Learning of Independent Experts' Criteria for Rescue Simulations", Journal of Universal Computer Science, Vol. 15, No. 13, 2701-2725, 2009.

[10] Taillandier T., Vo D. A., Amouroux E., & Drogoul A., "GAMA: a simulation platform that integrates geographical information data, agentbased modeling and multi-scale control", In Proceedings of Principles and practice of multi-agent systems, India, 2012.

[11] Kisko, T.M., Francis, R.L., Nobel C.R., "EVACNET4 User's Guide", University of Florida, 1998.

[12] Gregor, Marcel R., & Nagel K., "Large scale microscopic evacuation simulation", Pedestrian and Evacuation Dynamics, 547-553, 2008.

[13] Fahy R. F., "User's Manual, EXIT89 v 1.01, An Evacuation Model for High-Rise Buildings, National Fire Protection Association", Quincy, Mass, 1999.

[14] Fahy R. F., "EXIT89 – High-Rise Evacuation Model –Recent Enhancements and Example Applications" Interflam '96, International Interflam Conference – 7th Proceedings; Cambridge, England, pg. 1001-1005, 1996.

[15] Gobelbecker M., & Dornhege C., "Realistic cities in simulated environments- an open street map to RoboCup Rescue converter". In 4th Int'l Workshop on Synthetic Simulation and Robotics to Mitigate Earthquake Disaster (SRMED 2009), Graz, Austria, July 2009.

[16] Nair R., Ito T., Tambe M., & Marsella S., "Task allocation in the rescue simulation domain: A short note", Volume 2377 of Lecture Notes in Computer Science. Springer, Berlin 751–754, 2002.

[17] Boffo F., Ferreira P. R., & Bazzan A. L., "A comparison of algorithms for task allocation in robocup rescue", Proceedings of the 5th European workshop on multiagent systems, 537–548, 2007.

[18] Hunsberger L.,& Grosz B., "A combinatorial auction for collaborative planning", Proceedings of the fourth international conference on multiagent systems, 2000.

[19] Beatriz L., Silvia S., & Josep L., "Allocation in rescue operations using combinatorial auctions", Artificial Intelligence Research and Development, Vol. 100, 233-243, 2003.

[20] Chan C. K., & Leung H. F., "Multi-auction approach for solving task allocation problem", Lecture Notes in Computer Science, Vol 4078,

240-254, 2005.

[21] Sandholm T., "Algorithm for optimal winner determination in combinatorial auctions", Artificial Intelligence, Vol 135, 1-54, 2002.

[22] Arai K., & Sang T. X., "Multi Agent-based Rescue Simulation for Disable Persons with the Help from Volunteers in Emergency Situations", International Journal of Research and Reviews in Computer Science, Vol. 3, No. 2, April 2012.

[23] Arai K., & Sang T. X., "Fuzzy Genetic Algorithm for Prioritization Determination with Technique for Order Preference by Similarity to Ideal Solution", International Journal of Computer Science and Network Security, Vol. 11, No. 5, pp. 229-235, May 2011.

[24] Christensen K. M., & Sasaki Y., "Agent-Based Emergency Evacuation Simulation with Individuals with Disabilities in the Population", Journal of Artificial Societies and Social Simulation 11(3)9, 2008.

AUTHORS PROFILE

Kohei Aarai He received BS, MS and PhD degrees in 1972, 1974 and 1982, respectively. He was with The Institute for Industrial Science and Technology of the University of Tokyo from April 1974 to December 1978 and also was with National Space Development Agency of Japan from January, 1979 to March, 1990. During from 1985 to 1987, he was with Canada Centre for Remote Sensing as a Post Doctoral Fellow of National Science and Engineering Research Council of Canada. He moved to Saga University as a Professor in Department of Information Science on April 1990. He was a councilor for the Aeronautics and Space related to the Technology Committee of the Ministry of Science and Technology during from 1998 to 2000. He was a councilor of Saga University for 2002 and 2003. He also was an executive councilor for the Remote Sensing Society of Japan for 2003 to 2005. He is an Adjunct Professor of University of Arizona, USA since 1998. He also is Vice Chairman of the Commission-A of ICSU/COSPAR since 2008. He wrote 33 books and published 500 journal papers.

Relation between Rice Crop Quality (Protein Content) and Fertilizer Amount as Well as Rice Stump Density Derived from Helicopter Data

Kohei Arai 1
Graduate School of Science and Engineering
Saga University
Saga City, Japan

Osamu Shigetomi [2]
Saga Prefectural Agricultural Research Institute
Saga Prefectural Government, Japan

Masanoori Sakashita [1]
Information Science, Saga University
Saga, Japan

Yuko Miura [2]
Saga Prefectural Agricultural Research Institute
Saga Prefectural Government, Japan

Abstract—**Relation between protein content in rice crops and fertilizer amount as well as rice stump density is clarified with a multi-spectral camera data mounted on a radio-wave controlled helicopter. Estimation of protein content in rice crop and total nitrogen content in rice leaves through regression analysis with Normalized Difference Vegetation Index: NDVI derived from camera mounted radio-controlled helicopter is already proposed. Through experiments at rice paddy fields which is situated at Saga Prefectural Research Institute of Agriculture: SPRIA in Saga city, Japan, it is found that total nitrogen content in rice leaves is linearly proportional to fertilizer amount and NDVI. Also, it is found that protein content in rice crops is positively proportional to fertilizer amount for lower fertilizer amount while protein content in rice crop is negatively proportional to fertilizer amount for relatively high fertilizer amount.**

Keywords—Rice Crop; Rice Leaf; Total nitrogen content; Protein content; NDVI; Fertilizer amount; Rice stump density

I. INTRODUCTION

Vitality monitoring of vegetation is attempted with photographic cameras [1]. Grow rate monitoring is also attempted with spectral reflectance measurements [2]. Bi-Directional Reflectance Distribution Function: BRDF is related to the grow rate for tealeaves [3]. Using such relation, sensor network system with visible and near infrared cameras is proposed [4]. It is applicable to estimate total nitrogen content and fiber content in the tealeaves in concern [5]. Therefore, damage grade can be estimated with the proposed system for rice paddy fields [6]. This method is validated with Monte Carlo simulation [7]. Also Fractal model is applied to representation of shapes of tealeaves [8]. Thus the tealeaves can be asse3ssed with parameters of the fractal model. Vitality of tea trees are assessed with visible and near infrared camera data [9]. Rice paddy field monitoring with radio-control helicopter mounting visible and NIR camera is proposed [10] while the method for rice quality evaluation through total nitrogen content in rice leaves is also proposed [10]. The method which allows evaluation of rice quality with protein content in rice crop estimated with NDVI1 which is acquired with visible and NIR camera mounted on radio-control helicopter is also proposed [10]. The fact that protein content in rice crops is highly correlated with NDVI which is acquired with visible and Near Infrared: NIR camera mounted on radio-control helicopter is well reported [10]. It also is reported that total nitrogen content in rice leaves is correlated to NDVI as well.

Protein content in rice crop is negatively proportional to rice taste. Therefore, rice crop quality can be evaluated through NDVI observation of rice paddy field. Relation among total nitrogen content in rice leaves, amount of fertilizer amount, NDVI and protein content in rice crops as well as stump density has to be clarified in this paper.

The proposed method is described in the next section followed by experiments. The experimental results are validated in the following section followed by conclusion with some discussions.

II. PROPOSED METHOD FOR ESTIMATION OF PROTEIN CONTENT IN RICE CROPS

A. Radio Controlled Helicopter Based Near Infrared Cameras Utilizing Agricultural Field Monitoring System

The helicopter used for the proposed system is "GrassHOPPER" [2] manufactured by Information & Science Techno-Systems Co. Ltd. The major specification of the radio controlled helicopter used. Canon Powershot S1002 [3] (focal length=24mm) is mounted on the GrassHOPPER. It allows acquire images with the following Instantaneous Field of

---

[1] Normalized Difference Vegetation Index: NDVI is expressed with the following equation,
NDVI=(NIR-R)/(NIR+R)
where NIR, R denotes Near Infrared and Red wavelength region of reflectance
[2] http://www.ists.co.jp/?page_id=892
[3] http://cweb.canon.jp/camera/dcam/lineup/powershot/s110/index.html

View: IFOV at the certain altitudes, 1.1cm (Altitude=30m）

3.3cm (Altitude=100m）and 5.5cm（Altitude=150m）.

Spectral response functions of filters attached to the camera used are sensitive to Green, Red and Near Infrared bands.

In order to measure NIR reflectance, standard plaque whose reflectance is known is required. Spectralon[4] provided by Labsphere Co. Ltd. is well known as well qualified standard plaque. It is not so cheap that photo print papers are used for the proposed system. Therefore, comparative study is needed between Spectralon and the photo print papers.

The system consist Helicopter, NIR camera, photo print paper. Namely, photo print paper is put on the agricultural plantations, rice leaves in this case. Then farm areas are observed with helicopter mounted Visible and NIR camera. Total nitrogen content in rice leaves, protein content in rice crops can be estimated with the camera data based on the previously established regressive equation [12].

B. Rice Paddy Field at Saga Prefectural Agricultural Research Institute: SPARI

Specie of the rice crop is Hiyokumochi[4] which is one of the late growing types of rice species. Hiyokumochi[5] is one of low amylase (and amylopectin rich) of rice species (Rice No.216).

Paddy fields of the test site of rice paddy field at SPARI[6] which is situated at 33°13'11.5" North, 130°18'39.6"East, and the elevation of 52 feet. The paddy field C4-2 is for the investigation of water supply condition on rice crop quality. There are 14 of the paddy field subsections of which water supply conditions are different each other.

There are two types of water supply scheduling, short term and standard term. Water supply is stopped in the early stage of rice crop growing period for the short term water supply subsection fields while water supply is continued comparatively longer time period comparing to the short term water supply subsection fields.

Meanwhile, there are three types of water supply conditions, rich, standard, and poor water supply subsection fields. On the other hand, test sites C4-3 and C4-4 are for investigation of total nitrogen of chemical fertilizer amount dependency on rice crop quality. There are two types of paddy subsections, densely and sparsely planted paddy fields. Hiyokumochi rice leaves are planted 15 to 20 fluxes per m2 on June 22 2012. Rice crop fields are divided into 10 different small fields depending on the amount of nutrition including total nitrogen ranges from zero to 19 kg/10 a/total nitrogen.

Total nitrogen of chemical fertilizer amount is used to put into paddy fields for five times during from June to August. Although rice crops in the 10 different small fields are same

species, the way for giving chemical fertilizer amount are different. Namely, the small field No.1 is defined as there is no chemical fertilizer amount at all for the field while 9, 11, and 13 kg/10a/ total nitrogen of after chemical fertilizer amount are given for No.2 to 4, respectively, no initial chemical fertilizer amount though. Meanwhile, 9, 11, 13 kg/10 a/total nitrogen are given as after chemical fertilizer amount for the small field No.5, 6, and 7, respectively in addition to the 3 kg/10 a/total nitrogen of initial chemical fertilizer amount. On the other hand, 12, 14, and 16 kg/10 a /total nitrogen are given for the small fields No.5, 6, 7, respectively as after chemical fertilizer amount in addition to the initial chemical fertilizer amount of 3 kg/ 10 a/ total nitrogen for the small field No. 15, 17, 19, respectively. Therefore, rice crop grow rate differs each other paddy fields depending on the amount of total nitrogen of chemical fertilizer amount.

III. Experiments

A. Acquired Near Infrared Camera Imagery Data

Radio wave controlled helicopter mounted near infrared camera imagery data is acquired at C4-2, C4-3, C4-4 in SPARI on 18 and 22 August 2013 with the different viewing angle from the different altitudes. In the acquired camera images, there is Spectralon of standard plaque as a reference of the measured reflectance in between C4-3 and C4-4. Just before the data acquisition, some of rice crops and leaves are removed from the subsection of paddy fields for inspection of total nitrogen content in rice leaves. Using the removed rice leaves, total nitrogen content in rice leaves is measured based on the Keldar method and Dumas method[7] (a kind of chemical method) with Sumigraph NC-220F[8] of instrument. The measured total nitrogen content in rice leaves and protein content in rice crops are compared to the NDVI.

The camera images are acquired on 18 August and 22 August. Meanwhile, these images have influences due to shadow and shade of rice leaves and water situated under the rice leaves as well as narrow roads between rice paddy fields. In order to eliminate the influences, thresholding process is applied to the acquired images.

Measured total nitrogen contents in rice leaves of rice paddy fields of partitioned A1 to A8 and B1 to B8 on 14 and 22 August 2013 are shown in Table 1 and 2, respectively.

Before estimation of total nitrogen content in rice leaves, geometric correction is applied to the acquired camera image after extraction of intensive study areas. Also it is found that total nitrogen of chemical fertilizer amount; water management as well as plant density is different from each other partitioned rice paddy fields as aforementioned.

B. Total nitrogen Content in Rice Leaves

Total nitrogen content in the rice leaves seem to reflect the fact of chemical fertilizer amount of total nitrogen, water supply management, and plantation density, obviously. Fig.1 shows the relation between fertilizer amount and total nitrogen content in the rice leaves.

---

[4] http://www.labsphere.com/products/reflectance-standards-and-targets/reflectance-targets/spectralon-targets.aspx
[5] http://ja.wikipedia.org/wiki/%E3%82%82%E3%81%A1%E7%B1%B3
[6] http://www.pref.saga.lg.jp/web/shigoto/_1075/_32933/ns-nousisetu/nouse/n_seika_h23.html

[7] http://note.chiebukuro.yahoo.co.jp/detail/n92075
[8] http://www.scas.co.jp/service/apparatus/elemental_analyzer/sumigraph_nc-220F.html

TABLE I.   MEASURED TOTAL NITROGEN CONTENT IN RICE LEAVES ON 14 AUGUST 2013

Farm Area	Total nitrogen (%)
A1	2.61
A3	2.85
A5	2.84
A8	2.77
B1	2.82
B3	2.74
B5	3.16
B8	2.78

TABLE II.   MEASURED TOTAL NITROGEN CONTENT IN RICE LEAVES ON 22 AUGUST 2013

Farm Area	Total nitrogen (%)
A1	2.46
A2	2.88
A4	2.97
A5	2.89
A6	2.67
A8	3.22
B1	2.33
B2	2.79
B4	2.84
B5	2.85
B6	2.96
B8	3.14

(a)Overall

(b)Rice field A

(c)Rice field A
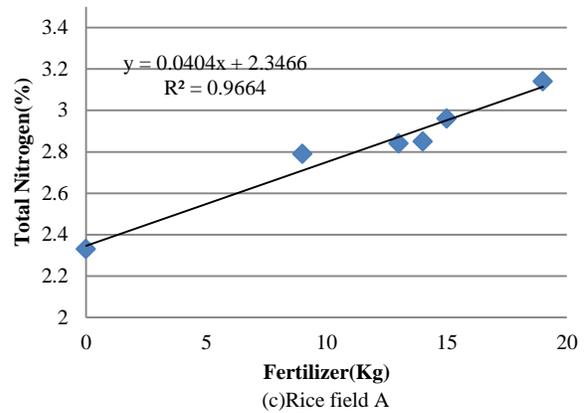
Fig. 1.   Relation between fertilizer amount and total nitrogen content in the rice leaves

The chemical fertilizer amount is put into paddy fields four times. Fertilizer amount denotes total chemical fertilizer amount. Fig.1 (a) shows overall relation between fertilizer amount and total nitrogen content in the rice leaves while Fig.1 (b) and (c) shows the relation for measured total nitrogen content in rice leaves on August 18 and August 22, respectively. Rice crops are harvested in the begging of October. Therefore, rice crops and rice leaves are grown up a little bit for four days. These figures show the proportional relation between both. The regressive equations for rice paddy field A is expressed in equation (1) while that for rice paddy field B is represented in equation (2), respectively.

$$y = 0.032x + 2.4717 \tag{1}$$
$$R^2 = 0.6535$$
$$y = 0.0404x + 2.3466 \tag{2}$$
$$R^2 = 0.9664$$

These regressive coefficients are very similar (the difference of proportional coefficients for both rice paddy fields is just 20.79 % while that of bias coefficients is 5.06 %). Therefore, the relationship between fertilizer amount and total nitrogen content in the rice leaves is clarified. In total, regressive equation between fertilizer amount and total nitrogen content in rice leaves is expressed with equation (3)

$$y = 0.0223x + 2.5733 \tag{3}$$
$$R^2 = 0.4659$$

R square value (determination value[9]) is around 0.5. This implies that the fertilizer amount is proportional to the total nitrogen in rice leaves.

C. NDVI and Protein Content in Rice Crops

Meanwhile, protein content in rice crops shows different relation against the relation between total nitrogen in rice leaves and fertilizer amount. Namely, there is proportional relation between protein content in rice crops and fertilizer amount ranged from zero to 12 Kg while there is negatively proportional relation between both for the fertilizer amount ranged from 12 to 16 Kg. Rice taste depends on protein content in the rice crops. Namely, protein rich rice crops taste
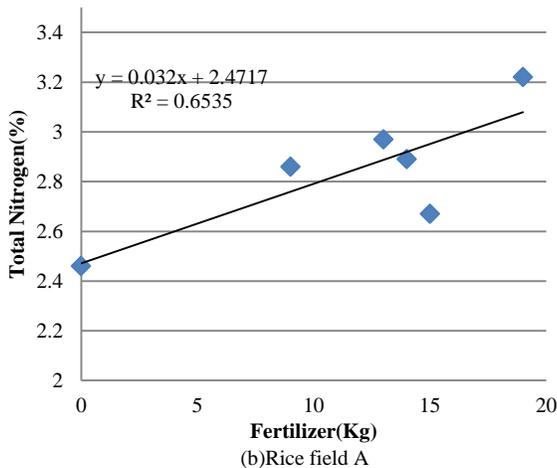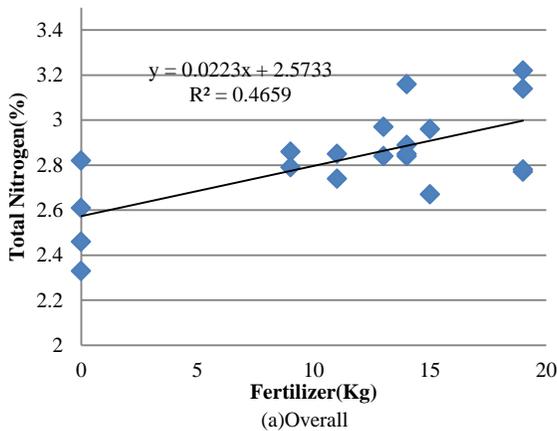
[9] $R^2 = 1 - \dfrac{\sum_{i=1}^{n}(y_i - f_i)^2}{\sum_{i=1}^{n}(y_i - m)^2}$ where y, f, and m denotes observed value, predicted value and mean value, respectively.

bad. Therefore, in accordance with increasing of fertilizer amount, total nitrogen content in rice leaves and NDVI of rice leaves are increased while protein content in rice crops is decreased as shown in Fig.2.
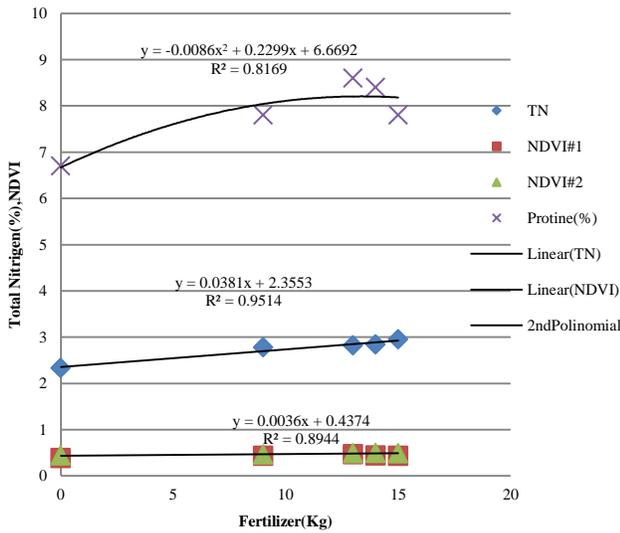
Fig. 2. Relation among fertilizer amount, total nitrogen content in rice leaves and NDVI of rice leaves as well as protein content in rice crops

Through the regressive analysis, it is found that there is proportional relation between fertilizer amount and NDVI with the following regressive equation,

$$y = 0.0036x + 0.4374 \qquad (4)$$
$$R^2 = 0.8944$$

Meanwhile, there must is the proportional relation between fertilizer content and total nitrogen content in rice leaves as shown in equation (5).

$$y = 0.0381x + 2.3553 \qquad (5)$$
$$R^2 = 0.9514$$

On the other hand, it seems that the relation between fertilizer amount and protein content in rice crop is different from the above relations. It is most likely the second order polynomial relation of equation (6) rather than proportional relation.

$$y = -0.0086x^2 + 0.2299x + 6.6692 \qquad (6)$$
$$R^2 = 0.8169$$

The determination index (R square value) is greater than 0.8. Therefore, it may say that there is saturation level of fertilizer amount. One of the reasons for this is due to the fact that the relation between NDVI and total nitrogen content in rice leaves differ from the relation between NDVI and protein content in rice crops as shown in Fig.6 (An Example).

On the other hand, remote controlled helicopter mounted visible and near infrared camera data are acquired on 18 and 22 August, total nitrogen content in rice leaves is measured on August 22 only though. Therefore, August 22 data show much reliable than August 18 data. For four days, rice leaves and rice crops are grown a little bit as shown in Fig.4.
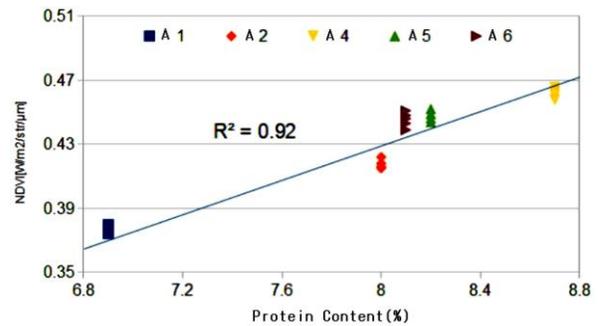
(a)Relation between protein content in rice crops and NDVI
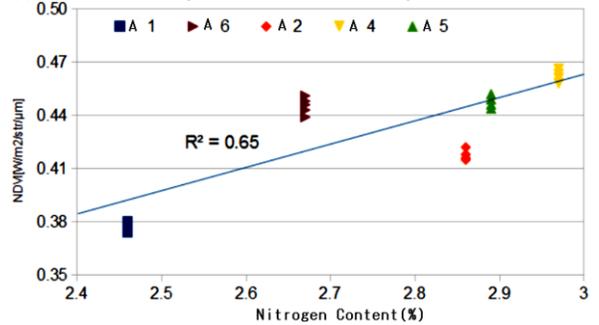
(b)Relation between total nitrogen content in rice leaves and NDVI

Fig. 3. Different relations between NDVI and total nitrogen content in rice leaves as well as protein content in rice crops
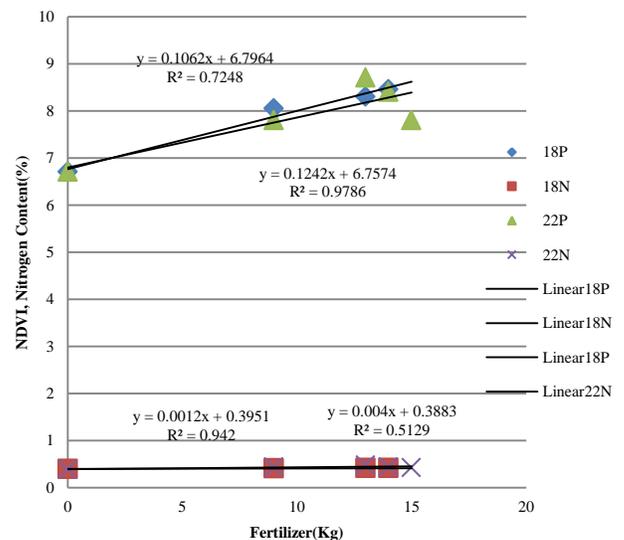
Fig. 4. Difference between August 18 and 22 data derived total nitrogen content and NDVI of rice leaves

D. Four Day Changes of NDVI and Protein Content in Rice Crops

NDVI and Total nitrogen content in rice leaves which are measured on 18 and 22 August are shown in Fig.5 (a) and (b), respectively. Both are increased a little bit. Also, the variances of these NDVI and total nitrogen content in rice leaves are increased, in particular, for NDVI.

(a)Total nitrogen content
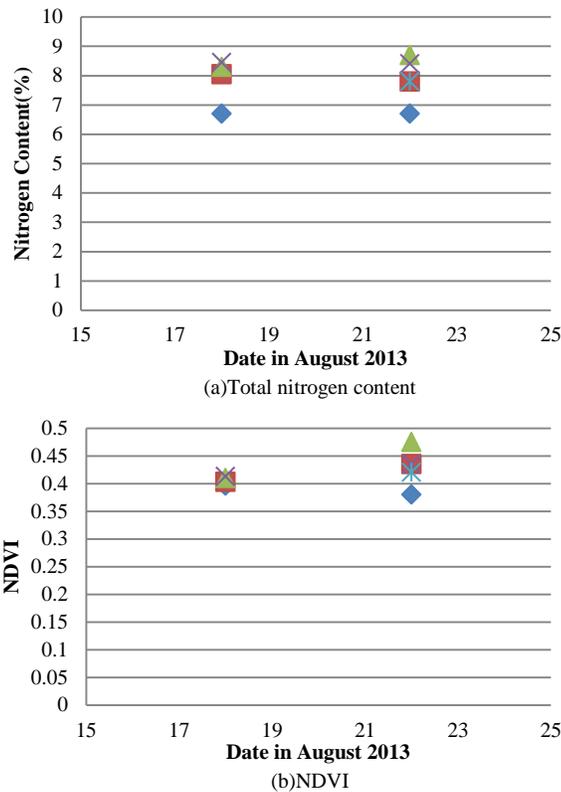
(b)NDVI

Fig. 5.   NDVI and Total nitrogen content in rice leaves which are measured on 18 and 22 August

E. Rice Stump Density

On the other hand, there are two rice stump densities, 15.15 and 21.21 stumps/ m^2 in the rice paddy fields A and B. NDVI, total nitrogen content in rice leaves and protein content in rice crops for each rice stump density are shown in Fig.6 (a), (b) and (c), respectively. NDVI and total nitrogen content in rice leaves are decreased in accordance with increasing of the density while protein content in rice crops is decreased with increasing of the density. This implies that rice crop quality of relatively high density of rice stump is better than that of poorly dense rice paddy field.

(a)NDVI

(b)Total nitrogen content
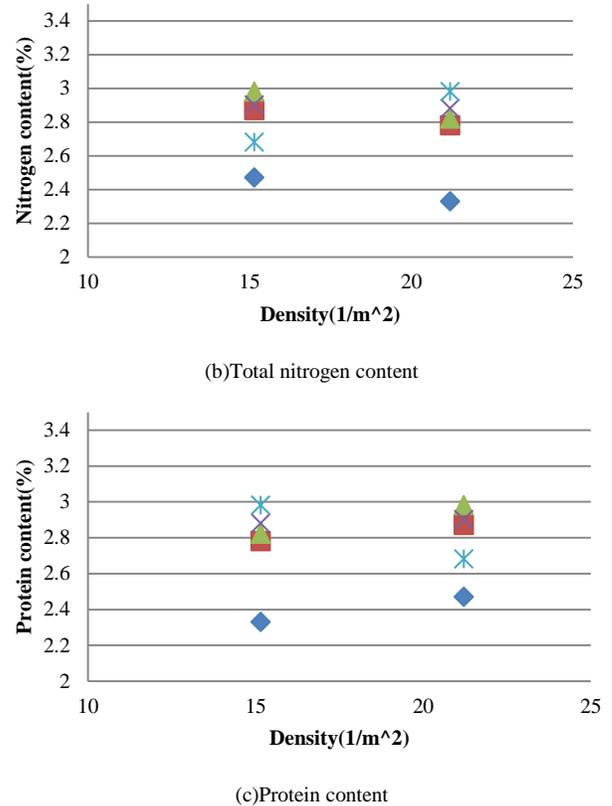
(c)Protein content

Fig. 6.   NDVI, total nitrogen content in rice leaves and protein content in rice crops for each rice stump density

IV.   CONCLUSION

Estimation of protein content in rice crop and total nitrogen content in rice leaves through regression analysis with Normalized Difference Vegetation Index: NDVI derived from camera mounted radio-control helicopter is proposed. Through experiments at rice paddy fields which is situated at Saga Prefectural Research Institute of Agriculture: SPRIA in Saga city, Japan, it is found that protein content in rice crops is highly correlated with NDVI which is acquired with visible and Near Infrared: NIR camera mounted on radio-control helicopter. It also is found that total nitrogen content in rice leaves is highly correlated to NDVI as well.

Protein content in rice crop is negatively proportional to rice taste. Therefore rice crop quality can be evaluated through NDVI observation of rice paddy field. It is found that total nitrogen content in rice leaves is linearly proportional to fertilizer amount and NDVI. Also, it is found that protein content in rice crops is positively proportional to fertilizer amount for lower fertilizer amount while protein content in rice crop is negatively proportional to fertilizer amount for relatively high fertilizer amount. It is also found that rice crop quality of low density of rice stump is better than that of highly dense rice paddy field.
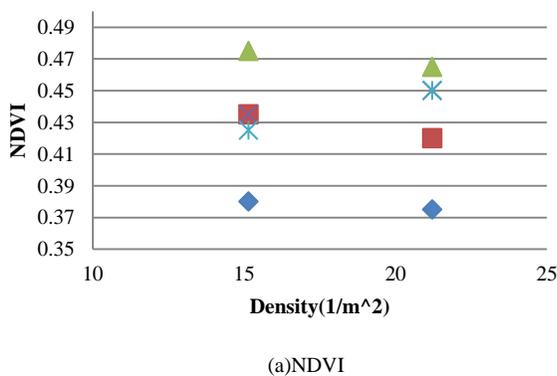
REFERENCES

[1] Wiegand, C., Shibayama , M, Yamagata , Y, Akiyama, T., 1989. Spectral Observations for Estimating the Growth and Yield of Rice, Journal of Crop Science, 58, 4, 673-683, 1989.

[2] Kohei Arai, Method for estimation of grow index of tealeaves based on Bi-Directional reflectance function:BRDF measurements with ground based netwrok cameras, International Journal of Applied Science, 2, 2, 52-62, 2011.

[3] Kohei Arai, Wireless sensor network for tea estate monitoring in complementally usage with Earth observation satellite imagery data based on Geographic Information System(GIS), International Journal of Ubiquitous Computing, 1, 2, 12-21, 2011.

[4] Kohei Arai, Method for estimation of total total nitrogen and fiber contents in tealeaves with grond based network cameras, International Journal of Applied Science, 2, 2, 21-30, 2011.

[5] Kohei Arai, Method for estimation of damage grade and damaged paddy field areas sue to salt containing sea breeze with typhoon using remote sensing imagery data, International Journal of Applied Science,2,3,84-92, 2011.

[6] Kohei Arai, Monte Carlo ray tracing simulation for bi-directional reflectance distribution function and grow index of tealeaves estimation, International Journal of Research and Reviews on Computer Science, 2, 6, 1313-1318, 2011.

[7] Kohei.Arai, Fractal model based tea tree and tealeaves model for estimation of well opened tealeaf ratio which is useful to determine tealeaf harvesting timing, International Journal of Research and Review on Computer Science, 3, 3, 1628-1632, 2012.

[8] Kohei.Arai, H.Miyazaki, M.Akaishi, Determination of harvesting timing of tealeaves with visible and near infrared cameradata and its application

to tea tree vitality assessment, Journal of Japanese Society of Photogrammetry and Remote Sensing, 51, 1, 38-45, 2012

[9] Kohei Arai, Osamu Shigetomi, Yuko Miura, Hideaki Munemoto, Rice crop field monitoring system with radio controlled helicopter based near infrared cameras through total nitrogen content estimation and its distribution monitoring, International Journal of Advanced Research in Artificial Intelligence, 2, 3, 26-37, 2013.

[10] Kohei Arai, Masanori Sakashita, Osamu Shigetomi, Yuko Miura, Estimation of Protein Content in Rice Crop and Total nitrogen Content in Rice Leaves Through Regression Analysis with NDVI Derived from Camera Mounted Radio-Control Helicopter, International Journal of Advanced Research in Artificial Intelligence, 3, 3, 13-19, 2013

AUTHORS PROFILE

Kohei Arai He received BS, MS and PhD degrees in 1972, 1974 and 1982, respectively. He was with The Institute for Industrial Science and Technology of the University of Tokyo from April 1974 to December 1978 and also was with National Space Development Agency of Japan from January, 1979 to March, 1990. During from 1985 to 1987, he was with Canada Centre for Remote Sensing as a Post-Doctoral Fellow of National Science and Engineering Research Council of Canada. He moved to Saga University as a Professor in Department of Information Science on April 1990. He was a councilor for the Aeronautics and Space related to the Technology Committee of the Ministry of Science and Technology during from 1998 to 2000. He was a councilor of Saga University for 2002 and 2003. He also was an executive councilor for the Remote Sensing Society of Japan for 2003 to 2005. He is an Adjunct Professor of University of Arizona, USA since 1998. He also is Vice Chairman of the Commission-A of ICSU/COSPAR since 2008. He is the Edito-in-Chief of IJACSA and IJISA. He wrote 33 books and published 500 journal papers.

Seamless Location Measuring System with Wifi Beacon Utilized and GPS Receiver based Systems in Both of Indoor and Outdoor Location Measurements

Kohei Arai 1
Graduate School of Science and Engineering
Saga University
Saga City, Japan

Abstract—A seamless location measuring system with WiFi beacon utilized and GPS receiver based systems in both of indoor and outdoor location measurements is proposed. Through the experiments in both of indoor and outdoor, it is found that location measurement accuracy is around 2-3 meters for the locations which are designated in both of indoor and outdoor.

Keywords—*GPS receiver; WiFi beacon; seamless location estimation*

I. INTRODUCTION

GPS based location estimation is quite popular. Mobile device, smart-phone, i-phone are utilizing GPS receivers for location estimation. It, however, does not work for indoor environments because of the fact that GPS satellite signals cannot be received in indoor environments. The location estimation accuracy of the GPS receiver based method is not so high. Furthermore, the accuracy of GPS based location estimation depends on many factors such as weather condition, the number of the acquired GPS satellites, circumstances (surrounding buildings, mountains, etc.), etc. On the other hands, WiFi-beacon can be used for location measurements in both indoor and outdoor environments. The location estimation accuracy depends on the situation of WiFi access points. Therefore, in general, WiFi beacon utilized location estimation accuracy is not good. It, however, still is somewhat useful for location estimation if the location accuracy requirement is not high. Therefore, WiFi beacon receiver based location estimation method is proposed here for both indoor and outdoor situations.

Bose and Heng classified WiFi-based positioning methods into Cell Identity (Cell-ID), Time of Arrival (TOA), Time Difference of Arrival (TDOA), Angle of Arrival (AOA), and signal strength categories [1]-[9]. Cell Identity (Cell-ID) is a basic wireless positioning system solution. It matches the target's position with its connection to an Access Point (AP). It does not require complex operations such as time synchronization and multiple APs. However, its low positional accuracy is the pitfall of its simplicity. Time of Arrival (TOA) measures a distance using the travel time of a radio signal from a transmitter to a receiver. Its application requires time synchronization of the transmitter and receiver, which is difficult to achieve for close ranges. To overcome the problem, Time Difference of Arrival (TDOA) was developed, which

utilizes the time difference between receiver and two or more receivers. That is to say, whereas TOA requires time synchronization of transmitters and receivers, TDOA needs just synchronization between receivers. Angle of Arrival (AOA) determines the position of a receiver by measuring the angle to it from a transmitter. An AP must use smart antennas and be capable of mounting them under static conditions.

Signal Strength based technique uses the signal attenuation property of the radio wave Received Signal Strength Indication (RSSI) to measure the distance from a receiver to transmitter using the distance-to-signal-strength relationship. One common approach of RSSI-based system is fingerprint approach, which entails two phases: a training phase and a tracking phase. In the training phase, the received signal strength information is filtered, interpolated, and eventually stored in a database as sample points. In the tracking phase, the position is determined by comparison with the received signal strength sample points stored in the database [10]. The accuracy of this system is a function of the sample points' sampling space, an estimation method and the structure of the database. However, such a method requires the time consuming on survey procedure or calibration process.

In order to find patients in hospitals, victims in group homes, etc., GPS receivers and WiFi beacon receivers in smart-phone, i-phone and tablet terminals are used in the proposed system. The location of WiFi access points the designated hospitals and the supposed group homes are known. Also, the specific location of the hospitals and group homes, for instance, the middle of the entrance door, is known. Therefore, the locations of the patients and the victims are estimated in both of indoor and outdoor situations in seamless basis. When they are in hospitals or group homes, their locations are estimated with WiFi beacon receivers while their location is estimated with WiFi beacon receiver and GPS receivers when they are in outside of hospitals or group homes with an accuracy of a couple of meters[1]. WiFi beacon based location estimation is helpful to improve GPS based location accuracy[2]. Also, location estimation can be done with WiFi

---

[1]http://wiki.openstreetmap.org/wiki/Accuracy_of_GPS_data

[2] http://www.quora.com/Why-is-location-accuracy-improved-when-wi-fi-is-enabled

beacon receiver in smart-phone, i-phone, and tablet terminal[3]. The WiFi beacon based location estimation accuracy around a couple of meters in an indoor situation [11]-[12].

The location estimation method proposed here is to use both GPS based method with improvement by WiFi beacon based method (it is referred to GPS based method hereafter) in outdoor situations and WiFi beacon based method in indoor situations as well as a calibration of estimated locations at the specific location of hospitals or group homes. Because of the locations of specific positions of hospitals or group homes are known, a calibration can be done through a comparison of the estimated locations of the designated specific positions between GPS based and WiFi beacon based methods. Thus the locations of the patients in hospitals and / or victims in group homes are estimated in seamless basis. Through experiments, it is found that the proposed method does work for seamless location estimation with an acceptable accuracy, 2-3 meters for finding the patients and the victims when they are out of hospitals or group homes when a disaster occurs.

The next section describes the proposed seamless basis location estimation method followed by some experiments. Then conclusion is described together with some discussions.

II. THE PROPOSED METHOD AND SYSTEM

The location estimation method proposed here is to use both GPS based method and WiFi beacon based method as well as a calibration of estimated locations at the specific location of hospitals or group homes. Because of the location of specific position of hospitals or group homes is known, a calibration can be done through a comparison of the estimated locations of the designated specific positions between GPS based and WiFi beacon based methods. Thus the locations of the patients in hospitals and / or victims in group homes are estimated in seamless basis.

Fig.1 shows flow chart of the proposed location estimation method. The location of smart-phone i-phone is estimated with GSP and WiFi beacon receivers equipped in the smart-phone and i-phone. The estimated locations are compared to the location of the designated known position in a prior to the location estimation such as the center of the entrance of the hospital or the group home. Then calibration of location estimation is done with the difference between the designated location and the estimated location with GPS and WiFi beacon. Thus the estimated location is calibrated. Repeat the calibration and location estimation is repeated.

The estimated locations are expressed with ISO 19155 of Place Identifier: PI. Example of the PI expression is shown below,

```
<allpi>
<placeidentifier>
<name>Kasasagi-Kaikan</name>
<latitude>33.24149339</latitude>
<longitude>130.28919659</longitude>
</placeidentifier>
```

[3] http://engineeringblog.yelp.com/2012/08/gps-vs-wifi-the-battle-for-location-accuracy-using-yelp-check-ins.html

```
<placeidentifier>
<name>Faculty Bldg. No.6</name>
<latitude>33.24139665</latitude>
<longitude>130.28864292</longitude>
</placeidentifier>
<placeidentifier>
<name>faculty Bldg. No.7</name>
<latitude>33.24118506</latitude>
<longitude>130.28842333</longitude>
</placeidentifier>
</allpi>
```
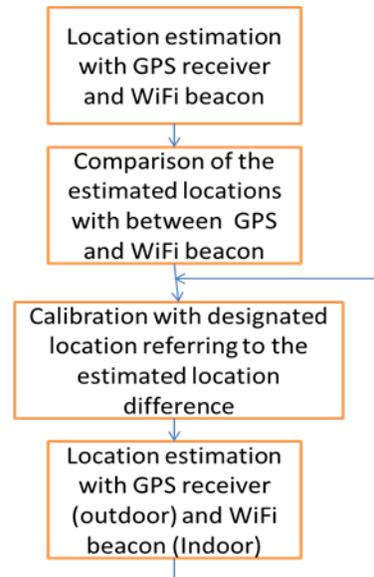

Fig. 1. Flow chart of the proposed location estimation method

The location name is located at the third line followed by latitude and longitude of the location. These name and latitude / longitude are aligned sequentially. PI expression is based on XML. Therefore, other information which is related to the location can be attached with a tag or tags. For instance, phone number, address, and the others. Therefore, these are referred crossly each other. Thus users can retrieve the location with the name, the phone number, the address, and the latitude / longitude.

III. EXPERIMENTS

A. *Location estimation accuracy with GPS receiver based method (Improvement by WiFi beacon receiver based method) in outdoor situation*

Although location estimation accuracy of the GPS receivers is well reported, there are a few reports on location estimation accuracy of WiFi beacon receivers. Therefore, the following experiments are conducted at the road situated at the prefectural border between Fukuoka and Saga, Japan in night time. Test site on the map is shown in Fig.2 while the photo of the test site in day time is shown in Fig.3. At the test site on the Sazanka road, WiFi access points and mobile devices are set up as are shown in Fig.4.

In order to avoid external noises, location estimation accuracy is measured in night time. The distance between two

locations, A and B is 10 m. Distance from A and B is measured with 1m step. Received signal strength is varied with the distance between the location A and the location apart from A with 1m step. Therefore distance between both locations can be estimated.

Fig. 2.   Test site location on topographic map

Fig. 3.   Day time photo of the test site situated at the prefectural border between Fukuoka and Saga, Japan

Received signal strength in unit of dBm is shown in Table 1 while the estimated distance between both locations is shown in Table 2, respectively.

As the results of the experiments, it is found that location estimation error of the method of location estimation with WiFi beacon is around 5(%).

TABLE I.   RECEIVED SIGNAL AT THE DIFFERENT LOCATIONS, A AND B

Distance(m) Signal_Level_from_A(dBm) Signal_Level_from_B(dBm)

0	-25	-58
1	-31.5	-57
2	-35.5	-56.5
3	-39	-55
4	-43	-52
5	-45	-50
6	-47;5	-47
7	-49	-45
8	-51.5	-48
9	-54	-38
10	-57.5	-27
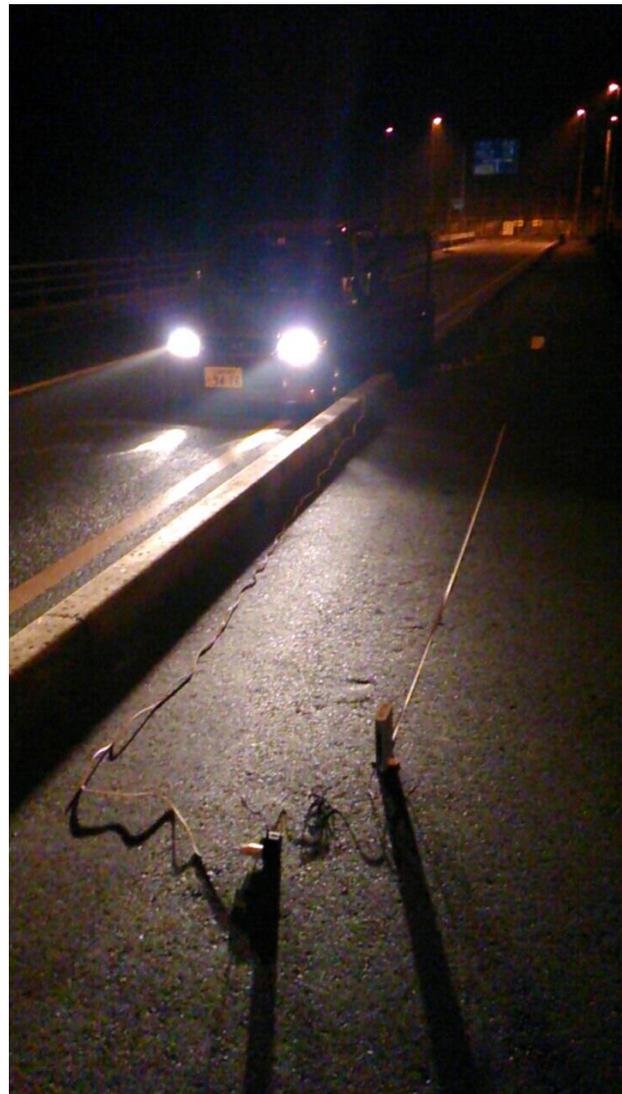
Fig. 4.   WiFi access points and mobile device are set up on the Sazanka road of the test site

TABLE II.   MEASURED DISTANCE ERRORS

Distance(m)	Calculated_Distance(m)	Error(%)
0	-0.28	28.0
1	1.06	5.66
2	1.89	-5.5
3	2.8	-6.67
4	4.15	3.61
5	5.0	0.0
6	6.16	2.6
7	6.84	-2.29
8	7.62	-4.99
9	8.89	-1.22
10	11.2	10.7

Location estimation accuracy of the GPS receiver based method is around 3.4 meters in average. Therefore, GPS receiver based method with the improvement by WiFi receiver based method achieved about 6 times much accurate location estimation.

B. Location estimation accuracy with WiFi beacon receiver based method in indoor situation

As described above, wireless channel signal strengths are changeful. Even immovable calibrating, the signal strengths still pulse up and down. Inconstant signal strengths on one position make estimating location difficult and inaccurate. Most research adopts mean value to solve this problem, but I think it's insufficient through inexact location estimating result. Using one mean value to stand for one position's wireless channel information is not enough. I present a Grid Segment Process to make some improvement. Assume one training process gains 100 signal strengths, I divide up these 100 signal strengths into 10 parts, each has 10 signal strengths. Then calculate mean value of each part and store them into radio map to substitute for original one mean value. Now I acquire 10 slices of mean values and have more information to estimate location. I call the divide procedure as Segment Process. Not only in offline calibration phase I do Segment Process, but in online estimation phase I execute it, as will introduce below. The mean value is used for expressing proper wireless channel characteristic. Using Segment Process to obtain more slices of mean values denotes more information to refer to and more accurate location estimation result. The received signal of each access point is converted into its color representative. This system use 3 signals information from 3 different AP's. Each access point has its basic color that different each other. The three AP (*AP1, AP2, & AP3*) use *red*, *green* and *blue* color respectively. The color map is based on signal strength information get from signal data collection process. The gradation of color is based on the *HSL (Hue Saturation Luminance)* value where *L* is a function of signal strength. Assuming S_{px} is a variable for signal strength (in percentage) for the position of *x* meter from the initial position. Then the color for the grid of *x* meter distance is measured by the formula:

$$L\text{-}Color\ AP1_x = 255 - (Hexadecimal(S_{px})*128/100)$$

where Hexadecimal(S) is function for convert the input into its hexadecimal value.

The gradation of color is based on the HSI (Hue Saturation Intensity) value where L is a function of signal strength.

The fission of the grid is half size and the color is based on the RGB combination of two adjacent colors. Then we will have a new grid in the more detail size as shown in Fig.5. The second stage of grid fusion is possible to create more detail color radio map grid. The accuracy of each color radio-map then investigates to measure the accuracy.

The effectiveness of this method is the interpolation using color grid fusion technique. Initial grid size could setup to a number that low cost on offline training. I start with grid size of 5 meters long with 2.5 widths (the corridor width). The initial color radio-map is created for this grid size that will have the initial error also 5 meters. Then too improve the accurate of the system, the initial map is interpolate in half size to determine the interpolation value (color) of middle point between two grids. Fig.6 shows the illustration of grid fusion technique. Also Fig.7 shows an example of location estimation result in the color radio-map representation.
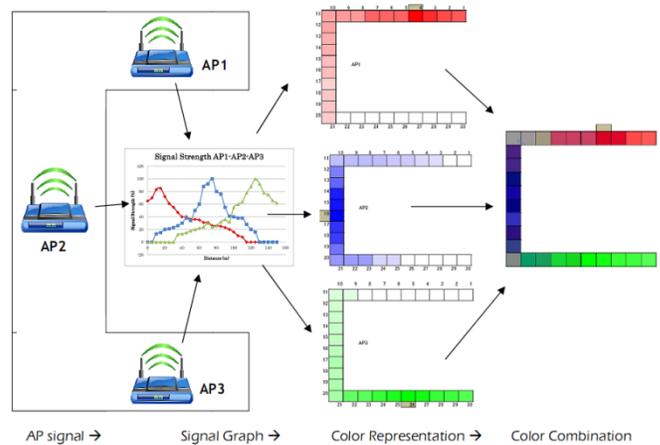
Fig. 5.   Diagram flow of Color Radio Map Method
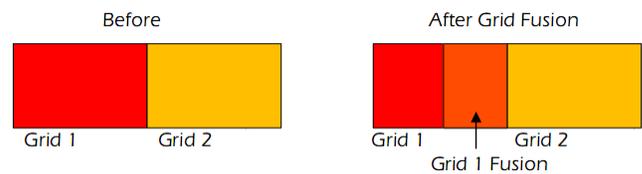
Fig. 6.   Grid fusion techniques
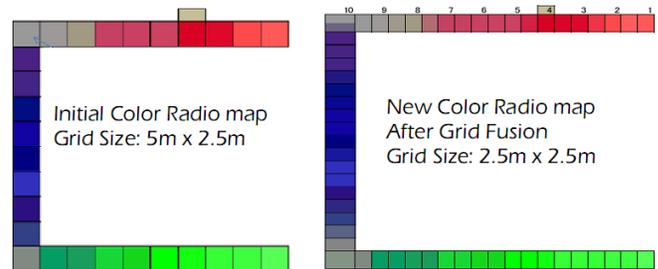
Fig. 7.   Example of an estimated result

I performed our experiment in the third floor of the Science and Engineering Faculty Building No.1, Saga University. This building has a layout like show in Fig.8 with the total dimension in rectangle is 150 × 3 meters. The building is equipped with 802.11b wireless LAN environment. To form the radio map, the environment was modeled as a space of 30 locations in grid of 5 x 3 meters each. The position of AP and initial online tracking position is show in Fig.5.
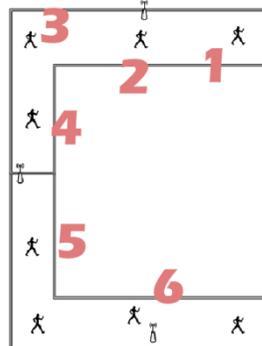
Fig. 8.   Floor layout of the Bldg. in the experiment

As the result of the experiment, it is found that the location estimation accuracy is approximately 2.5m.

C. Calibration of estimated location

Application software is developed which allows location estimation with GPS and WiFi beacon receivers. The estimated location is expressed with PI. Example of the estimated locations with GPS and WiFi beacon is shown in Fig.9. Not only latitude and longitude but also direction of the target location from the current position is displayed onto smart-phone and / or i-phone as shown in Fig.10. The direction can be calculated with the following equation.

$$\theta = \operatorname{atan}(2\beta/\alpha) \tag{1}$$

where α and β are calculated with the estimated locations.

ISO19155: Place Identifier (PI)

Fig. 9.   Example of the estimated locations displayed onto smart-phone or i-phone

Example of the estimated and actual location is shown in Fig.11. In comparison of the actual location and the estimated locations with GPS and WiFi receivers are quite clearly different each other with around 5 meters. Location estimation accuracies of GPS and WiFi beacon based methods depend on circumstances, surrounding building, in this case.
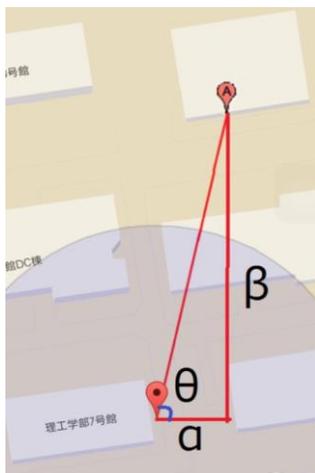
Fig. 10. Estimation of the direction of the target location from the current location
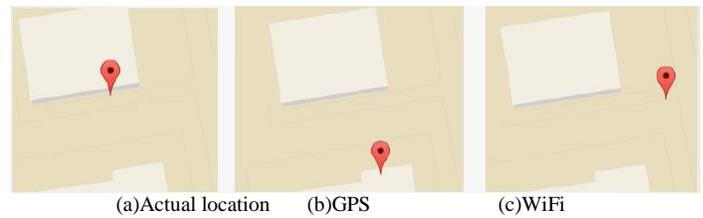
Fig. 11. Actual and the estimated locations with GPS and WiFi beacon receivers equipped in smart-phone and i-phone

Using the difference between the actual location and the estimated locations with GPS and WiFi beacon receivers can be calibrated. Thus the estimated location is switched to GPS based method to WiFi beacon based method when the patients and the victims are getting into hospitals and or group homes from the outside and vise versa.

IV.   CONCLUSION

A seamless location measuring system with WiFi beacon utilized and GPS receiver based systems in both of indoor and outdoor location measurements is proposed. Through the experiments in both of indoor and outdoor, it is found that location measurement accuracy is around 2-3 meters for the locations which are designated in both of indoor and outdoor. It is also found that GPS receiver based location estimation method with improvement by using WiFi beacon based method works well. Approximately 6 times better accuracy is achieved in comparison between GPS based method and the proposed GPS based method with improvement with WiFi beacon based method.

These GPS and WiFi beacon receivers are equipped in smart-phone and / or i-phone. Therefore, the locations of the patients in hospitals, the victims in group homes can be estimated with 2-3 meters of accuracy if they have the smart-phone and / or i-phone with the developed application software.

REFERENCES

[1]   P. Bahl, V.N. Padmanabhan, RADAR: an in-building RF-based user location and tracking system, INFOCOM 2000. 19th Annual Joint Conference of the IEEE Computer and Communications Societies, Proceedings IEEE 2 (2000) 775–784 vol.772.

[2]   A. Bose, F. Chuan Heng, A Practical Path Loss Model for Indoor WiFi Positioning Enhancement, Information, Communications & Signal Processing, 2007 6th International Conference, 2007, pp. 1–5.

[3]   Y. Chen, X. He, Contribution of pseudolite observations to GPS precise surveys, KSCE Journal of Civil Engineering 12 (1) (2008) 31–36.

[4]   Y.K. Cho, J.-H. Youn, N. Pham, Performance tests for wireless real-time localization systems to improve mobile robot navigation in various indoor environments, in: C. Balaguer, M. Abderrahim (Eds.), Robotics and Automation in Construction, InTech Education and Publishing, 2008, pp. 355–372.

[5]   Y. Fukuju,M. Minami, H.Morikawa, T. Aoyama, DOLPHIN: An Autonomous Indoor Positioning System in Ubiquitous Computing Environment, Proceedings of the IEEE Workshop on Software Technologies for Future Embedded Systems, IEEE Computer Society, 2003.

[6] S. Han, J. Kim, C.-H. Park, H.-C. Yoon, J. Heo, Optimal detection range of RFID tag for RFID-based positioning system using the k-NN algorithm, Sensors 9 (6) (2009) 4543–4558.

[7] C. Hu, W. Chen, Y. Chen, D. Liu, Adaptive Kalman filtering for vehicle navigation, Journal of Global Positioning Systems 2 (1) (2003) 6.

[8] J. Yim, C. Park, J. Joo, S. Jeong, Extended Kalman filter for wireless LAN based indoor positioning, Decision Support System 45 (4) (2008) 960–971.

[9] W.-S. Jang, M.J. Skibniewski, A wireless network system for automated tracking of construction materials on project sites, Journal of Civil Engineering and Management 14 (1) (2008) 9.

[10] H.M. Khoury, V.R. Kamat, Evaluation of position tracking technologies for user localization in indoor construction environments, Automation in Construction 18 (4) (2009) 444–457.

[11] Arai, K., Tolle Herman, Akihiro Serita, Mobile Devices Based 3D Image Display Depending on Users' Actions and Movements, International Journal of Advanced Research in Artificial Intelligence, 2, 6, 77-83, 2013.

[12] Kohei Arai, Herman Tolle, Color radio-map interpolation for efficient fingerprint WiFi-based indoor location estimation, International Journal of Advanced Research in Artificial Intelligence, 2, 3, 10-15, 2013

AUTHORS PROFILE

Kohei Aarai He received BS, MS and PhD degrees in 1972, 1974 and 1982, respectively. He was with The Institute for Industrial Science and Technology of the University of Tokyo from April 1974 to December 1978 and also was with National Space Development Agency of Japan from January, 1979 to March, 1990. During from 1985 to 1987, he was with Canada Centre for Remote Sensing as a Post Doctoral Fellow of National Science and Engineering Research Council of Canada. He moved to Saga University as a Professor in Department of Information Science on April 1990. He was a councilor for the Aeronautics and Space related to the Technology Committee of the Ministry of Science and Technology during from 1998 to 2000. He was a councilor of Saga University for 2002 and 2003. He also was an executive councilor for the Remote Sensing Society of Japan for 2003 to 2005. He is an Adjunct Professor of University of Arizona, USA since 1998. He also is Vice Chairman of the Commission-A of ICSU/COSPAR since 2008. He wrote 33 books and published 500 journal papers.

Methods for Wild Pig Identifications from Moving Pictures and Discrimination of Female Wild Pigs based on Feature Matching Methods

Kohei Arai 1

Graduate School of Science and Engineering
Saga University
Saga City, Japan

Kensuke Kubo 3

3 Fujitsu Kyushu Network Technologies, Ltd.
Fukuoka Japan

Katsumi Sugawa 3

3 Fujitsu Kyushu Network Technologies, Ltd.
Fukuoka Japan

Indra Nugraha Abdullah 2

2 Jakarta Office, Yamaha Co. Ltd.
Jakarta, Indonesia

Abstract—**Methods for wild pig identifications and discrimination of female wild pigs based on feature matching methods with acquired Near Infrared: NIR moving pictures are proposed. Trials and errors are repeated for identifying wild pigs and for discrimination of female wild pigs through experiments. As a conclusion, feature matching methods with the target nipple features show a better performance. Feature matching method of FLANN shows the best performance in terms of feature extraction and tracking capabilities.**

Keywords—*OpenCV; Canny filter; Template matching; Feature matching*

I. INTRODUCTION

Wildlife damage in Japan is around 23 Billion Japanese Yen a year in accordance with the report from the Ministry of Agriculture, Japan. In particular, wildlife damages by deer and wild pigs are dominant (10 times much greater than the others) in comparison to the damage due to monkeys, bulbuls (birds), rats. Therefore, there are strong demands to mitigate the wildlife damage as much as we could. It, however, is not so easy to find and capture the wildlife due to lack of information about behavior. For instance, their routes, lurk locations are unknown and not easy to find. Therefore, it is difficult to determine the appropriate location of launch a trap.

The purpose of this research work is to identify the wildlife, in particular, wild pigs for mitigation of wildlife damage. In particular, it is effective to capture female wild pigs (wild boar lays the child) for mitigation of wildlife damage. Therefore, there are very strong demands of capturing female wild pigs.

In order to identify the wild pigs and discriminate female wild pigs from the moving pictures acquired with Near Infrared: NIR camera, computer vision of technologies are utilized. First, target of wild pigs is attempted to extract from the moving pictures. Contour extraction and edge extraction are attempted. Secondly, background and target are attempted to separate. Using a template of nipple image (a small portion of image), discrimination of female wild pigs is attempted.

Then feature matching methods are used for female wild pig discriminations with nipple features acquired from the moving pictures.

The following section describes research background followed by the proposed methods for wild pig identification and discrimination of female wild pigs. Then experiments are described followed by conclusion with some discussions.

II. RESEARCH BACKGROUND

According to the West, B. C., A. L. Cooper, and J. B. Armstrong. 2009. Managing wild pigs: A technical guide. Human-Wildlife Interactions Monograph 1:1–55[1], there are the following wild pig damages,

Ecological

Impacts to ecosystems can take the form of decreased water quality, increased propagation of exotic plant species, increased soil erosion, modification of nutrient cycles, and damage to native plant species [1]-[5].

Agricultural Crops

Wild pigs can damage timber, pastures, and, especially, agricultural crops [6]-[9].

Forest Restoration

Seedlings of both hardwoods and pines, especially longleaf pines, are very susceptible to pig damage through direct consumption, rooting, and trampling [10]-[12].

Disease Threats to Humans and Livestock

Wild pigs carry numerous parasites and diseases that potentially threaten the health of humans, livestock, and wildlife [13]-[15].

Humans can be infected by several of these, including diseases such as brucellosis, leptospirosis, salmonellosis, toxoplasmosis, sarcoptic mange, and trichinosis. Diseases of

---

[1] www.berrymaninstitute.org/publications,

significance to livestock and other animals include pseudorabies, swine brucellosis, tuberculosis, vesicular stomatis, and classical swine fever [14], [16]-[18].

There also are some lethal techniques for damage managements. One of these is trapping. It is reported that an intense trapping program can reduce populations by 80 to 90% [19]. Some individuals, however, are resistant to trapping; thus, trapping alone is unlikely to be successful in entirely eradicating populations. In general, cage traps, including both large corral traps and portable drop-gate traps, are most popular and effective, but success varies seasonally with the availability of natural food sources [20]. Cage or pen traps are based on a holding container with some type of a gate or door [21].

III. PROPOSED METHOD AND SYSTEM

A. Proposed System

Fig.1 shows an example of the system for trapping and capturing of wild pigs which consists of the trap cage and the video camera.

Fig. 1. Proposed system for trapping and acquiring moving picture of wild pigs

In the trap cage, there is bait. When wild pigs get in the trap cage, ultrasonic sensor sensed them. Then the entrance doors are shut downed. These processes are monitored and captured with the near infrared video camera with near infrared Light Emission Diode: LED. Because wild pigs are active in nighttime, Near Infrared: NIR camera with NIR LED is used.

The proposed system for trapping of wild pigs and for capturing their moving pictures is illustrated in Fig.2.

There are two ultrasonic sensors which are attached at the front and the back ends of the cage. When wild pigs get in the cage, then they are sensed with the ultrasonic sensors. Meantime, trap obstruction is activated. Drop-gates are then shut downed immediately after they are sensed with the ultrasonic sensors. Thus the wild pigs are trapped in the cage. These processes are monitored and captured with NIR camera with NIR LED. The captured moving pictures are transmitted through Bluetooth and then the transmitted moving pictures

are transferred to the data collection center through WiFi networks or LAN. There are sensor control and battery box as well as solar panel for electricity supply.
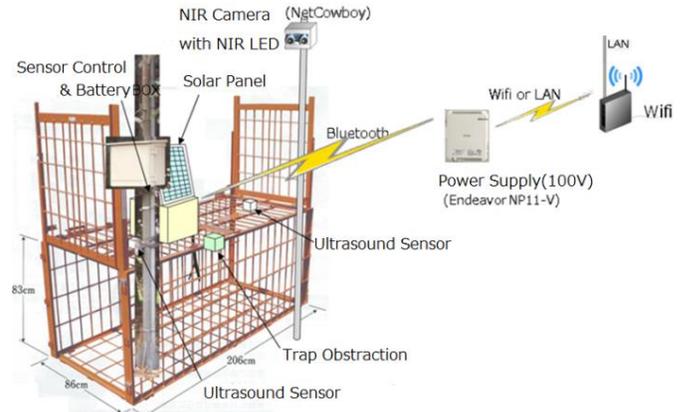
Fig. 2. Proposed system for trapping of wild pigs and for capturing their moving pictures

Outlooks of the NIR camera (NetCowboy) with NIR LED and ultrasonic sensors are shown in Fig. 3 (a) and (b), respectively. Meanwhile, specifications of these camera and sensor are shown in Table 1 and 2, respectively

TABLE I. SPECIFICATION OF NIR CAMERA (NETCOWBOY)

Pixel	1.3 M
Resolution	1280×1024
Frame rate	1280 x 1024：7.5fps, 640 x 480：30fps
Dimension	52mm (W) × 65mm (D) × 70mm (H)
Weight	85g
Operating condition	0 - 40deg.C
Interface	USB 2.0
IR Illumination	7 NIR LED

TABLE II. FEATURES OF ULTRASONIC RANGE FINDER[2]

Supply Voltage	5 V (DC)
Supply Current	30 mA (Typ), 35 mA (Max)
Range	3cm to 3m
Input Trigger	Positive TTL pulse, 2μS min, 5μS (Typ)
Echo Pulse	Positive TTL pulse, 115 μS to 18.5 mS
Echo Hold-off	750 μS from fall of Trigger pulse
Burst Frequency	40 kHz for 200 μS
Delay before next measurement	200 μS
Dimension	22 mm H x 46 mm W x 16 mm D

(a)NIR camera   (b)Ultrasonic sensor
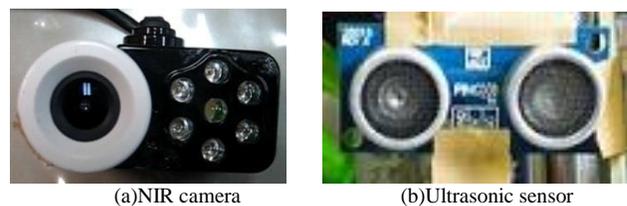
Fig. 3. Outlook of NIR camera with NIR LED and ultrasonic sensor used in the proposed system for trapping and capturing of wild pigs

---

[2] Parallax ultrasonic sensor,
http://www.parallax.com/dl/docs/prod/acc/PingDocs.pdf

B. *Proposed Moving Picture Analysis Methods*

Moving pictures are acquired with high resolution mode of 1280 by 1024 pixels. Therefore, frame rate is 7.5 fps. OpenCV is used for acquisition, processing, and analysis because it is totally easy to use. OpenCV is an open source computer vision library which is written in C and C++ and runs under Linux, Windows, and Mac OS X. It can be downloaded from *http://sourceforge.net/projects/opencvlibrary*

There so many library software for image processing and analysis. First, object has to be extracted from the moving picture. Then object contour has to be extracted. For the contour extraction and tracing, Canny filter related spatial filters are attempted. After that, it would be better to remove the background. The following background removals is attempted,

cv2.createBackgroundSubtractorMOG()

In order to discriminate female wild pigs, template matching method is applied with a template of small portion of nipple images. The following correlation functions are attempted for template matching,

CV_TM_SQDIFF , CV_TM_SQDIFF_NORMED , CV_TM_CCORR , CV_TM_CCORR_NORMED , CV_TM_CCOEFF, CV_TM_CCOEFF_NORMED

Also feature matching methods are applied for discrimination of female wild pigs. There are many feature matching methods in the OpenCV library. A couple of feature matching methods are attempted for the discriminations. The followings are typical feature matching methods which are provided from OpenCV,

- BruteForce
- BruteForce-L1
- BruteForce-SL2
- BruteForce-Hamming
- BruteForce-Hamming(2)
- FlannBased

The FlannBasedMatcher interface is used in the proposed method in order to perform a quick and efficient matching by using the FLANN (*Fast Approximate Nearest Neighbor Search Library*). Also Brute-Force matcher which is simple matching method is used in the proposed method. It takes the descriptor of one feature in first set and is matched with all other features in second set using some distance calculation. For both, feature descriptor is needed. Speeded-up Robust Feature: SURF is used in the proposed method.

IV. EXPERIMENTS

A. *Preliminary Image Processing*

One shot image of the acquired moving pictures is shown in Fig.4 as an example. This is a female wild pig on the route from habitat area to go to the calms feed. Wild boar children are followed by the female wild pig. By using the difference between the current and the previous frame of wild pig

(targeted object), it is possible to extract the female wild pig. Also, it is possible to remove the background by frame by frame. Fig.5 shows the resultant image of the background removals.

Edge and contour extractions are attempted with Canny and sharp Canny filters. Fig.6 (a) shows the resultant image of Canny filter while Fig.6 (b) shows that of the sharp Canny filter. In the process, lower and higher thresholds are adequately set obviously. Through a comparison between Fig.6 (a) and (b), sharp Canny filter seems superior to Canny filter. It, however, is not sufficient for extraction.

Fig. 4. Portion of original image of the targeted object of female wild pig in concern

Fig. 5. Resultant image of background removal from the original image in frame by frame basis

(a)Canny filter
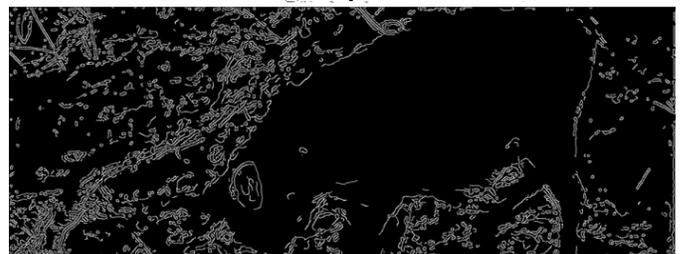
(b)Sharp Canny filter

Fig. 6. resultant images of edge and contour extractions

B. Descrimination of Female Wild pigs

Secondly, discrimination of female wild pigs is attempted with template matching and feature matching. Fig.7 shows an example of template image of nipple which indicates female wild pigs.

Fig. 7.   Template image of nipple which is an indicator of female wild pigs

By using template matching software which is provided by OpenCV, nipple feature is matched and tracked. An example of template matching image with template image is shown in Fig.8. It seems does work well for female wild pig discrimination and tracking. It, however, does not work so well when the wild pig moves so fast and the portion of nipple is occluded and disappeared which are shown in Fig.9 (a) and (b), respectively. Also influence due to the both target moving speed and occlusion of the different object behind the other object is shown in Fig.9 (c).

Fig. 8.   Example of resultant image of template matching with the template image of nipple portion of image

(a)Move so fast

(b)Nipple portion cannot be seen

(c)Cub behind male adult wild pig

Fig. 9.   Influences due to target speed and occlusion in template matching

Other than these, feature matching methods are attempted for discrimination of female wild pigs. In order to describe the feature of female wild pigs, Scale-Invariant Feature Transform: SIFT and SURF based feature descriptors are used for representation of nipple features. SURF descriptor based feature matching and tracking is attempted. Fig.10 shows an example of the resultant image of SURF feature matching.
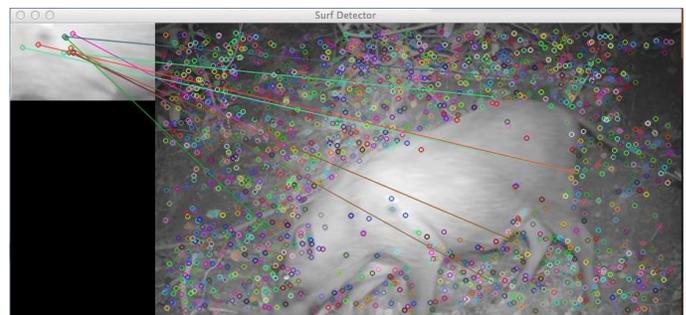
Fig. 10. Resultant image of SURF based feature description and feature matching

The SURF based feature description and feature matching is not good enough for feature tracking. Sometime it works well, but it does not work well as shown in Fig.10. Therefore, another feature matching methods are attempted after that.
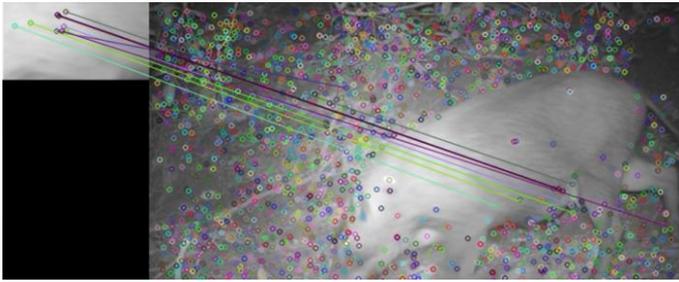
Fig. 11. Example of the resultant image of FLANN

Those are SURF Brute-Force and FLANN. The performance of discrimination is almost similar between both. Fig.11 shows an example of the resultant image of FLANN.

Nipple of features is matched so well. In particular, tracking capability of the FLANN feature matching is superior to the other template matching and SURF matching as well as SURF Brute-Force matching.

C. Proposed System for Wild Pig Montoring Hardware System

One of the issues for damage management due to wild pigs is how to count the number of female wild pigs in the area in concern. Although the proposed methods and systems above work well, the hardware system is costly. The hardware system proposed here is cheap version of the system for monitoring the number of female wild pigs. Because the areas where suffers from wild pig damage are situated almost all over the Japanese island. Such situation is common to the countries in the world. Therefore, the cheap version of hardware system for monitoring is required.

Android tablet terminal which equipped communication capability (Bluetooth, WiFi) and camera is not so expensive. For instance, Android tablet terminal of KEIAN M716S V2 with 7 inches display does cost about 7280 Japanese Yen. Major specification and outlook of the Android tablet terminal is shown in Table 3.

TABLE III.   SPECIFICATION OF ANDROID TABLET TERMINAL OF KEIAN M716S V2

Dimension	OS	weight
800x480	Android 4.4.2	305g

NIR LED is also cheap. Therefore, one set of wild pig monitor does cost about 10000 Japanese Yen. The length of the route in the area in concern is a couple of hundred meters. Therefore, 30 sets of the monitoring system would cover the entire route of wild pigs. The total cost of the hardware system an area is around 300000 Japanese Yen. Obviously it is cheaper than damage cost.

Event driven application software is installed in the Android tablet terminal. When relatively large changes are detected in the current frame compared to the previous frame, the event driven software is activated. Then target object is detected with target extraction and contour extraction. Then size of target object is measured from the contour. Discrimination between adult and cub is done depending on the measured size. After that discrimination between male and female is done depending on presence or absence of nipple.

Along with the suspicious route of wild pigs, the monitoring hardware systems are set every 10 meters. The number of incoming and outgoing wild pigs is counted for each block with 10 meters long. Thus total number of wild pigs can be estimated.

V.   CONCLUSION

Methods for wild pig identifications and discrimination of female wild pigs based on feature matching methods with acquired Near Infrared: NIR moving pictures are proposed. Trials and errors are repeated for identifying wild pigs and for discrimination of female wild pigs through experiments. As a conclusion, feature matching methods with the target nipple features show a better performance. Feature matching method of FLANN shows the best performance in terms of feature extraction and tracking capabilities.

Further study is required for wide area of spatial distribution of wild pigs. Spatial distribution of wild pigs in a relatively small size of area in concern can be estimated by the proposed system and method. Kiriging can be used for a much wide area in concern using estimated the number of wild pigs of the small size of areas.

REFERENCES

[1]   Patten, D. C. 1974. Feral hogs — boon or burden. Proceedings of the Sixth Vertebrate Pest Conference 6:210–234.

[2]   Singer, F. J., W. T. Swank, and E. E. C. Clebsch. 1984. Effects of wild pig rooting in a deciduous forest. Journal of Wildlife Management. 48:464–473.

[3]   Stone, C. P., and J. O. Keith. 1987. Control of feral ungulates and small mammals in Hawaii's national parks: research and management strategies. Pages 277–287 in C. G. J. Richards and T. Y. Ku, editors. Control of mammal pests. Taylor and Francis, London, England, and New York and Philadelphia, USA.

[4]   Cushman, J. H., T. A. Tierney, and J. M. Hinds. 2004. Variable effects of feral pig disturbances on native and exotic plants in a California grassland. Ecological Applications 14:1746–1756.

[5]   Kaller, M. D., and W. E. Kelso. 2006. Swine activity alters invertebrate and microbial communities in a coastal plain watershed. American Midland Naturalist 156:163–177.

[6]   Bratton, S. P. 1977. The effect of European wild boar on the flora of the Great Smoky Mountains National Park. Pages 47–52 in G. W. Wood, editor. Research and management of wild hog populations. Belle W. Baruch Forest Science Institute, Clemson University, Georgetown, South Carolina, USA.

[7]   Lucas, E. G. 1977. Feral hogs — problems and control on National Forest lands. Pages 17–22 in G. W. Wood, editor. Research and management of wild hog populations. Belle Baruch Forest Science Institute, Clemson University, Georgetown, South Carolina, USA.

[8]   Thompson, R. L. 1977. Feral hogs on National Wildlife Refuges. Pages 11–15 in G. W. Wood, editor. Research and management of wild hog populations. Belle W. Baruch Forest Science Institute, Clemson University, Georgetown, South Carolina, USA.

[9] Schley, L, and T. J. Roper. 2003. Diet of wild boar *Sus scrofa* in Western Europe, with particular reference to consumption of agricultural crops. Mammal Review 33:43–56.

[10] Whitehouse, D. B. 1999. Impacts of feral hogs on corporate timberlands in the southeastern United States. Pages 108–110 *in* Proceedings of the Feral Swine Symposium, June 2–3, 1999, Ft. Worth, Texas, USA.

[11] Mayer, J. J., E. A. Nelson, and L. D. Wike. 2000. Selective depredation of planted hardwood seedlings by wild pigs in a wetland restoration area. Ecological Engineering, 15(Supplement 1): S79–S85.

[12] Campbell, T. A., and D. B. Long. 2009. Feral swine damage and damage management in forested ecosystems. Forest Ecology and Management 257:2319–2326

[13] Forrester, D. J. 1991. Parasites and diseases of wild mammals in Florida. University of Florida Press, Gainesville, Florida, USA.

[14] Williams, E. S., and I. K. Barker. 2001. Infectious diseases of wild mammals. Iowa State University Press, Ames, Iowa, USA.

[15] Sweeney, J. R., J. M. Sweeney, and S. W. Sweeney. 2003. Feral hog. Pages 1164–1179 *in* G. A. Feldhamer, B. C. Thompson, and J. A. Chapman, editors. Wild mammals of North America. Johns Hopkins University Press, Baltimore, Maryland, USA.

[16] Nettles, V.F., J. L. Corn, G. A. Erickson, and D. A. Jessup. 1989. A survey of wild swine in the United States for evidence of hog cholera. Journal of Wildlife Diseases 25:61–65.

[17] Davidson, W. R., and V. F. Nettles, editors. 1997. Wild swine. Pages 104–133 *in* Field manual of wildlife diseases in the southeastern United States. Second edition. Southeastern Cooperative Wildlife Disease Study, Athens, Georgia, USA.

[18] Davidson, W. R., editor. 2006. Wild swine. Pages 105–134 *in* Field manual of wildlife diseases in the southeastern United States. Third edition. Southeastern Cooperative Wildlife Disease Study, Athens, Georgia, USA.

[19] Choquenot, D. J., R. J. Kilgour, and B. S. Lukins. 1993. An evaluation of feral pig trapping. Wildlife Research, 20:15– 22.

[20] Barrett, R. H., and G. H. Birmingham. 1994. Wild pigs. Pages D65–D70 *in* S. Hyngstrom, R. Timm, and G. Larsen, editors. Prevention and control of wildlife damage. Cooperative Extension Service, University of Nebraska, Lincoln, Nebraska, USA.

[21] Mapston, M. E. 1999. Feral hog control methods. Pages 117–120 *in* Proceedings of the Feral Swine Symposium, June 2–3, 1999, Fort Worth, Texas, USA.

AUTHORS PROFILE

Kohei Aarai He received BS, MS and PhD degrees in 1972, 1974 and 1982, respectively. He was with The Institute for Industrial Science and Technology of the University of Tokyo from April 1974 to December 1978 and also was with National Space Development Agency of Japan from January, 1979 to March, 1990. During from 1985 to 1987, he was with Canada Centre for Remote Sensing as a Post Doctoral Fellow of National Science and Engineering Research Council of Canada. He moved to Saga University as a Professor in Department of Information Science on April 1990. He was a councilor for the Aeronautics and Space related to the Technology Committee of the Ministry of Science and Technology during from 1998 to 2000. He was a councilor of Saga University for 2002 and 2003. He also was an executive councilor for the Remote Sensing Society of Japan for 2003 to 2005. He is an Adjunct Professor of University of Arizona, USA since 1998. He also is Vice Chairman of the Commission-A of ICSU/COSPAR since 2008. He is Editor-in-Chief of IJACSA and IJISA. He wrote 33 books and published 500 journal papers.

Changes in Known Statements After New Data is Added

Sylvia Encheva

Stord/Haugesund University College

Bjørnsonsg. 45,

5528 Haugesund,

Norway

Abstract—**Learning spaces are broadly defined as spaces with a noteworthy bearing on learning. They can be physical or virtual, as well as formal and informal. The formal ones are customary understood to be traditional classrooms or technologically en-hanced active learning classrooms while the informal learning spaces can be libraries, lounges, cafés, etc.. Students' as well as lecturers' preferences to learning spaces along with the effects of these preferences on teaching and learning have been broadly discussed by many researchers. Yet, little is done to employ mathematical methods for drawing conclusions from available data as well as investigating changes in known statements after new data is added. To do this we suggest use of ordering rules and ordered sets theories.**

Keywords—*Ordering rules; Ordered sets; Implications*

I. INTRODUCTION

Interest in building, teaching in, and researching the impact of technologically enhanced learning spaces appears to have grown exponentially, [3]. Learning spaces are usually divided into formal and informal, [7]. The first ones are customary understood to be classrooms while the latter can be libraries, lounges or cafés. At the same time, today's teaching and learning processes are heavily effected by an increasing use of laptop computers, smart phones and tablets. All these various opportunities can be viewed with respect to students' preferences and learning effectiveness. To do this we suggest support taken from ordering rules and ordered sets theories, [5].

Modern information technology tools allow good oppor-tunities for collecting, storing and even classifying data. A number of scientific fields like for example automation and decision support systems, [4], require ordering of elements and rules.

The theory of ordering rules is often applied for ordering elements with respect to attributes' values. Ordering rules like "if the value of an object x on an attribute a is ordered ahead of the value of another object y on the same attribute, then x is ordered ahead of y", are presented in [10] and [11]. This rises a natural question on whether it is possible to combine several ordering rules and draw reasonable conclusions afterwards.

The rest of the paper goes as follows. Some terms from the fields of ordered sets and ordered relations are presented in Section II. Their application is discussed in Section III followed by a conclusion in Section IV.

II. ORDERED SETS AND RELATIONS

Two very interesting problems are considered in [2], namely the problem of determining a consensus from a group of orderings and the problem of making statistically significant statements about ordering.

A relation I is an *indifference* relation when given AIB neither $A > B$ nor $A < B$ has place in the componentwise ordering. A partial ordering whose indifference relation is transitive is called a *weak ordering*. A *total ordering* is a binary relation which is transitive, antisymmetric, and total ($p \leq q$ or $q \leq p$).

If given two alternatives, a person is finally choosing only one. the natural extension of to more than two elements is known as the 'majority rule' or the 'Condorcet Principle'. A relation $R(L_1, L_2, ..., L_k)$ is constructed by saying that the pair $(a, b) \in R$ if (a, b) belong to the majority of relations L_i.

The following three linear orderings

$$a \quad b \quad c$$
$$b \quad c \quad a$$
$$c \quad a \quad b$$

leading to

$$R = \{(a, b), (b, c), (c, a)\}$$

(three-way tie), illustrate the 'paradox of voting'. A 'social welfare function' maps k-tuples of the set of linear orderings of any $b \subset A$ to single linear orderings of B, where A is a set of at least three alternatives, [1].

Two elements a and b where $a \neq b$ and $a, b \in P$ are comparable if $a \leq b$ or $b \leq a$, and incomparable otherwise. If $\forall a, b$ where $a, b \in P$ are comparable, then P is chain. If $\forall a, b$ where $a, b \in P$ are incomparable, then P is antichain.

Interesting set-relational approach for computer adminis-tration of psychological investigations has been employed in [12].

Below we list some definitions and formulas as in [10]. The authors also introduce order relations into attribute values.

An information function I_a is a total function mapping an object of U to an exact value in V_a.

Definition 1: [9] An information table is a quadruple:

$$IT = (U, At, \{V_a | a \in At\}, \{I_a | a \in At\}),$$

where U is a finite nonempty set of objects, At is a finite nonempty set of attributes, V_a is a nonempty set of values for $a \in At$, $I_a : U \rightarrow V_a$ is an information function.

Definition 2: Let U be a nonempty set and $\succ$ be a binary relation on U. The relation $\succ$ is a weak order if it satisfies the two properties:

Asymmetry:

$$x \succ y \Longrightarrow \neg(y \succ x),$$

Negative transitivity:

$$(\neg(x \succ y), \neg(y \succ z)) \Longrightarrow \neg(x \succ z).$$

An important implication of a weak order is that the following relation,

$$x \sim y \Longleftrightarrow (\neg(x \succ y), \neg(y \succ x))$$

is an equivalence relation. For two elements, if $x \sim y$, we say x and y are indiscernible by $\succ$. The equivalence relation $\sim$ induces a partition $U/\sim$ on U, and an order relation $\succ^\star$ on $U/\sim$ can be defined by

$$[x]_\sim \succ^\star [y]_\sim \Longleftrightarrow x \succ y$$

where $[x]_\sim$ is the equivalence class containing x. Any two distinct equivalence classes of $U/\sim$, can be compared since $\succ^\star$ is a linear order.

Definition 3: An ordered information table is a pair

$$OIT = (IT, \{\succ_a \mid a \in At\}),$$

where IT is a standard information table and $\succ_a$ is a weak order on V_a.

An ordering of values of a particular attribute a naturally induces an ordering of objects, namely, for $x, y \in U$:

$$x \succ_{\{a\}} y \Longleftrightarrow I_a(x) \succ_a I_a(y),$$

where $\succ_{\{a\}}$ denotes an order relation on U induced by the attribute a. An object x is ranked ahead of another object y if and only if the value of x on the attribute a is ranked ahead of the value of y on a. The relation $\succ_{\{a\}}$ has exactly the same properties as that of $\succ_a$. That is, x is ranked ahead of y if and only if x is ranked ahead of y according to all attributes in A.

Data mining in an ordered information table may be formulated as finding association between orderings induced by attributes.

Definition 4: Consider two subsets of attributes $A, B \subseteq At$. For two expressions $\phi \in E(A)$ and $\psi \in E(B)$, an ordering rule is read "if ϕ then ψ" and denoted by $\phi \Rightarrow \psi$. The expression ϕ is called the rule's antecedent, while the expression ψ is called the rule's consequent.

III. Graphical Representation of Correlations Between Ordering Rules

Recent enthusiasm for shifting the manner in which institutions of higher education approach and conceptualize classroom space has been fueled by a host of articles extolling the potential transformative power of formal learning spaces on

teaching practices and learning outcomes, [3]. Handling such large amount of data resulting from both physical and mental processes requires solid well formalized techniques like f. ex. those included in the field of artificial intelligence.

It is worth mentioning that ordinary majority voting is unable to handle situations with incomplete or changing data. Ordered sets and ordering rules can accommodate both very nicely. They are particularly applicable in cases when some of the elements are compared while others are not or different conclusions are drawn by different groups and non of them should be ignored in a decision making process.
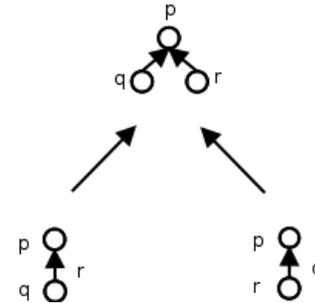
Fig. 1. q and r imply p

Suppose students are suggested to express their preferences with respect to two different learning spaces x, y based on three attributes a, b, c. Their preferences related to learning spaces are first collected and conclusions can be drawn afterwards supported by ordered sets theory.

An ordering rule states how orderings of objects by attributes in A determines orderings of objects by attributes in B. For example, an ordering rule,

$$(a, \succ) \wedge (b, \preceq) \Rightarrow (c, \succ),$$

can be re-expressed as

$$x \succ_{\{a\}} y \wedge x \preceq_{\{b\}} y \Rightarrow x \succ_{\{c\}} y.$$

That is, for two arbitrary objects x and y, if x is ranked ahead of y by attribute a, and at the same time, x is not ranked ahead of y by attribute b, then x is ranked ahead of y by attribute c.

In order to facilitate readability we introduce three new notations p, q, r, where:

p stands for $x \succ_{\{a\}} y$,

q stands for $x \preceq_{\{b\}} y$, and

r stands for $x \succ_{\{c\}} y$.

Obviously, p, q, r generate six implications where one of them implies any of the other two. When two of them imply the third we obtain a rule similar to

$$x \succ_{\{a\}} y \wedge x \preceq_{\{b\}} y \Rightarrow x \succ_{\{c\}} y.$$

The three possible rules are illustrated in Fig. 1, Fig. 2, and Fig. 3. They can be used to draw conclusions when only
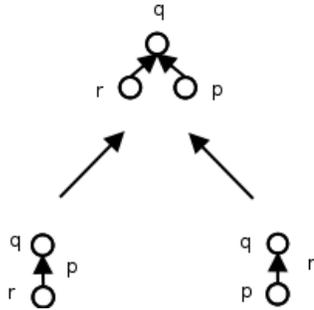
Fig. 2. p and r imply q
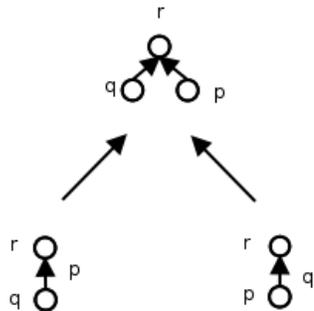
Fig. 3. p and q imply r

couples of spaces are evaluated and also when a conclusion involving all of them is required.

We can extract much more information if we connect all these implications as in Fig. 4. The applied implication rules are based on the theory presented in Section II.
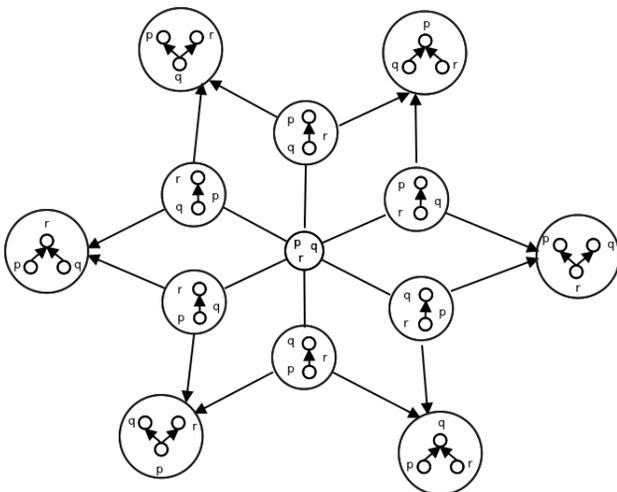
Fig. 4.   Illustration of ordering rules

The graph in Fig. 5 shows that comparing two cases where an element is a rule's antecedent in one case or a rule's consequent in the other one is operating with two disjoint sets of implications.

Any two non disjoint sets of implications, i.e. pares of implications sharing one implication, generate a rule where
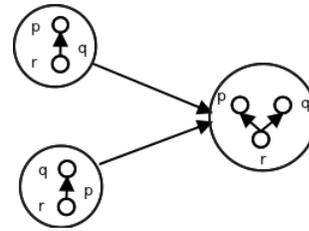
Fig. 5. p and q are implied by r

one element is an antecedent and another rule where another element is a consequent, see f. ex. Fig. 6.
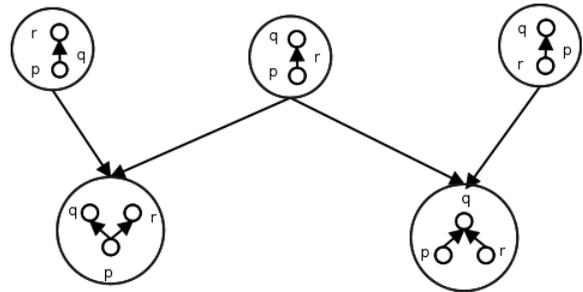

Fig. 6.   Two sets of implications

Formal classroom space shapes the behavior of lecturers and students, [3]. A ranking system can be used for drawing automated conclusions when different initial rules are assumed. For ranking systems the rule illustrated in Fig. 6 can be used to show how one ordering combined with two different orderings can lead to two different conclusions.

Remark: Learning spaces should not be considered as a part of knowledge space theory, [6] and [8]. Knowledge spaces refer to states of knowledge of a person.

IV.   CONCLUSION

Appropriate combination of ordering rules sharing common elements leads to new conclusions. Closed sets coupled with ordering rules can be applied in decision support processes and development of machine learning techniques.

In future work we intend to investigate opportunities to involve more than three elements and rules in an ordering rules deductive system.

REFERENCES

[1]   K. J. Arrow, *Social Choice and Individual Values*, Wiley, New York, 2nd ed. 1963.

[2]   K. P. Bogart, *Some social sciences applications of ordered sets*, In: I. Rival, Editor, Ordered Sets, Reidel, Dordrecht, pp. 759–787, 1982.

[3]   D. C. Brooks, *Space and Consequences: The Impact of Different Formal Learning Spaces on Instructor and Student Behaviour*, Journal of Learning Spaces, Vol.1, No 2, 2012.

[4]   C. Carpineto and G. Romano, *Concept Data Analysis: Theory and Applications*, John Wiley and Sons, Ltd., 2004.

[5]   B. A. Davey and H. A. Priestley, *Introduction to lattices and order*, Cambridge University Press, Cambridge, 2005.

[6]   J.-P. Doignon and J.-C. Falmagne, *Knowledge Spaces*, Springer-Verlag, 1999.

[7] J.-P. Doignon and J.-C. Falmagne, *Learning Spaces*, Springer-Verlag, 2011.

[8] J. -C. Falmagne, D. Albert, C. Doble, D. Eppstein, and X. Hu, *Knowledge Spaces: Applications in Education*, Springer, 2013.

[9] Z. Pawlak, *Rough Sets, Theoretical Aspects of Reasoning about Data*, Kluwer Academic Publishers, Dordrecht, 1991.

[10] Y. Sai and Y. Y. Yao, *Analyzing and Mining Ordered Information Tables*, Journal of Computer Science and Technology, vol. 18, No.6, 771–779, 2003.

[11] Y. Sai and Y. Y. Yao, *On Mining Ordering Rules*, New Frontiers in Artificial Intelligence, Lecture Notes in Computer Science, vol. 2253, pp. 316–321, 2001.

[12] K. Yordzhev and I. Peneva, *Computer Administering of the Psychological Investigations: Set-Relational Representation*, Open Journal of Applied Sciences, 2, pp. 110–114, 2012. http://www.scirp.org/journal/PaperInformation.aspx?PaperID=20331

Evaluation of Reception Facilities for Ship-generated Waste

Sylvia Encheva

Stord/Haugesund University College

Bjørnsonsg. 45,

5528 Haugesund,

Norway

Abstract—**Waste management plans usually address all types of ship-generated waste and cargo residues originating from ships calling at ports. Well developed waste management plan is a serious step towards reduction of the environmental impact of ship-generated waste. Such important and at the same time complex considerations can be supported by application of modern mathematical theories. Evaluation of waste management plans based on application of grey theory is presented in this work.**

Keywords—*Waste management, grey theory, assessments*

I. INTRODUCTION

Waste management plans usually address all types of ship-generated waste including sewage, and cargo residues originating from ships. The volume of waste produces pressure on the environment, particularly with respect to ship-generated waste disposal at home ports and ports of call. Well developed waste management plan is a serious step towards reduction of the environmental impact of ship-generated waste. Obviously, there is a serious need for research on developing intelligent tools for evaluating such plans considering their importance and complexity.

Boolean logic is often used in the process of decision making, [4] and [16]. Thus if a response does not appear to be necessarily true, the system selects false. While Boolean logic appears to be sufficient for most everyday reasoning, it is certainly unable to provide meaningful conclusions in presence of inconsistent and/or incomplete input [5], [6]. This problem can be resolved by applying many-valued logic.

In real life situations qualities are often assessed by using linguistic terms. In order to facilitate such a process which is usually based on incomplete information we propose Grey theory, [7]. This theory is particularly useful with respect to working in situations where the information about elements (or parameters) is incomplete, the information about structure is incomplete, the information about boundaries is incomplete, and the behavior information of movement is incomplete. Occurrence of incomplete information is the main reason of being grey.

The rest of the paper is organized as follows. Basic terms and concepts are presented in Section II. The main results are described in Section III. Section IV contains the conclusion of this work.

II. BACKGROUND

Grey theory is an effective method used to solve uncertainty problems with discrete data and incomplete information. The theory includes five major parts: grey prediction, grey relational analysis, grey decision, grey programming and grey control, [2], [3], and [8]. A quantitative approach for assessing the qualitative nature of organizational visions is presented in [10].

The Grey theory in this work follows [7].

Definition 1: A grey system is defined as a system containing uncertain information presented by a grey number and grey variables.

Definition 2: Let X be the universal set. Then a grey set G of X is defined by its two mappings $\overline{\mu}_G(x)$ and $\underline{\mu}_G(x)$.

$$\begin{cases} \overline{\mu}_G(x) : x \to [0,1] \\ \underline{\mu}_G(x) : x \to [0,1] \end{cases}$$

$\overline{\mu}_G(x) \geq \underline{\mu}_G(x), x \in X, X = R$, $\overline{\mu}_G(x)$ and $\underline{\mu}_G(x)$ are the upper and lower membership functions in G respectively.

When $\overline{\mu}_G(x) = \underline{\mu}_G(x)$, the grey set G becomes a fuzzy set. It shows that grey theory considers the condition of the fuzziness and can deal flexibly with the fuzziness situation.

The grey number can be defined as a number with uncertain information. For example, the ratings of attributes are described by the linguistic variables; there will be a numerical interval expressing it. This numerical interval will contain uncertain information. A grey number is often written as $\otimes G$, $(\otimes G = G|_{\underline{\mu}}^{\overline{\mu}})$.

Definition 3: Lower-limit, upper-limit, and interval grey numbers.

$\otimes G = [\underline{G}, \infty]$ - if only the lower limit of G can be possibly estimated and G is defined as a lower-limit grey number.

$\otimes G = [-\infty, \overline{G}]$ - if only the upper limit of G can be possibly estimated and G is defined as a upper-limit grey number.

$\otimes G = [\underline{G}, \overline{G}]$ - the lower and upper limits of G can be estimated and G is defined as an interval grey number.

Grey number operation is an operation defined on sets of intervals, rather than real numbers. Some basic operation

laws of grey numbers $\otimes G_1 = [\underline{G}_1, \overline{G}_1]$ and $\otimes G_2 = [\underline{G}_2, \overline{G}_2]$ on intervals where the four basic grey number operations on the interval are the exact range of the corresponding real operation follow:

$$\otimes G_1 + \otimes G_2 = [\underline{G}_1 + \underline{G}_2, \overline{G}_1 + \overline{G}_2]$$

$$\otimes G_1 - \otimes G_2 = [\underline{G}_1 - \overline{G}_2, \overline{G}_1 - \underline{G}_2]$$

$$\otimes G_1 \times \otimes G_2 = [\min(\underline{G}_1\underline{G}_2, \underline{G}_1\overline{G}_2, \overline{G}_1\underline{G}_2, \overline{G}_1\overline{G}_2), \max(\underline{G}_1\underline{G}_2, \underline{G}_1\overline{G}_2, \overline{G}_1\underline{G}_2, \overline{G}_1\overline{G}_2)]$$

$$\otimes G_1 \div \otimes G_2 = [\underline{G}_1, \overline{G}_1] \times \left[\frac{1}{\underline{G}_2}, \frac{1}{\overline{G}_2}\right]$$

The length of a grey number $\otimes G$ is defined as

$$L(\otimes G) = [\overline{G} - \underline{G}].$$

Definition 4: [7] For two grey numbers $\otimes G_1 = [\underline{G}_1, \overline{G}_1]$ and $\otimes G_2 = [\underline{G}_2, \overline{G}_2]$, the possibility degree of $\otimes G_1 \leq \otimes G_2$ can be expressed as follows:

$$P\{\otimes G_1 \leq \otimes G_2\} = \frac{\max(0, L^\star - \max(0, \overline{G}_1 - \underline{G}_2))}{L^\star}$$

where $L^\star = L(\otimes G_1) + L(\otimes G_2)$.

For the position relationship between $\otimes G_1$ and $\otimes G_2$, there exist four possible cases on the real number axis. The relationship between $\otimes G_1$ and $\otimes G_2$ is determined as follows:

- If $\underline{G}_1 = \underline{G}_2$ and $\overline{G}_1 = \overline{G}_2$, we say that $\otimes G_1$ is equal to $\otimes G_2$, denoted as $\otimes G_1 = \otimes G_2$. Then $P\{\otimes G_1 \leq \otimes G_2\} = 0.5$.

- If $\underline{G}_2 > \overline{G}_1$, we say that $\otimes G_2$ is larger than $\overline{G}_1$, denoted as $\otimes G_2 > \otimes G_1$. Then $P\{\otimes G_1 \leq \otimes G_2\} = 1$.

- If $\overline{G}_2 > \overline{G}_1$, we say that $\otimes G_2$ is smaller than $\overline{G}_1$, denoted as $\otimes G_2 < \otimes G_1$. Then $P\{\otimes G_1 \leq \otimes G_2\} = 0$.

- If there is an inter-crossing part in them, when $P\{\otimes G_1 \leq \otimes G_2\} > 0.5$, we say that $\otimes G_2$ is larger than $\overline{G}_1$, denoted as $\otimes G_2 > \otimes G_1$. When $P\{\otimes G_1 \leq \otimes G_2\} < 0.5$, we say that $\otimes G_2$ is smaller than $\overline{G}_1$, denoted as $\otimes G_2 < \otimes G_1$.

Suppose a decision group has K persons, then the attribute weight of attribute Q_j can be calculated as

$$\otimes w_j = \frac{1}{K}\left[\otimes w_j^1 + \otimes w_j^2 + + \otimes w_j^K\right]$$

where $\otimes w_j^K, j = 1, 2, ..., n$ is the attribute weight of K-th decision maker and can be described by grey number $\otimes w_j^K = [\underline{w}_j^K, \overline{w}_j^K]$.

The rating values are

$$\otimes G_{ij} = \frac{1}{K}\left[\otimes G_{ij}^1 + \otimes G_{ij}^2 + + \otimes G_{ij}^K\right]$$

where $\otimes G_{ij}^K, i = 1, 2, ..., m, j = 1, 2, ..., n$ is the attribute rating value of K-th decision maker and can be described by the grey number $\otimes G_{ij}^K = [\underline{G}_{ij}^K, \overline{G}_{ij}^K]$.

The weighted normalized grey decision matrix can be established as

$$D^\star = \begin{bmatrix} \otimes V_{11} & \otimes V_{12} & \cdots & \otimes V_{1n} \\ \otimes V_{21} & \otimes V_{22} & \cdots & \otimes V_{2n} \\ & & \cdots & \\ \otimes V_{m1} & \otimes V_{m2} & \cdots & \otimes V_{mn} \end{bmatrix}$$

where $\otimes V_{ij} = \otimes G_{ij} \times \otimes w_j$.

$$S^{\max} = \left\{ \begin{array}{l} \left[\max_{1\leq i\leq m} \underline{V}_{i1}, \max_{1\leq i\leq m} \overline{V}_{i1}\right], \\ \left[\max_{1\leq i\leq m} \underline{V}_{i2}, \max_{1\leq i\leq m} \overline{V}_{i2}\right], \\ ..., \\ \left[\max_{1\leq i\leq m} \underline{V}_{in}, \max_{1\leq i\leq m} \overline{V}_{in}\right] \end{array} \right\}$$

The grey possibility degree between plan alternatives in set $Pl = \{Pl_1, Pl_2, ..., Pl_m\}$ and ideal referential plan alternative $Pl^{\max}$.

$$P\{Pl_i \leq Pl^{\max}\} = \frac{1}{n}\sum_{1\leq j\leq n} P\{\otimes V_{ij} \leq \otimes G_j^{\max}\}$$

A smaller $P\{Pl_i \leq Pl^{\max}\}$ implies worse ranking order of Pl_i.

A historical review and bibliometric analysis of grey system theory is presented in [14]. Application of grey theory for predication of electric power demand can be seen in [13].

The Analytic Hierarchy Process (AHP), [11] facilitates development of a hierarchical structure of complex evaluation problems. This way subjective judgment errors can be avoided and an increase of the likelihood for obtaining reliable results can be achieved. AHP employs paired comparisons in order to obtain ratio scales. Both actual measurements and subjective opinions can be used in the process. Grey relational analysis method and analytic network process [12] approach were used in [9].

III. DECISION-MAKING

The regulation on waste delivered to shore enforced by 2004 requires vessels entering ports within the European Economic Community (EEC) to report current status of waste on-board. This includes the amount of waste being produced, delivered in port, and planned to be delivered in next port of call. Prior to arrival all the required data has to be delivered to port authorities. Such information is of special interest regarding environmental reporting.

Cruise ships often generate waste that prevails their maximum storage capacity long before they have access to shore

TABLE I.   ATTRIBUTE WEIGHTS

Scale	
Not satisfactory	[0.0, 0.2]
Somewhat atisfactory	[0.21, 0.4]
Average	[0.41, 0.5]
Good	[0.51, 0.8]
Very good	[0.81, 0.9]
Exellent	[0.91, 1.0]

TABLE II.   WEIGHTED NORMALIZED DECISION TABLE

	A1	A2	A3	A4
Pl1	[6.41,6.83]	[3.46,3.84]	[6.25, 6.81]	[3.52, 3.86]
Pl2	[5.46,5.72]	[5.34,5.75]	[7.32, 7.57]	[4.14, 4.76]
Pl3	[4.34,4.66]	[5.11,0.23]	[5.75, 6.13]	[6.25, 6.78]
Pl4	[4.93,5.28]	[4.33,4.62]	[4.32, 4.74]	[4.93, 5.08]
Pl5	[3.75,4.12]	[4.83,4.91]	[5.14, 5.63]	[5.55, 6.12]

waste disposal facilities. According to MARPOL 73/78 discharge of treated waste water is allowed 4 Mi off shore, while some regional port policies require discharge treated waste water 12 Mi off shore.

Establishment and operation of reception facilities for ship-generated waste is a very important regarding protection of the external environment. The reception facilities can be fixed, floating and mobile units. Examples of ship-generated waste include oily waste, sewage, cargo residues and garbage.

While large oil spills in the see are followed by marine pollution authorities, small spills cased by pumping oily bilge water overboard and refueling receive considerably less attention. They however have also negative effects on the marine environment. Marine bilge pump out services are to be used instead of pumping oily bilge water overboard. The latter may contain diesel and petrol, as well as lubricant and hydraulic oils.

Reception facilities are often ranked according to availability of the pre-treatment equipment and processes, methods of recording actual use of the port reception facilities, methods of recording amounts of received and disposed ship-generated waste and cargo residues. The impact of cruise ship generated waste on home ports and ports of call is studied in [1].

Actual use of reception facilities is sometimes stimulated by the so-called "no-special-fee" system. Thus 'fees covering the cost of the reception, handling and final disposal of ship-generated wastes are included in the harbor fee or otherwise charged to the ship, irrespective of whether any wastes are actually delivered', [17]. Recent port waste management plan for ship-generated waste can be found in [18].

In this work five plan alternatives $Pl1, Pl2, Pl3, Pl4$ and $Pl5$ are ranked with respect to four attributes. These attributes address provision of facilities to receive $A1$, treat $A2$, safely dispose of ship-generated waste $A3$, and use of green energy $A4$. We however are not to provide all numerical details due to agreed upon anonymity restrictions. Instead we present a graphical illustration for comparing the plan alternatives.

Further on we use the rule: the grater values the better. The calculations are done based on real data and according to the theory presented in [7]. This means calculating of linguistic ratings for weights and linguistic ratings for attributes, first and building a weighted normalized decision table afterwards. Linguistic ratings for applied weights presented in Table I and weighted normalized decision table is shown in Table II.

The possibility degrees are $P\{Pl_i \leq Pl^{\max}\} = \{0.65, 0.78, 0.72, 0.61, 0.67\}$. In other words $Pl2 > Pl3 > Pl5 > Pl1 > Pl4$. According to the performed calculations the second alternative should be chosen.

Fig. 1.   Plan alternative $Pl2$ and attributes

Applying grey theory in our case results in ordering proposed plan alternatives when all attributes are taken in consideration. In order to make decisions some authorities are interested to see how different plan alternatives are ranked with respect to each attribute. We answer that question in Fig. 1. Since the second alternative $Pl2$ is listed as the best according the executed calculations, we show where $Pl2$ is placed with respect to each attribute. $Pl2$ appears to be the best alternative according to $A2$ and $A3$, and is number two according to $A1$, and number four according to $A4$. Alternative $Pl3$ is highlighted Fig. 2.
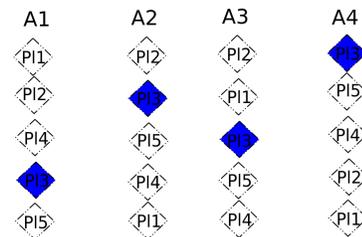
Fig. 2.   Plan alternative $Pl3$ and attributes

Similar figures can be made for alternative $Pl5$ if for some reasons alternatives $Pl2$ and $Pl3$ cannot be accepted.

Instead of developing graphical representations one can study the weighted normalized decision table. The latter however proves to be quite difficult when populated with larger amount of data.

IV.   CONCLUSION

Quite often different elements in waste management plans are evaluated independently of each other, which leads to multi-criteria decision inconsistencies. The presented approach can be used to evaluate all elements in such plans and compare those plans in order to make an optimal decision.

We have also compared the five plans applying Analytic Hierarchy Process, [15]. The outcomes conforms what has already been obtained with the Grey theory approach.

REFERENCES

[1] N. Butt, The impact of cruise ship generated waste on home ports and ports of call: A study of Southampton, Marine Policy, vol.31(5), pp. 591–598, 2007.

[2] J. L. Deng, *Control problems of grey systems*, System and control letters, vol. 5, 288-294, 1982.

[3] J. L. Deng, *Introduction to grey system theory*, Journal of grey systems, 1, vol. 1-24, 1989.

[4] R. L. Goodstein, *Boolean Algebra*, Dover Publications, 2007.

[5] E. Gradel, M. Otto and E. Rosen, *Undecidability results on two- variable logics*, Archive of Mathematical Logic, vol. 38, pp. 313–354, 1999.

[6] N. Immerman, A. Rabinovich, T. Reps, M. Sagiv and G. Yorsh, *The boundery between decidability and undecidability of transitive closure logics*, In: CSL'04, 2004.

[7] S. Liu and Y. Lin, *Grey information*, Springer, 2006

[8] Y.C. Hu, *Grey relational analysis and radical basis function network for determining costs in learning sequences*, Applied mathematics and computation, vol. 184, pp. 291-299, 2007.

[9] C. Mi and W. Xia, *Prioritizing technical requirements in QFD by integrating grey relational analysis method and analytic network process approach*, Grey Systems: Theory and Application, vol. 5(1), pp. 117 – 126, 2015

[10] F. Rahimnia, M. Moghadasian and E. Mashreghi, *Application of grey theory organizational approach to evaluation of organizational vision*, Grey Systems: Theory and Application, vol. 1, (1), pp. 33–46, 2011.

[11] T. L. Saaty, *Principia Mathematica Decernendi: Mathematical Principles of Decision Making*, Pittsburgh, Pennsylvania: RWS Publications, 2010.

[12] T. L. Saaty, M. S. Ozdemir and J. S. Shang, *The Rationality of Punishment - Measuring the Severity of Crimes: An AHP-Based Orders-of-Magnitude Approach*, International Journal of Information Technology and Decision Making, vol. 14(1), pp. 5–16, 2015.

[13] X. Shen and Z. Lu, *The Application of Grey Theory Model in the Predication of Jiangsu Province's Electric Power Demand*, 2nd AASRI Conference on Power and Energy Systems (PES2013), AASRI Procedia, vol. 7, pp. 81–87, 2014.

[14] M-S. Yin, *Fifteen years of grey system theory research: A historical review and bibliometric analysis*, Expert Systems with Applications, vol. 40(7), pp. 2767–2775, 2013.

[15] J. Wang, *Multi-criteria decision-making approach with incomplete certain information based on ternary AHP*, Journal of Systems Engineering and Electronics, vol. 17(1), pp. 109–114, 2006.

[16] J. E. Whitesitt, Boolean Algebra and Its Applications, Dover Publications, 1995.

[17] http://www.helcom.fi/shipping/waste/en_GB/waste/

[18] http://www.bristolport.co.uk/sites/default/pfiles/files/bpc-waste-management-plan-2013-issue-3-revision-2-final.pdf

A Comparison between Regression, Artificial Neural Networks and Support Vector Machines for Predicting Stock Market Index

Alaa F. Sheta
Computers and Systems Department
Electronics Research Institute Giza,
Egypt

Sara Elsir M. Ahmed
Computer Science Department
Sudan University of Science and Technology
Khartoum, Sudan

Hossam Faris
Business Information Tech. Dept.
The University of Jordan
Amman, Jordan

Abstract—Obtaining accurate prediction of stock index significantly helps decision maker to take correct actions to develop a better economy. The inability to predict fluctuation of the stock market might cause serious profit loss. The challenge is that we always deal with dynamic market which is influenced by many factors. They include political, financial and reserve occasions. Thus, stable, robust and adaptive approaches which can provide models have the capability to accurately predict stock index are urgently needed. In this paper, we explore the use of Artificial Neural Networks (ANNs) and Support Vector Machines (SVM) to build prediction models for the S&P 500 stock index. We will also show how traditional models such as multiple linear regression (MLR) behave in this case. The developed models will be evaluated and compared based on a number of evaluation criteria.

Index Terms—Stock Market Prediction; S&P 500; Regression; Artificial Neural Networks; Support Vector Machines.

I. Introduction

Understanding the nature of the relationships between financial markets and the country economy is one of the major components for any financial decision making system [1]–[3]. In the past few decades, stock market prediction became one of the major fields of research due to its wide domain of financial applications. Stock market research field was developed to be dynamic, non-linear, complicated, non-parametric, and chaotic in nature [4]. Much research focuses on improving the quality of index prediction using many traditional and innovative techniques. It was found that significant profit can be achieved even with slight improvement in the prediction since the volume of trading in stock markets is always huge. Thus, financial time series forecasting was explored heavenly in the past. They have shown many characteristics which made them hard to forecast due to the need for traditional statistical method to solve the parameter estimation problems. According to the research developed in this field, we can classify the techniques used to solve the stock market prediction problems to two folds:

- **Econometric Models**: These are statistical based approaches such as linear regression, Auto-regression and Auto-regression Moving Average (ARMA) [5], [6]. There are number of assumptions need to be considered

while using these models such as linearity and stationary of the the financial time-series data. Such non-realistic assumptions can degrade the quality of prediction results [7], [8].

- **Soft Computing based Models**: Soft computing is a term that covers artificial intelligence which mimic biological processes. These techniques includes Artificial Neural Networks (ANN) [9], [10], Fuzzy logic (FL) [11], Support Vector Machines (SVM) [12], particle swarm optimization (PSO) [13] and many others.

ANNs known to be one of the successfully developed methods which was widely used in solving many prediction problem in diversity of applications [14]–[18]. ANNs was used to solve variety of problems in financial time series forecasting. For example, prediction of stock price movement was explored in [19]. Authors provided two models for the daily Istanbul Stock Exchange (ISE) National 100 Index using ANN and SVM. Another type of ANN, the radial basis function (RBF) neural network was used to forecast the stock index of the Shanghai Stock Exchange [20]. In [21], ANNs were trained with stock data from NASDAQ, DJIA and STI index. The reported results indicated that augmented ANN models with trading volumes can improve forecasting performance in both medium-and long-term horizons. A comparison between SVM and Backpropagation (BP) ANN in forecasting six major Asian stock markets was reported in [22]. Other soft computing techniques such as Fuzzy Logic (FL) have been used to solve many stock market forecasting problems [23], [24].

Evolutionary computation was also explored to solve the prediction problem for the S&P 500 stock index. Genetic Algorithms (GAs) was used to simultaneously optimize all of a Radial Basis Function (RBF) network parameters such that an efficient time-series is designed and used for business forecasting applications [25]. In [26], author provided a new prediction model for the S&P 500 using Multigene Symbolic Regression Genetic Programming (GP). Multigene GP shows more robust results especially in the validation/testing case than ANN.

In this paper, we present a comparison between traditional regression model, the ANN model and the SVM model for predicting the S&P 500 stock index. This paper is structured as follows. Section II gives a brief idea about the S&P 500 Stock Index in the USA. In Section III, we provide an introduction to linear regression models. A short introduction to ANN and SVM is provided in Section IV and Section V, respectively. The adopted evaluation methods are presented in Section VI. In Section VII, we describe the characteristics of the data set used in this study. We also provide the experimental setup and results produced in this research.

II. S&P 500 Stock Index

The S&P 500, or the Standard & Poor's 500, is an American stock market index. The S&P 500 presented its first stock index in the year 1923. The S&P 500 index with its current form became active on March 4, 1957. The index can be estimated in real time. It is mainly used to measure the stock prices levels. It is computed according to the market capitalization of 500 large companies. These companies are having stock in the The New York Stock Exchange (NYSE) or NASDAQ. The S&P 500 index is computed by S&P Dow Jones Indices. In the past, there were a growing interest on measuring, analyzing and predicting the behavior of the S&P 500 stock index [27]–[29]. John Bogle, Vanguard's founder and former CEO, who started the first S&P index fund in 1975 stated that:

> The rise in the S&P 500 is a virtual twin to the rise in the total U.S. stock market, so of course investors, and especially index fund investors, who received their fair share of those returns, feel wealthier,"

In order to compute the price of the S&P 500 Index, we have to compute the sum of market capitalization of all the 500 stocks and divide it by a factor, which is defined as the Divisor (D). The formula to calculate the S&P 500 Index value is given as:

$$Index\ Level = \frac{\sum P_i \times S_i}{D}$$

P is the price of each stock in the index and S is the number of shares publicly available for each stock.

III. Regression Analysis

Regression analysis have been used effectively to answer many question in the way we handle system modeling and advance associations between problem variables. It is important to develop such a relationships between variables in many cases such as predicting stock market [13], [14], [30], [31]. It is important to understand how stock index move over time.

A. Single Linear Regression

In order to understand how linear regression works, assume we have n pairs of observations data set $\{x_i, y_j\}_{i=1,..,n}$ as given in Figure 1. Our objective is to develop a simple relationship between the two variables x (i.e. input variable)
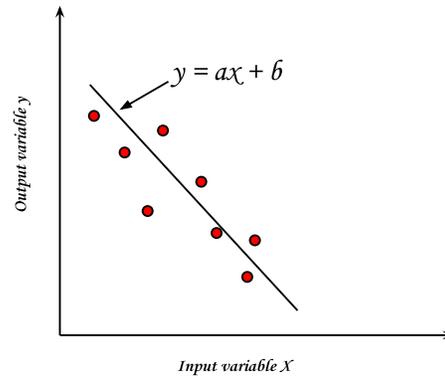

Fig. 1. Simple Linear Model

and y (i.e output variable) so that we can develop a line equation (see Equation 1).

$$y = a + bx \tag{1}$$

where a is a constant (i.e. bias) and b is the slope of the line. It is more likely that the straight line will not pass by all the points in the graph. Thus, Equation 1 shall be re-written as follows:

$$y = a + bx + \epsilon \tag{2}$$

where ϵ represents the error difference between the values of x_i and y_i at any sample i. Thus, to find the best line that produce the most accurate relationship between x and y. We have to formulate the problem as an optimization problem such that we can search and find the best values of the parameters (i.e. $\hat{a}$ and $\hat{b}$). In this case, we need to solve an error minimization problem. To minimize the sum of the error over the whole data set. We need to minimize the function L given in Equation 3.

$$L = \sum_{i=1}^{n} \epsilon_i^2 = \sum_{i=1}^{n} (y_i - a - bx_i)^2 \tag{3}$$

To find the optimal values for $\hat{a}$ and $\hat{b}$ we have to differentiate L with respect to a and b.

$$\frac{\partial L}{\partial \hat{a}} = -2 \sum_{i=1}^{n} (y_i - \hat{a} - \hat{b}x_i) = 0$$

$$\frac{\partial L}{\partial \hat{b}} = -2 \sum_{i=1}^{n} (y_i - \hat{a} - \hat{b}x_i)x_i = 0 \tag{4}$$

By simplification of Equations 4, we get to the following two equations:

$$n\,\hat{a} + \sum_{i=1}^{n} x_i\,\hat{b} = \sum_{i=1}^{n} y_i$$

$$\sum_{i=1}^{n} x_i\,\hat{a} + \sum_{i=1}^{n} x_i^2\,\hat{b} = \sum_{i=1}^{n} x_i y_i \tag{5}$$

Equations 5 is called least square (LS) normal equations. The solution of these normal equations produce the least square estimate for $\hat{a}$ and $\hat{b}$.

B. Multiple Linear Regression

The simple linear model Equation 2 can be expanded to a multivariate system of equations as follows:

$$y = a_1 x_1 + a_2 x_2 + \cdots + a_n x_j \qquad (6)$$

where x_j is the jth independent variable. In this case, we need to use LS estimation to compute the optimal values for the parameters $a_1, \ldots, a_j$. Thus, we have to minimize the optimization function L, which in this case can be presented as:

$$L = \sum_{i=1}^{n} \epsilon_i^2 = \sum_{i=1}^{n} (y_i - \hat{a_1} x_1 - \hat{a_2} x_2 - \ldots \hat{a_n} x_n)^2 \qquad (7)$$

To get the optimal values of the parameters $\hat{a_1}, \ldots, \hat{a_n}$, we have to compute the differentiation for the functions:

$$\frac{\partial L}{\partial \hat{a_1}} = \frac{\partial L}{\partial \hat{a_2}} = \cdots = \frac{\partial L}{\partial \hat{a_j}} = 0 \qquad (8)$$

Solving the set of Equations 8, we can produce the optimal values of the model parameters and solve the multiple regression problem. This solution is more likely to be biased by the available measurements. If you we have large number of observations the computed estimate of the parameters shall be more robust. This technqiue provide poor results when the observations are small in number.

IV. Artificial Neural Networks

ANNs are mathematical models which were inspired from the understanding of some ideas and aspects of the biological neural systems such as the human brain. ANN may be considered as a data processing technique that maps, or relates, some type of input stream of information to an output stream of processing. Variations of ANNs can be used to perform classification, pattern recognition and predictive tasks [15], [19], [20], [22], [30].

Neural network have become very important method for stock market prediction because of their ability to deal with uncertainty and insufficient data sets which change rapidly in very short period of time. In Feedforward (FF) Multilayer Perceptron (MLP), which is one of the most common ANN systems, neurons are organized in layers. Each layer consists of a number of processing elements called neurons; each of which contains a summation function and an activation function. The summation function is given by Equation 9 and an activation function can be a type of sigmoid function as given in Equation 10.

Training examples are used as input the network via the input layer, which is connected to one, or more hidden layers. Information processing takes place in the hidden layer via the connection weights. The hidden layers are connected to an output layer with neurons most likely have linear sigmoid function. A learning algorithms such as the BP one might be used to adjust the ANN weights such that it minimize the error difference between the actual (i.e. desired) output and the ANN output [32]–[34].

$$S = \sum_{i=0}^{n} w_i x_i \qquad (9)$$

$$\phi(S) = \frac{1}{1 + e^{-S}} \qquad (10)$$

There are number of tuning parameters should be designated before we can use ANN to learn a problem. They include: the number of layers in the hidden layer, the type of sigmoid function for the neurons and the adopted learning algorithm.

V. Support vector machines

Support vector machine is a powerful supervised learning model for prediction and classification. SVM was first introduced by Vladimir Vapnik and his co-workers at AT&T Bell Laboratories [35]. The basic idea of SVM is to map the training data into higher dimensional space using a nonlinear mapping function and then perform linear regression in higher dimensional space in order to separate the data [36]. Data mapping is performed using a predetermined kernel function. Data separation is done by finding the optimal hyperplane (called the Support Vector with the maximum margin from the separated classes. Figure 2 illustrates the idea of the optimal hyperplane in SVM that separates two classes. In the left part of the figure, lines separated data but with small margins while on the right an optimal line separates the data with the maximum margins.

A. Learning Process in SVM

Training SVM can be described as follows; suppose we have a data set $\{x_i, y_j\}_{i=1,\ldots,n}$ where the input vector $x_i \in \Re^d$ and the actual $y_i \in \Re$. The modeling objective of SVM is to find the linear decision function represented in the following equation:

$$f(x) \leq w, \ \ \phi_i(x) > +b \qquad (11)$$

where w and b are the weight vector and a constant respectively, which have to be estimated from the data set. ϕ is a nonlinear mapping function. This regression problem can be formulated as to minimize the following regularized risk function:

$$R(C) = \frac{C}{n} \sum_{i=1}^{n} L_\varepsilon(f(x_i), y_i) + \frac{1}{2} \|w\|^2 \qquad (12)$$

where $L_\varepsilon(f(x_i), y_i)$ is known as $\varepsilon-$intensive loss function and given by the following equation:

$$L_\varepsilon(f(x), y) = \begin{cases} |f(x) - y| - \varepsilon & |f(x) - y| \geq \varepsilon \\ 0 & otherwise \end{cases} \qquad (13)$$

To measure the degree of miss classification to achieve an acceptable degree of error, we use slack variables ξ_i and
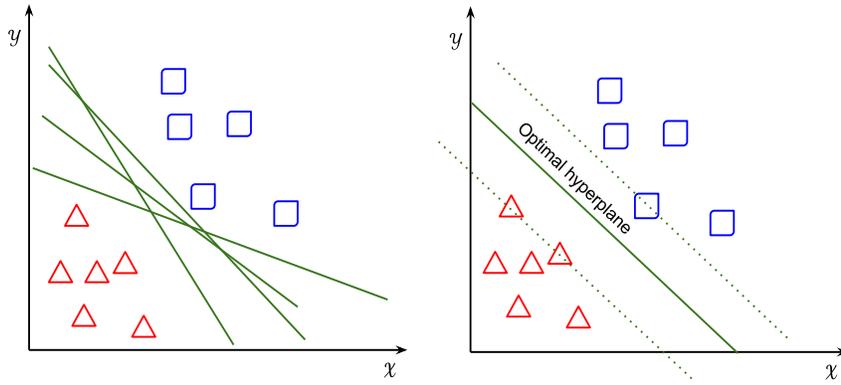
Fig. 2. Optimal hyperplane in Support Vector Machine
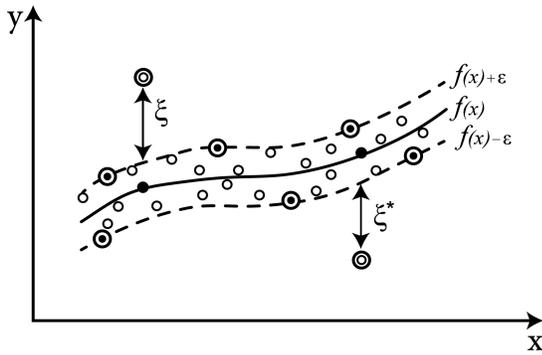
Fig. 3. Optimal hyperplane with slack variables

ξ_i^* as shown in Figure 3. This addition makes the problem presented as a constrained minimum optimization problem (See Equation 14).

$$Min. \; R(w, \xi_i^*) = \frac{1}{2} \|w\|^2 + C \sum_{i=1}^{n} (\xi_i + \xi_i^*) \qquad (14)$$

Subject to:

$$\begin{cases} y_i - <w, x_i> -b & \leq \varepsilon + \xi_i \\ <w, x_i> +b - y_i & \leq \varepsilon + \xi_i^* \\ \xi_i, \xi_i^* & \geq 0 \end{cases} \qquad (15)$$

where C is a regularized constant greater than zero. Thus it performs a balance between the training error and model flatness. C represents a penalty for prediction error that is greater than ε. ξ_i and ξ_i^* are slack variables that form the distance from actual values to the corresponding boundary values of ε. The objective of SVM is to minimize ξ_i, ξ_i^* and w^2.

The above optimization with constraint can be converted by means of Lagrangian multipliers to a quadratic programming problem. Therefore, the form of the solution can be given by the following equation:

$$f(x) = \sum_{i=1}^{n} (\alpha_i - \alpha_i^*) K(x_i, x) + b \qquad (16)$$

TABLE I
COMMON SVM KERNEL FUNCTIONS

Polynomial Kernel	$K(x_i, x_j) = (x_i.x_j + 1)^d$
Hyperbolic Tangent Kernel	$K(x_i, x_j) = tanh(c_1(x_i.x_j) + c_2)$
Radial Basis Kernel	$p: K(x_i, x_j) = exp(|x_j - x_i|/2p^2)$

where α_i and α_i^* are Lagrange multipliers. Equation 16 is subject to the following constraints:

$$\sum_{i=1}^{n} (\alpha_i - \alpha_i^*) = 0 \qquad (17)$$

$$0 \leq \alpha_i \leq C \quad i = 1, \dots, n$$

$$0 \leq \alpha_i^* \leq C \quad i = 1, \dots, n$$

$K(.)$ is the kernel function and its values is an inner product of two vectors x_i and x_j in the feature space $\phi(x_i)$ and $\phi(x_j)$ and satisfies the Mercer's condition. Therefore,

$$K(x_i, x_j) = \phi(x_i).\phi(x_j) \qquad (18)$$

Some of the most common kernel functions used in the literature are shown in Table I. In general, SVMs have many advantages over classical classification approaches like artificial neural networks, decision trees and others. These advantages include: good performance in high dimensional spaces; and the support vectors rely on a small subset of the training data which gives SVM a great computational advantage.

VI. EVALUATION CRITERION

In order to assess the performance of the developed stock market predication models, a number of evaluation criteria will be used to evaluate these models. These criteria are applied to measure how close the real values to the values predicted using the developed models. They include Mean Absolute Error (MAE), Root Mean Square Error (RMSE) and correlation coefficient R. They are given in Equations 19, 20 and 21, respectively.

$$MAE = \frac{1}{n} \sum_{t=1}^{n} |(y_i - \hat{y}_i)| \qquad (19)$$

$$RMSE = \sqrt{\frac{1}{n} \sum_{i=1}^{n} (y_i - \hat{y}_i)^2} \qquad (20)$$

$$R = \frac{\sum_{i=1}^{n}(y_i - \overline{y})(\hat{y}_i - \overline{\hat{y}})}{\sqrt{\sum_{i=1}^{n}(y_i - \overline{y})^2 \sum_{i=1}^{n}(\hat{y}_i - \overline{\hat{y}})^2}} \qquad (21)$$

where y is actual stock index values, $\hat{y}$ is the estimated values using the proposed technqiues. n is the total number of measurements.

VII. EXPERIMENTAL RESULTS

A. S&P 500 Data Set

In this work, we use 27 potential financial and economic variables that impact the stock movement. The main consideration for selecting the potential variables is whether they have significant influence on the direction of (S&P 500) index in the next week. While some of these features were used in previous studies [30]. The list, the description, and the sources of the potential features are given in Table III show the 27 features of data set.

The categories of these features include: S&P 500 index return in three previous days SPY(t-1), SPY(t-2), SPY(t-3); Financial and economic indicators (Oil, Gold, CTB3M, AAA); The return of the five biggest companies in S&P 500 (XOM, GE, MSFT, PG, JNJ); Exchange rate between USD and three other currencies (USD-Y, USD-GBP, USD-CAD); The return of the four world major indices (HIS, FCHI, FTSE, GDAXI); and S&P 500 trading volume (V).

S&P 500 stock market data set used in our case consists of 27 features and 1192 days of data, which cover five-year period starting 7 December 2009 to 2 September 2014. We sampled the data on a weekly basis such that only 143 samples were used in our experiments. The S&P 500 data were split into 100 samples as training set and data for 43 samples as testing set.

B. Multiple Regression Model

The regression model shall have the following equation system.

$$y = a_0 + \sum_{i=1}^{27} a_i x_i \qquad (22)$$

The values of the parameters $a's$ shall be estimated using LS estimation to produce the optimal values of the parameters $\hat{a}'s$. The produced linear regression model can be presented as given in Table II. The actual and Estimated S&P 500 index values based the MLR in both training and testing cases are shown in Figure 4 and Figure 5. The scattered plot of the actual and predicted responses is shown in Figure 6.
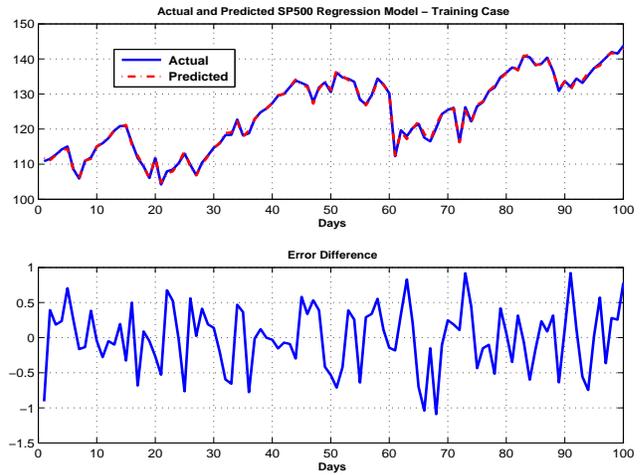

Fig. 4. Regression: Actual and Estimated S&P 500 Index values in Training Case
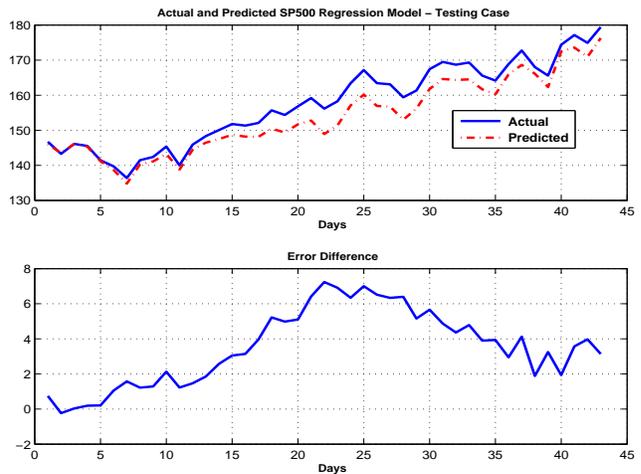
Fig. 5. Regression: Actual and Estimated S&P 500 Index values in Testing Case
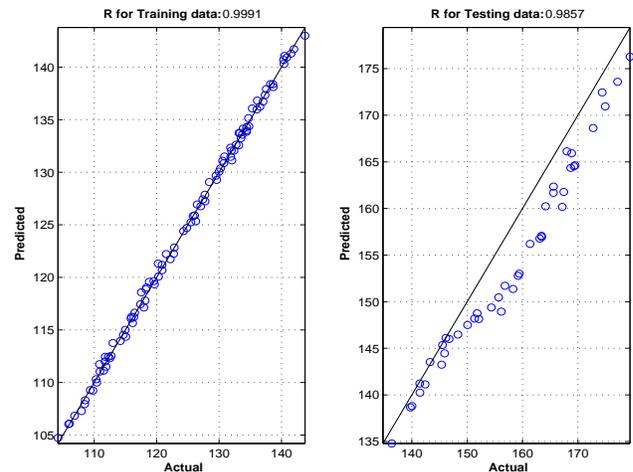

Fig. 6. Regression Scattered Plot

TABLE II
A REGRESSION MODEL WITH INPUTS: $x_1, \ldots, x_{27}$

$$
\begin{aligned}
\hat{y} = \quad & -0.0234 * x_1 + 0.13 * x_2 + 0.021 * x_3 + 0.021 * x_4 - 0.021 * x_5 \\
- \quad & 10.303 * x_6 + 6.0031 * x_7 + 0.7738 * x_8 + 0.2779 * x_9 - 0.43916 * x_{10} \\
- \quad & 0.27754 * x_{11} + 0.12733 * x_{12} - 0.058638 * x_{13} + 13.646 * x_{14} + 9.5224 * x_{15} \\
- \quad & 0.0003 * x_{16} + 0.24856 * x_{17} - 0.0016 * x_{18} + 0 * x_{19} - 2.334 \times 10^{-9} * x_{20} \\
+ \quad & 0.16257 * x_{21} + 0.63767 * x_{22} - 0.14301 * x_{23} + 0.08 * x_{24} + 0.074 * x_{25} \\
- \quad & 0.0002 * x_{26} + 0.026301 * x_{27} + 6.9312
\end{aligned}
\tag{23}
$$

TABLE III
THE 27 POTENTIAL INFLUENTIAL FEATURES OF THE S&P 500 INDEX [30]

Variable	Feature	Description
x_1	SPY(t-1)	The return of the S&P 500 index in day $t-1$ Source data: finance.yahoo.com
x_2	SPY(t-2)	The return of the S&P 500 index in day $t-2$ Source data: finance.yahoo.com
x_3	SPY(t-3)	The return of the S&P 500 index in day $t-3$ Source data: finance.yahoo.com
x_4	Oil	Relative change in the price of the crude oil Source data: finance.yahoo.com
x_5	Gold	Relative change in the gold price Source data: www.usagold.com
x_6	CTB3M	Change in the market yield on US Treasury securities at 3-month constant maturity, quoted on investment basis Source data: H.15 Release - Federal Reserve Board of Governors
x_7	AAA	Change in the Moody's yield on seasoned corporate bonds - all industries, Aaa Source data: H.15 Release - Federal Reserve Board of Governors
x_8	XOM	Exxon Mobil stock return in day t-1 Source data: finance.yahoo.com
x_9	GE	General Electric stock return in day t-1 Source data: finance.yahoo.com
x_{10}	MSFT	Micro Soft stock return in day t-1 Source data: finance.yahoo.com
x_{11}	PG	Procter and Gamble stock return in day t-1 Source data: finance.yahoo.com
x_{12}	JNJ	Johnson and Johnson stock return in day t-1 Source data: finance.yahoo.com
x_{13}	USD-Y	Relative change in the exchange rate between US dollar and Japanese yen Source data: OANDA.com
x_{14}	USD-GBP	Relative change in the exchange rate between US dollar and British pound Source data: OANDA.com
x_{15}	USD-CAD	Relative change in the exchange rate between US dollar and Canadian dollar Source data: OANDA.com
x_{16}	HIS	Hang Seng index return in day t-1 Source data: finance.yahoo.com
x_{17}	FCHI	CAC 40 index return in day t-1 Source data: finance.yahoo.com
x_{18}	FTSE	FTSE 100 index return in day t-1 Source data: finance.yahoo.com
x_{19}	GDAXI	DAX index return in day t-1 Source data: finance.yahoo.com
x_{20}	V	Relative change in the trading volume of S&P 500 index Source data: finance.yahoo.com
x_{21}	CTB6M	Change in the market yield on US Treasury securities at 6-month constant maturity, quoted on investment basis Source data: H.15 Release - Federal Reserve Board of Governors
x_{22}	CTB1Y	Change in the market yield on US Treasury securities at 1-year constant maturity, quoted on investment basis Source data: H.15 Release - Federal Reserve Board of Governors
x_{23}	CTB5Y	Change in the market yield on US Treasury securities at 5-year constant maturity, quoted on investment basis Source data: H.15 Release - Federal Reserve Board of Governors
x_{24}	CTB10Y	Change in the market yield on US Treasury securities at 10-year constant maturity, quoted on investment basis Source data: H.15 Release - Federal Reserve Board of Governors
x_{25}	BBB	Change in the Moody's yield on seasoned corporate bonds - all industries, Baa Source data: H.15 Release - Federal Reserve Board of Governors
x_{26}	DJI	Dow Jones Industrial Average index return in day t-1 Source data: finance.yahoo.com
x_{27}	IXIC	NASDAQ composite index return in day t-1 Source data: finance.yahoo.com

C. Developed ANN Model

The proposed architecture of the MLP Network consists of three layers with single hidden layer. Thus input layer of our neural network model has 27 input nodes while the output layer consists of only one node that gives the predicted next week value. Empirically, we found that 20 neurons in the hidden layer achieved the best performance. The BP algorithm is used to train the MLP and update its weight. Table IV shows the settings used for MLP. Figure 7 and Figure 8 show the actual and predicted stock prices for training and testing cases of the developed ANN. The scattered plot for the developed ANN model is shown in Figure 9.

D. Developed SVM Model

SVM with an RBF kernel is used to develop the S&P 500 index model. The RBF kernel has many advantages such as

TABLE IV
THE SETTING OF MLP

Maximum number of epochs	500
Number of Hidden layer	1
Number of neurons in hidden layer	20
Learning rate	0.5
Momentum	0.2

the ability to map non-linearly the training data and the ease of implementation [37]–[39]. The values of the parameters C and σ have high influence on the accuracy of the SVM model. Therefore, we used grid search to obtain these values. It was found that the best performance can be obtained with $C = 100$ and $\sigma = 0.01$. Figure 10 and Figure 11 show the actual and predicted stock prices for training and testing cases of the developed SVM model. The scattered plot for the developed SVM model is shown in Figure 12.
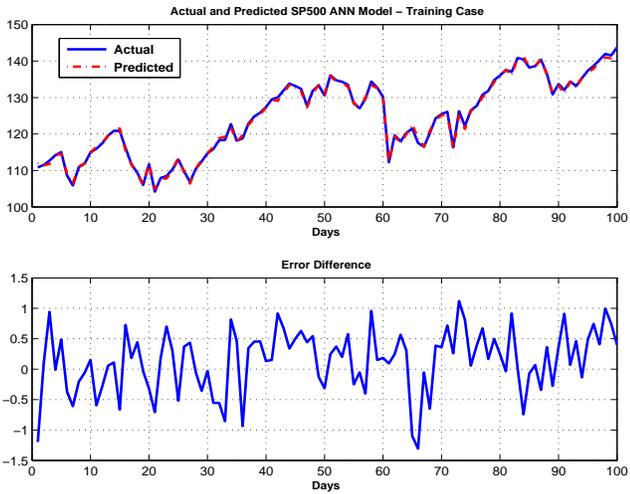
Fig. 7.   ANN: Actual and Estimated S&P 500 Index values in Training Case
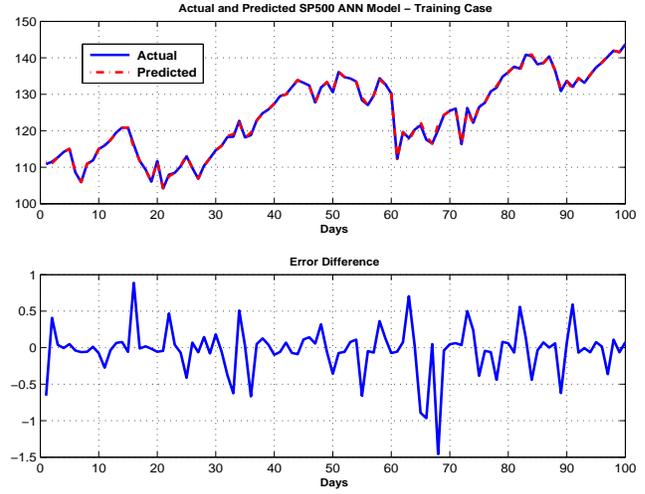
Fig. 10.   SVM: Actual and Estimated S&P 500 Index values in Training Case
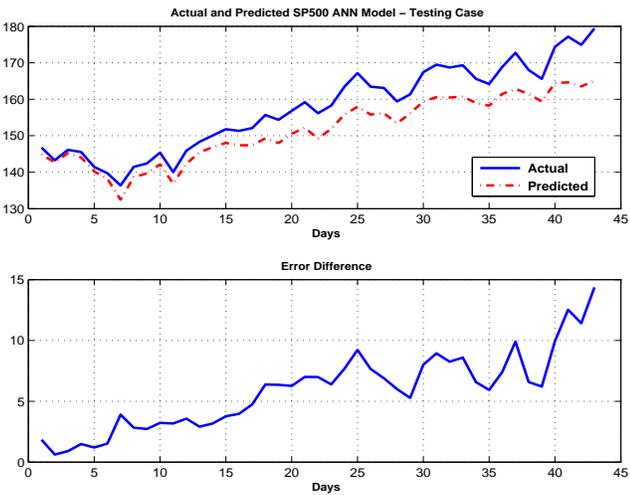

Fig. 8.   ANN: Actual and Estimated S&P 500 Index values in Testing Case
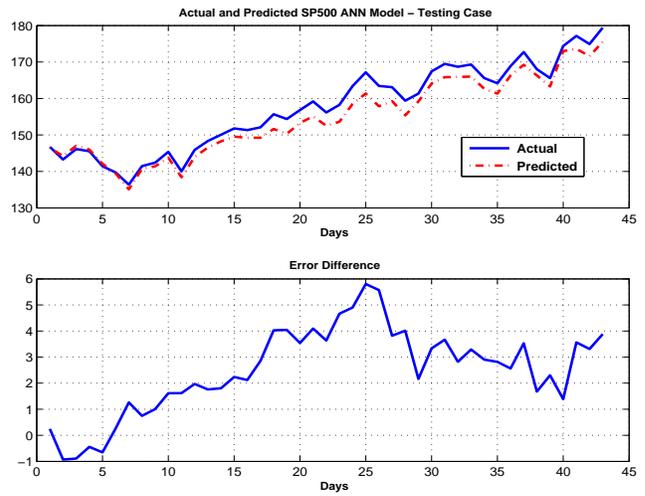
Fig. 11.   SVM: Actual and Estimated S&P 500 Index values in Testing Case
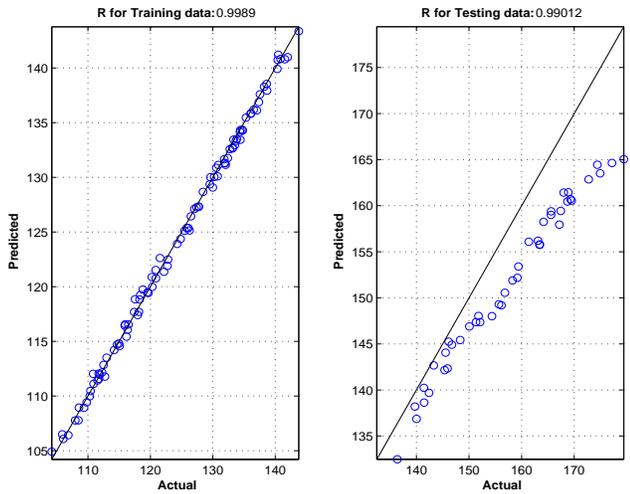

Fig. 9.   ANN Scattered Plot
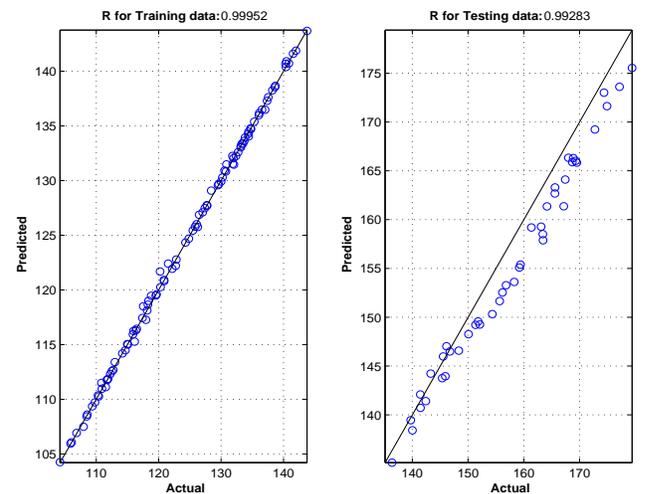
Fig. 12.   SVM Scattered Plot

E. Comments on the Results

The calculated evaluation criterion of the regression, MLP and SVM models for training and testing cases are shown in Table V. Based on these results it can be noticed that SVM outperformed the MLP and MLR models in both training and testing cases. SVMs has many advantages such as using various kernels which allows the algorithm to suits many classification problems. SVM are more likely to avoid the problem of falling into local minimum.

VIII. CONCLUSIONS AND FUTURE WORK

In this paper, we explored the use MLP and SVM to develop models for prediction the S&P 500 stock market index. A 27 potential financial and economic variables which impact the stock movement were adopted to build a relationship between the stock index and these variables. The basis for choosing these variables was based on their substantial impact on the course of S&P 500 index. The data set was sampled on a weekly bases. The developed SVM model with RBF kernel model provided good prediction capabilities with respect to the regression and ANN models. The results were validated using number of evaluation criteria. Future research shall focus on exploring other soft computing techniques to solve the stock market prediction problems.

REFERENCES

[1] S. Hoti, M. McAleer, and L. L. Pauwels, "Multivariate volatility in environmental finance," *Math. Comput. Simul.*, vol. 78, no. 2-3, pp. 189–199, Jul. 2008. [Online]. Available: http://dx.doi.org/10.1016/j.matcom.2008.01.038

[2] Q. Wen, Z. Yang, Y. Song, and P. Jia, "Automatic stock decision support system based on box theory and svm algorithm," *Expert System Application*, vol. 37, no. 2, pp. 1015–1022, Mar. 2010. [Online]. Available: http://dx.doi.org/10.1016/j.eswa.2009.05.093

[3] M. Kampouridis, A. Alsheddy, and E. Tsang, "On the investigation of hyper-heuristics on a financial forecasting problem," *Annals of Mathematics and Artificial Intelligence*, vol. 68, no. 4, pp. 225–246, Aug. 2013. [Online]. Available: http://dx.doi.org/10.1007/s10472-012-9283-0

[4] T. Z. Tan, C. Quek, and G. S. Ng, "Brain-inspired genetic complementary learning for stock market prediction," in *Proceedings of the IEEE Congress on Evolutionary Computation, CEC 2005, 2-4 September 2005, Edinburgh, UK*, 2005, pp. 2653–2660. [Online]. Available: http://dx.doi.org/10.1109/CEC.2005.1555027

[5] A. C. Harvey and P. H. J. Todd, "Forecasting economic time series with structural and box-jenkins models: A case study," *Journal of Business & Economic Statistics*, vol. 1, no. 4, pp. 299–307, 1983. [Online]. Available: http://dx.doi.org/10.2307/1391661

[6] Y. B. Wijaya, S. Kom, and T. A. Napitupulu, "Stock price prediction: Comparison of ARIMA and artificial neural network methods - an indonesia stock's case," in *Proceedings of the 2010 Second International Conference on Advances in Computing, Control, and Telecommunication Technologies*, ser. ACT'10. Washington, DC, USA: IEEE Computer Society, 2010, pp. 176–179. [Online]. Available: http://dx.doi.org/10.1109/ACT.2010.45

[7] L. Yu, S. Wang, and K. K. Lai, "A neural-network-based nonlinear metamodeling approach to financial time series forecasting," *Appl. Soft Comput.*, vol. 9, no. 2, pp. 563–574, Mar. 2009. [Online]. Available: http://dx.doi.org/10.1016/j.asoc.2008.08.001

[8] S. Walczak, "An empirical analysis of data requirements for financial forecasting with neural networks," *J. Manage. Inf. Syst.*, vol. 17, no. 4, pp. 203–222, Mar. 2001. [Online]. Available: http://dl.acm.org/citation.cfm?id=1289668.1289677

[9] M.-D. Cubiles-de-la Vega, R. Pino-Mejías, A. Pascual-Acosta, and J. Muñoz García, "Building neural network forecasting models from time series ARIMA models: A procedure and a comparative analysis," *Intell. Data Anal.*, vol. 6, no. 1, pp. 53–65, Jan. 2002. [Online]. Available: http://dl.acm.org/citation.cfm?id=1293993.1293996

[10] R. Majhi, G. Panda, and G. Sahoo, "Efficient prediction of exchange rates with low complexity artificial neural network models," *Expert System Application*, vol. 36, no. 1, pp. 181–189, Jan. 2009. [Online]. Available: http://dx.doi.org/10.1016/j.eswa.2007.09.005

[11] M. R. Hassan, "A combination of hidden markov model and fuzzy model for stock market forecasting," *Neurocomputing*, vol. 72, no. 1618, pp. 3439 – 3446, 2009. [Online]. Available: http://www.sciencedirect.com/science/article/pii/S0925231209001805

[12] W. Huang, Y. Nakamori, and S. Wang, "Forecasting stock market movement direction with support vector machine," *Computers & Operations Research*, vol. 32, no. 10, pp. 2513–2522, 2005.

[13] R. Majhi, G. Panda, G. Sahoo, A. Panda, and A. Choubey, "Prediction of S&P 500 and DJIA stock indices using particle swarm optimization technique," in *The IEEE World Congress on Computational Intelligence on Evolutionary Computation (CEC2008)*. IEEE, 2008, pp. 1276–1282.

[14] Y. Zhang and L. Wu, "Stock market prediction of S&P 500 via combination of improved bco approach and bp neural network," *Expert Syst. Appl.*, vol. 36, no. 5, pp. 8849–8854, 2009.

[15] S. O. Olatunji, M. Al-Ahmadi, M. Elshafei, and Y. A. Fallatah, "Saudi arabia stock prices forecasting using artificial neural networks," pp. 81–86, 2011.

[16] T.-S. Chang, "A comparative study of artificial neural networks, and decision trees for digital game content stocks price prediction," *Expert Syst. Appl.*, vol. 38, no. 12, pp. 14 846–14 851, Nov. 2011. [Online]. Available: http://dx.doi.org/10.1016/j.eswa.2011.05.063

[17] E. Guresen, G. Kayakutlu, and T. U. Daim, "Using artificial neural network models in stock market index prediction," *Expert System Application*, vol. 38, no. 8, pp. 10 389–10 397, Aug. 2011. [Online]. Available: http://dx.doi.org/10.1016/j.eswa.2011.02.068

[18] P.-C. Chang, D.-D. Wang, and C.-L. Zhou, "A novel model by evolving partially connected neural network for stock price trend forecasting," *Expert Syst. Appl.*, vol. 39, no. 1, pp. 611–620, Jan. 2012. [Online]. Available: http://dx.doi.org/10.1016/j.eswa.2011.07.051

[19] Y. Kara, M. Acar Boyacioglu, and O. K. Baykan, "Predicting direction of stock price index movement using artificial neural networks and support vector machines: The sample of the istanbul stock exchange," *Expert Syst. Appl.*, vol. 38, no. 5, pp. 5311–5319, May 2011. [Online]. Available: http://dx.doi.org/10.1016/j.eswa.2010.10.027

[20] W. Shen, X. Guo, C. Wu, and D. Wu, "Forecasting stock indices using radial basis function neural networks optimized by artificial fish swarm algorithm," *Know.-Based Syst.*, vol. 24, no. 3, pp. 378–385, Apr. 2011. [Online]. Available: http://dx.doi.org/10.1016/j.knosys.2010.11.001

[21] X. Zhu, H. Wang, L. Xu, and H. Li, "Predicting stock index increments by neural networks: The role of trading volume under different horizons," *Expert System Application*, vol. 34, no. 4, pp. 3043–3054, May 2008. [Online]. Available: http://dx.doi.org/10.1016/j.eswa.2007.06.023

[22] W.-H. Chen, J.-Y. Shih, and S. Wu, "Comparison of support-vector machines and back propagation neural networks in forecasting the six major asian stock markets," *International Journal of Electron Finance*, vol. 1, no. 1, pp. 49–67, Jan. 2006. [Online]. Available: http://dx.doi.org/10.1504/IJEF.2006.008837

[23] P.-C. Chang, C.-Y. Fan, and J.-L. Lin, "Trend discovery in financial time series data using a case based fuzzy decision tree," *Expert System Application*, vol. 38, no. 5, pp. 6070–6080, May 2011. [Online]. Available: http://dx.doi.org/10.1016/j.eswa.2010.11.006

[24] M. R. Hassan, K. Ramamohanarao, J. Kamruzzaman, M. Rahman, and M. Maruf Hossain, "A HMM-based adaptive fuzzy inference system for stock market forecasting," *Neurocomput.*, vol. 104, pp. 10–25, Mar. 2013. [Online]. Available: http://dx.doi.org/10.1016/j.neucom.2012.09.017

[25] A. F. Sheta and K. De Jong, "Time-series forecasting using ga-tuned radial basis functions," *Inf. Sci. Inf. Comput. Sci.*, vol. 133, no. 3-4, pp. 221–228, Apr. 2001. [Online]. Available: http://dx.doi.org/10.1016/S0020-0255(01)00086-X

[26] A. Sheta, S. E. M. Ahmed, and H. Faris, "Evolving stock market prediction models using multi-gene symbolic regression genetic programming," *Artificial Intelligence and Machine Learning AIML*, vol. 15, pp. 11–20, 6 2015.

TABLE V
EVALUATION CRITERIA FOR THE DEVELOPED MODELS

	Regression		ANN		SVM-RBF	
	Training	Testing	Training	Testing	Training	Testing
Correlation coefficient	0.998	0.995	0.999	0.990	0.9995	0.9928
Mean absolute error	0.373	4.961	0.433	5.869	0.1976	2.6454
Root mean squared error	0.482	5.749	0.529	6.666	0.3263	3.0006
Relative absolute error	4.429%	11.838%	4.683%	58.335%	2.134%	7.993%
Root relative squared error	4.982%	12.313%	5.040%	57.569%	3.109%	8.5579%

[27] D. D. Thomakos, T. Wang, and J. Wu, "Market timing and cap rotation," *Math. Comput. Model.*, vol. 46, no. 1-2, pp. 278–291, Jul. 2007. [Online]. Available: http://dx.doi.org/10.1016/j.mcm.2006.12.036

[28] S. Lahmiri, "Multi-scaling analysis of the S&P500 under different regimes in wavelet domain," *Int. J. Strateg. Decis. Sci.*, vol. 5, no. 2, pp. 43–55, Apr. 2014. [Online]. Available: http://dx.doi.org/10.4018/ijsds.2014040104

[29] S. Lahmiri, M. Boukadoum, and S. Chartier, "Exploring information categories and artificial neural networks numerical algorithms in S&P500 trend prediction: A comparative study," *Int. J. Strateg. Decis. Sci.*, vol. 5, no. 1, pp. 76–94, Jan. 2014. [Online]. Available: http://dx.doi.org/10.4018/IJSDS.2014010105

[30] S. T. A. Niaki and S. Hoseinzade, "Forecasting s&p500 index using artificial neural networks and design of experiments," *Journal of Industrial Engineering International*, vol. 9, no. 1, pp. 1–9, 2013.

[31] A. Sheta, H. Faris, and M. Alkasassbeh, "A genetic programming model for S&P 500 stock market prediction," *International Journal of Control and Automation*, vol. 6, pp. 303–314, 2013.

[32] A. Nigrin, *Neural networks for pattern recognition*, ser. A Bradford book. Cambridge, Mass, London: The MIT Press, 1993. [Online]. Available: http://opac.inria.fr/record=b1126290

[33] J. Leonard and M. A. Kramer, "Improvement of the backpropagation algorithm for training neural networks," *Computer Chemical Engineering*, vol. 14, pp. 337–343, 1990.

[34] A. K. Jain, J. Mao, and K. Mohiuddin, "Artificial neural networks: A tutorial," *IEEE Computer*, vol. 29, pp. 31–44, 1996.

[35] V. Vapnik, *The Nature of Statistical Learning Theory*. Springer, New York, 1995.

[36] ——, "An overview of statistical learning theory," *IEEE Transactions on Neural Networks*, vol. 5, pp. 988–999, 1999.

[37] Y. B. Dibike, S. Velickov, D. Solomatine, and M. B. Abbott, "Model induction with support vector machines: introduction and applications," *Journal of Computing in Civil Engineering*, 2001.

[38] R. Noori, M. Abdoli, A. A. Ghasrodashti, and M. Jalili Ghazizade, "Prediction of municipal solid waste generation with combination of support vector machine and principal component analysis: A case study of mashhad," *Environmental Progress & Sustainable Energy*, vol. 28, no. 2, pp. 249–258, 2009.

[39] W. Wen-chuan, X. Dong-mei, C. Kwok-wing, and C. Shouyu, "Improved annual rainfall-runoff forecasting using pso–svm model based on eemd," 2013.

Cogntive Consistency Analysis in Adaptive Bio-Metric Authentication System Design

Gahangir Hossain
Electrical & Computer Engineering
Indiana University-Purdue
University Indianapolis
Indianapolis, IN USA

Habibah Khan
Instructional Design & Technology
The University of Memphis
Memphis, TN USA

Md.Iqbal Hossain
Electrical & Computer Engineering
The University of Memphis
Memphis, TN USA

Abstract—**Cognitive consistency analysis aims to continuously monitor one's perception equilibrium towards successful accomplishment of cognitive task. Opposite to cognitive flexibility analysis – cognitive consistency analysis identifies monotone of perception towards successful interaction process (e.g., biometric authentication) and useful in generation of decision support to assist one in need. This study consider fingertip dynamics (e.g., keystroke, tapping, clicking etc.) to have insights on instantaneous cognitive states and its effects in monotonic advancement towards successful authentication process. Keystroke dynamics and tapping dynamics are analyzed based on response time data. Finally, cognitive consistency and confusion (inconsistency) are computed with Maximal Information Coefficient (MIC) and Maximal Asymmetry Score (MAS), respectively. Our preliminary study indicates that a balance between cognitive consistency and flexibility are needed in successful authentication process. Moreover, adaptive and cognitive interaction system requires in depth analysis of user's cognitive consistency to provide a robust and useful assistance.**

Keywords—Cognitive authentication; Cognitive consistency; Fingertip dynamics; Maximal Information Coefficient; Bivatiate plot

I. INTRODUCTION

With the increase of adaptive interfaces including natural gestures, touch-screen, tactile, speech enable, implicit and tangible interactions; fingertips (keystrokes, mouse click and tapping interfaces) are still dominating since their invention [1]. Users like to perform authentic interaction by a fingertip. Slip of tip might hinder the user in robust interaction and authentication process just because of inflexibility of accessibility and authentication schemes. This becomes more challenging when the users need assistance from the interaction system. Meanwhile, the system strategically requires a robust user authentication, adaptation and automation to tie its users continuously into its loop. Question arises: how to maximize authentic accessibility to benefit user in assistive interaction? The challenging accessibility problem requires a different usability engineering solution than we currently practice. Analysis of end-user's cognitive pattern of interaction and deficiencies may improve the future interface accessibility towards authentic and adaptive accessibility design. More specifically, cognitive approach of authentication may allow some flexibility in user authentication process based on users'

past history of success and present consistent interactions (monotone), even though unsuccessful in authentication process.

Cognitive consistency analysis is the fundamental principle in social cognition and important factor in balancing interests through adaptive collaborative system design. The analysis uncovers three key factors that tend toward (cognitive) consistency: perception, emotion, and action. More specifically, the process helps the system to reveal user's intrinsic conscious conflict situation that leads to adaptive behavior.

In an adaptive authentication, cognitive consistency analysis is a critical research process, that aims to (1) identify progressive interests in biometric authentication, (2) develops understanding of inherent meaning, values and motives in cognitive activities, (3) study adaptive interaction trends with connection to current research, (4) construct models of the relations between cognitive capability, personal profile and participants' actions, (5) elucidate the fundamental contradiction which are developing as a result of action based on ideologically frozen understanding, (6) participate in a program to see new ways of the situation, (7) Theoretically ground the principles applied in the analysis.

With the holistic goal of adaptive authentication system development, two specific aims are analyzed through the research. First specific aim is to understand consistent or inconsistent interactions during authentic interaction. The second specific aim is to co-analyze user's past history of successful authentication record with the degree of present cognitive activity to provide an essential decision support in authentication process. This study covers the first aim with two different datasets. Moreover, the conditions with understandings are compared, ideologies are criticized, and immanent possibilities for action are discovered.

The rest of the paper is organized as following: In section 2, gives brief descriptions on cognitive approaches in fingertip dynamics and authentication with general and mixed frameworks. Section 3, explains the methods used in cognitive consistency analysis process. Exploratory analyses of cognitive effort on some benchmark biometric data sets are shown in section 4. Finally, the research is concluded with findings and future works in section 5.

II. Fingertips Dynamics Approaches

Fingertips dynamics includes finger related user interactions including keystroke, key tapping, and mouse clicking. Roman and Vanue [1] reviewed a classification of the state-of-the-art behavioral biometrics related to user's skills, style, preference, knowledge, motor-skills or strategy that users use in their everyday task accomplishment. Fingertips dynamics fall into the behavioral biometrics classification and play an importance role in conjunction to everyday hand related activities. Keystroke dynamics biometric pattern analysis and user modeling are proposed by Killourhy[3]. Subjects typed a strong password and their key pressing response times are recoded to have up key, holding and down key and their combination response analysis. Ahmed and Traore's [2] proposed new biometric fingertips with mouse clicking dynamics, which was improved in Nakkabi et al. [4] in terms of clicking response time. Poh and Tistarelli[9] customized biometric authentication systems by a novel method with discriminative score. Liang et al. [10] proposed a combined analysis of fingertips dynamics with head pose estimation. The real-time fingertip gesture tracking is proposed in Oka et al. [13] which determine an appropriate threshold value for image binarization during initialization by examining the histogram of an image of a user's hand placed open on a desk.
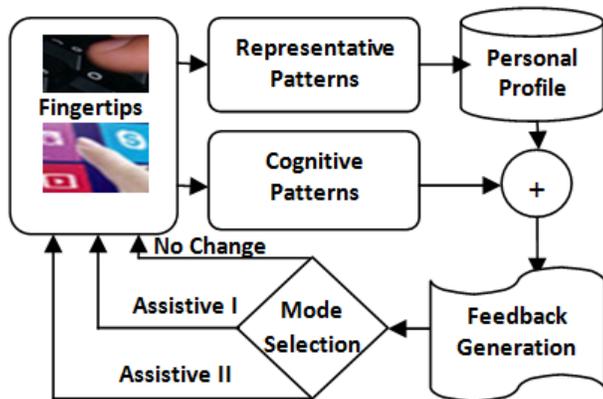

Fig. 1. Overview of proposed cognitive biometric authentication system with flexible feedbacks
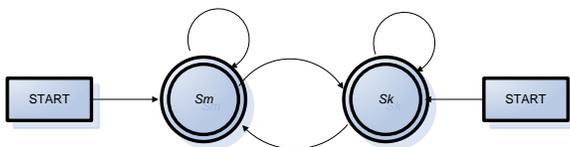

Fig. 2. Keystroke and mouse click are complementary; Sm and Sk stands for the mouse clicking state and keystroke state respectively

Cognitive issues in fingertips includes but not limited to: mental effort, consistencies (monotone) in action, dissonance, bias and more. The cognitive mechanisms of touch are proposed in some works including, Rola [13], Jone et al. [14] gives more elaboration of tactile sensory systems with brain signal analysis. Hossain et al.'s work [5, 6] proposes some relevant cognitive mechanism of cognitive workload during assistive technology interaction. These literatures prove an

important grounding in cognitive analysis of fingertips dynamics. Fishel[9] proposed a direct measure of fingertip strength through a robust micro-vibration sensor for bio-metric fingertips.

A. The General Structure

In keystroke and tapping dynamics, user identifiable patterns are considered as representative patterns and recorded as personal profile. Cognitive patterns relates to mental activities which are related to user's task performance in terms of response time in case of fingertip dynamics. For example, the monotone in response times in every key (or dot) a user press (or tap) in authentication process. Combining both type of patterns are proposed in cognitive approach of authentication system. More specifically, the combined approach is considered to be useful in better assistance it's used in need. Figure 1 shows a functional block diagram of cognitive authentication systems with assistive modes. The assistive modes may vary based on flexibility of design principles.

B. The Mixed or Hybrid Structure

Keystroke and mouse clicking are still considered as primary input mechanisms. While the keystroke is considered as feed-forward interaction, the mouse click is considered as feedback interaction which is mostly replaced by tapping interaction essential in authentication process. These two interaction mechanisms works as two wings of a bird in robust interaction. It is quiet impossible for a user to accomplish a task depending only on key pressing or tapping/mouse interaction rather a combination of keyboard and mouse click/ tapping. Although keystroke and mouse clicks are sometimes complementary, their combination makes the interaction more natural. The main idea of mixed cognitive authentication is to allow the user a natural way of access rights with a combined or individual approach of fingertips and dynamics. Key objectives are: (a) to identify similarity and differences of cognitive efforts a user experiences during continuous fingertips and (b) to analyze the leverage of the differences towards adaptive authentication design. Figure 2 shows a state diagram of cognitive authentication with possible beginning and ending states of keyboard and mouse clicks use in action. Measures of cognitive effort dynamics become important and challenging research issue.

This work analyzed the keystroke response time and fingertips dynamics to have insights of cognitive efforts and their differences.

C. Theoretical Background

Naturally, we expect and have a preference for monotonic interaction in our lives as well as other things including in authentication process. We need consistency in the whole interaction (e.g., key pressing) process of authentication. This section explains cognitive consistency analysis with a theory and mathematical modeling techniques.

1) Cognitive consistency theory

Consistency becomes like a form of human gravity. It holds everything down and together. It helps us to understand the world and our place in it. The fundamental thrust of consistency theories is to enforce equilibrium among one's

cognitions. Cognitive consistency can be defined with - cognitive consistency theory[7 -9], that focuses on the balance individuals create cognitively when inconsistencies create tensions and thus motivate our brains and body to respond. The fundamental thrust of cognitive consistency theory is to enforce equilibrium among one's cognitions. Cognitive consistency theory shows how people motivate themselves to work and adjust inconsistent measures. Three steps of consistency theory are: (1) estimation of expected consistency, (2) resolving inconsistencies that create a state of dissonance, and (3) the dissonance drives us to restore consistency. This theory is the basis for equilibrium for individuals in authentication process. However, the importance of positive and negative outcomes to reduce stressful choices relates to cognitive dissonance theory of Leon Festinger[18, 19]. Although, the cognitive consistency theory touches on both issues, it focuses on the affects of inconsistencies in interaction process motivating to react and consequent actions.

Fingertips dynamics represent finger related user interactions including keystroke, key tapping, and mouse clicking. Cognitive issues in fingertips includes but not limited to: cognitive effort, consistencies (monotone) in action, dissonance, bias and more. For example, consider in keystroke and tapping dynamics. User identifiable patterns are considered as representative patterns and recorded as personal profile. Cognitive patterns are some derived patterns from online task performance in terms of response time in fingertip dynamics. Combining both type of patterns are proposed in cognitive approach of authentication system.

Main research goal is to have an adaptive interface that can understand consistency of mental state in fingertip dynamics. More specifically, the goal is to have a robust and effective user accessibility framework which is useful in flexible user authentication process. Cognitive analysis of fingertips dynamics can be combined with users' prior interaction behavior profiles to have more effective authentication system. Cognitive effort, load, and cost are some analysis considered in consistent authentication interface design.

Figure 3, illustrates an example of lock pattern tapping interaction and cognitive analysis to understand user's consistent and dissonance interactions. Figure3, a & b shows the schematic of interaction process. Relative response time between dots or dot-to-dot transition may uncover the cognitive consistence. Main assumption behind the consistency identification is that, user with a balance consistence-dissonance value need no assistance from the system in authentication process.

III. THE CRITICAL ANALYSIS

This work analyzed two datasets: the keystroke dynamics dataset [3], which is publicly available as a benchmark dataset and the lock pattern tapping [18] dataset - used with permission from the author. Both dataset are passed through the institutional review board (IRB) for secondary evaluation. Maximal Information-based Nonparametric Exploration (MINE) tool [17] is used in consistency and dissonance analysis.
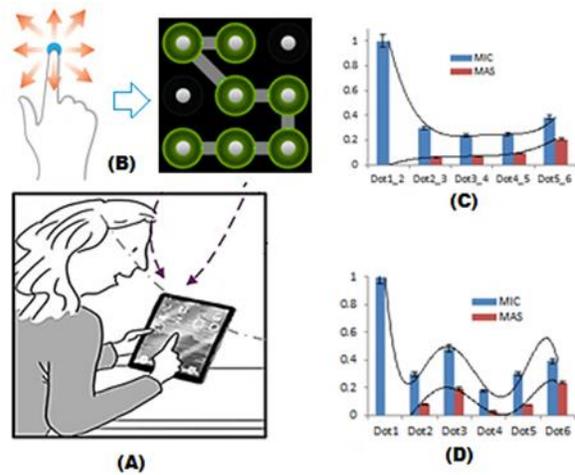

Fig. 3. Cognitive authentication in lock pattern tapping (fingertips) dynamics analysis

A. Technical Analysis

The consistency is analyzed with maximal information coefficient (MIC), which is a non-parametric measure of two-variable dependence. The MIC is widely used to identify important relationships in data sets and to characterize them. Different relationship types give rise to characteristic matrices with different properties. For instance, strong relationships yield characteristic matrices with high peaks, monotonic relationships yield symmetric characteristic matrices, and complex relationships yield characteristic matrices whose peaks are far from the origin. The MIC is used to measure relationship strength between two responses (say, dot1 and dot2) in terms of response time. Let the two response variables be defined as D and A, respectively. The MIC can be written as –

$$MIC(M) = \max_{DA<B(n)} Mutual(M)_{D,A}$$
$$= \max_{DA<B(n)} \frac{I*(M,D,A)}{\log(\min D,A)}$$

where B(n) = n is the search-grid size, I(M, D, A) is the maximum mutual information over all grids D-by-A, of the distribution induced by M on a grid having D and A bins.

The Maximum Asymmetry Score (MAS)captures the deviation from monotonicity, and useful for detecting periodic relationships to have idea about cognitive dissonance. It can be defined as:

$$MAS(M) = \max_{DA<B(n)} |Mutual(M)_{D,A} - |Mutual(M)_{A,D}|$$

The Maximum Edge Value (MEV) measures the closeness to being a function is defined as:

$$MEV(D) = \max_{XY<B(n)} \{M(D)_{X,Y} : X = 2 \tilde{~} or \tilde{~} Y = 2\}.$$

Cognitive consistency visualization and analysis:

Box plot and robust bi-variant bag plots are used to visualize fingertips dynamics (consistencies) in terms of data location, spread, skewness and outliers.
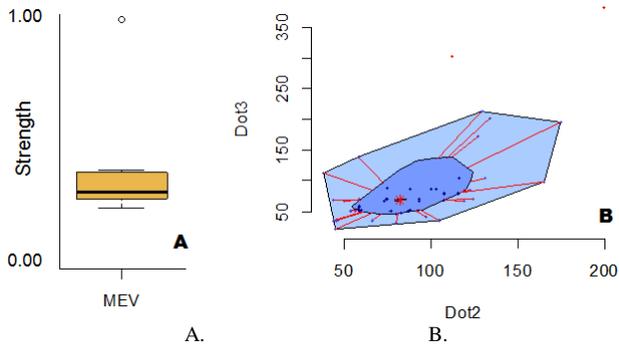
Fig. 4. Bi-variate plots illustration of two consicutive dots responsetime. *Left* - A. the box plot and *Right* - B. the bag plot

Boxplot shows the difference in cognitive levels at fingertips inconsistencies and control. Boxes show the median, 25th and 75th percentiles, error bars show 10th and 90th percentiles, and filled symbols show outliers (figure 4A).

In bag plot, the representation consists of three nested polygons: 'bag', 'fence' and 'loop' (figure 4B). The bag is the inner polygon, which is a construction of the smallest depth region containing at least 50% of the total number of observations, also known as Tukey depth around the center point of median (Tukey median). The most outer polygon known as fence (which is not drawn in the figure) but computed for the outlier points identification. Observations outside the fence are flagged as outliers. The 'fence' polygon can be obtained by inflating the bag (relative to the Tukey median) by a factor ρ. According to Rousseeuw et al. [21] ρ = 3, a recent work [22] prefers ρ = 2.58, as that allows the fence to contain 99% of the observations when the projected bivariate scores follow standard normal distributions. The convex hull of the observations that are not marked as outlier creates another polygon known as loop. The highest possible Tukey depth (median) is also marked in orange color near the center of the graph. The importance of use of bagplot is not only it's robustness against outliers, but also invariant under afine transformation.

B. Datasets

The Keystroke Dynamics - Benchmark Data Set is the accompaniment to Kevin and Roy [3]. The data consist of keystroke-timing information from 51 subjects (typists), each typing a password (.tie5Roanl) 400 times. The second dataset is – the lock pattern tapping dataset [20] – according to [20] a total of 32 different participants successfully completed lock pattern task assigned to them using the mobile application. Participants were 20 male and 12 female with different age groups (from 19 to 56 years old), cultural and educational backgrounds, and having different levels of experience interacting with touch-screen smart phones. They performed the test on different Android phones: Samsung Galaxy SII (18), Nexus S (8), HTC Legend (4) and HTC Vision (2). With email permission from [20], this dataset is used in this study for secondary evaluation.

MIC, MAS and MEV are performed in both dataset to identify underlying monotone, inconsistencies and functional closeness, respectively. Bi-variate box and bag plots are performed visual illustration of cognitive states that shows the trends in monotone and consistencies.

IV. RESULTS AND DISCUSSIONS

Understanding cognitive states are important in accessible and adaptive system development. Ideas presented through this research are transformative and critical (not qualitative or quantitative) and aim to bring additive flexibilities in adaptive interaction design. Finger tapping is gaining increasing popularity; hence, the MIC-MAS trends are analyzed that is observed in finger tapping dataset. Figure 3 shows partial result of monotonic interaction and dissonance in lock pattern tapping interaction. Figure3, c & d illustrates the dot-to-dot and in dot cognitive response time relations, respectively. Figure 3C, shows that the increasing number of transition to remember increases more gap (delay). Result shows partial dot-to-dot and in-dot monotonic interaction and inconsistencies in terms of MIC and MAS. In dot-to-dot transition (Figure 3c), user shows monotonically decreasing relative responses which reaches in a steady state in between dot transitions (dot2-3, dot3-4, dot4-5) which was analyzed on all correct lock pattern response data. Moreover, user has an increase of cognitive inconsistencies (dissonance) with increase of dot-to-dot transition options (dot2-3, dot3-4, dot4-5, and dot5-6). Relative in-dot response time (figure3d) shows a stable pattern of MAS value (dissonance) always lower than consistent dot visit (MIC value), which is similar to dot-to-dot analysis, but no steady trend is observed. So, the dot-to-dot transition MIC-MAS relationship uncovers more cognitive mental aspects in authentication process.

Similar to figure 3c &3d, in keystroke data analysis, key up to next key down response time and key holding time MIC MAS are separately computed and plotted in figure 5. The cognitive consistency and inconsistency trends in key up-down and key holding response times are shown in figure5 (up) and (down), respectively. While the tapping interaction shows a frequent sinusoidal trend, keystroke interaction shows a delayed period in sinusoids.

Figure 6, shows the box plot of the complete data set with additional MINE tool, the maximum edge value (MEV) in lock pattern tapping data. According to keystroke dynamics dataset [3], users are instructed to try different log patterns. Their tapping time and performance are logged in terms of response time. This study performed an analysis of correlative activities with MIC and MAS. Box plots in figure6, represent overall analysis on MIC, MAS and MAV values. The DD analysis (the right part of the figure) indicates a consistent responses by test subjects in successfully password typing. In figure 7, holding time (H) and key-up-to-key-down (UD) time analysis shows, inconsistencies in MAS value. Whereas, more inconsistencies (dissonance) are observed in holding time (H), cognitively meaning that subject is more confused in selecting and pressing keys related to password.

Deeper lock-pattern tapping analysis is performed with a comparative tapping response time analysis in within and between dots and their transition.

Fig. 6. Box plot of lock pattern tapping data. D in the top right corner of figure A represents the results from the response time analysis on dots. Where D2D represents the response time analysis on dot-to-dot. The Y-axis represents strength in 0.00-1.00 scale

These are illustrated with bag plots in figure 8. Similarly, in password typing (keystroke dynamics) dataset, inter key holding time and key transition time (key up and key down) and their comparisons are illustrated with bag-plots in figure 9. Both box plots and bi-variate bag plots combined illustrates the underlying cognitive factors in authentication.

Both in, in-dot and key-holding, subjects have similar cognitive states (gray dotted line on box plots figure A, and figure8A), then in dot-to-dot and key-up to key-down time. This observation, illustrates that they have more consistencies in finger tapping memory (recall) task then decision (switching) task. Existence of more sparse outliers, in later bags indicates decision inconsistencies in selecting transitions (C and D parts in figure8 and 9). For instance, the last bag plot of both cases is smaller because of sparse outlier.

Having MIC, MAS and MAV values; and outliers' situation, some derived feature values with keystroke dynamics and finger tapping datasets, a representative feature vector can be created to apply machine learning approaches towards cognitive authentication system design.

Fig. 5. Trends of user cognitive involvement in keystroke change (top) and key holding (bottom)
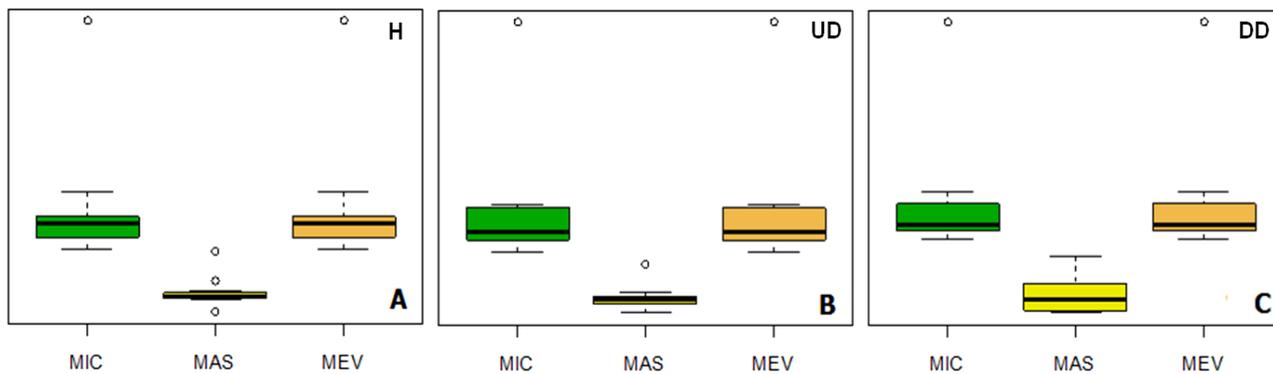

Fig. 7. Box plot of keystroke dynamics dataset[3]. DD in the top right corner in right plot C, represents the results from the key-down to key-down response time analysis. Whereas, H represents the key holding response time, and UD represents the key-up to key-down response times plot. The Y-axis represents strength in 0.00-1.00 scale

V. CONCLUSION

Rapid increase of accessible technology needs continuous access of user's ability based authentic interaction - an adaptive-cognitive authentication protocol becomes an important issue. This study started with the old principle of cognitive consistency and inconsistencies (dissonance) theories with novel applications in adaptive authentication system development. Exploratory analyses are performed to identify trends of cognitive activities. Some instances of cognitive processes (perception, attention, and action/decision-making) are considered in this analysis. The associated properties - emotion, intuition, collaborative action etc. can be derived with more analysis.

By fingertips dynamics, we can consider tapping, double tapping, long press, scroll, pan, flick, two finger tapping, two finger scroll, pinch, zoom, and rotate during interaction. This paper presents a compilation of user interface requirements that arise in fingertip dynamics based cognitive, assistive and adaptive interaction design. It draws implications imposed by the user interaction requirements on the architectures of cognitive consistent system. It defines a special class of cognitively defined authentication systems. Various cognitive mechanisms of providing efficient mental states can be included with similar framework. This paper also draws attention to the need for more non-parametric analysis in cognitive system design.

This paper provided a way of cognitive consistency analysis in keystroke based user interface requirements for constructing good user experience. A special user interface design needs to have assistive (helps it's user in need) and adaptive (learns and updates personal profile) properties, that can be accomplished through consistency analysis. This analysis presents opportunities to improve the system performance relying on the special structure of such interactions. Some ways to exploit this structure are pointed out through this study. Additional research could be warranted in the following areas to further exploit the nature of such problems. One may experiment with various task outcomes and cognitive load schemas for memorizing passwords and lock patterns of computations across user sessions.

Additional cognitive analysis could be gained by learning across cognitive dissonance theory [18, 19]. Such learning may involve cognitively confused patterns in test items.

More trial and time could be devoted to devising and experimenting with algorithms that are essential and connected to robust and online accessibility.

REFERENCES

[1] V. Y. Roman, and G. Venu, "Behavioural biometrics: a survey and classification." International Journal of Biometrics 1, no. 1 pp. 81-113, 2008

[2] A. E. Ahmed and I. Traore, "A New Biometrics Technology based on Mouse Dynamics", IEEE Transactions on Dependable and Secure Computing, Vol. 4 No. 3, pp.165-179, 2007.

[3] K. S. Killourhy, and A. M. Roy, "Comparing anomaly-detection algorithms for keystroke dynamics," Dependable Systems & Networks, pp.125-134, 2009. IEEE Computer Society Press, Los Alamitos, California, 2009.

[4] Y. Nakkabi, I. Traore, A. A. E Ahmed, "Improving Mouse Dynamics Biometric Performance using Variance Reduction with Separate Extractors", IEEE Transactions on Systems, Man and Cybernetics—Part A: Systems and Humans, Vol. 40, No. 6, pp.1345 – 1353,2010.

[5] G. Hossain and M. Yeasin, Cognitive Load Based Adaptive Assistive Technology Design for Reconfigured Mobile Android Phone, MobiCASE 2011, pp.370-380, Los Angeles, CA, USA, 2011.

[6] G. Hossain, A. S. Shaik, and M. Yeasin, Cognitive Load and Usability Analysis of RMAP for people who are blind or visually impaired. In Proceedings of the 29th ACM International Conf. on Design of Communication (SIGDOC) ACM, Pisa, Italy, 2011.

[7] P. Tannenbaum, The Congruity Principles: Retrospective Reflection and Recent Research. In Theories of Cognitive Consistency: A Sourcebook. Abelson, R. & others (eds.) Rand McNally & Co.; Skokie, 111, 1968.

[8] M. Venkatesan, Cognitive Consistency and Novelty Seeking. In Ward, S. & Robertson, T. (eds.) Consumer Behaviour: Theoretical Sources. Prentice-Hall, Inc; Englewood Cliffs, New Jersey, 1973.

[9] T. Newcomb, Interpersonal Balance. In Abelson, R. et al Theory of Cognitive Consistency: A Sourcebook. Rand McNally & Co. Skokie, 111, 1968

[10] N. Poh and M. Tistarelli, "Customizing biometric authentication systems via discriminative score calibration." In Computer Vision and Pattern Recognition (CVPR), 2012 IEEE Conference on, pp. 2681-2686. IEEE, 2012.

[11] H. Liang, Y. Junsong, and D. Thalmann. "Hand pose estimation by combining fingertip tracking and articulated ICP." In Proceedings of the 11th ACM SIGGRAPH International Conference on Virtual-Reality Continuum and its Applications in Industry, pp. 87-90. ACM, 2012.

[12] V. Štruc, Z. Jerneja, V. Boštjan, and N. Pavešić. "Beyond parametric score normalisation in biometric verification systems." IET Biometrics 3, no. 2 (2014): 62-74.

[13] K. Oka, S. Yoichi, and K. Hideki, "Real-time fingertip tracking and gesture recognition." Computer Graphics and Applications, IEEE 22, no. 6 (2002): 64-71.

[14] E. T. Rolls, "The affective and cognitive processing of touch, oral texture, and temperature in the brain." Neuroscience & Biobehavioral Reviews 34, no. 2 pp.237-245, 2010.

[15] L. A. Jones, and A. M. Smith. "Tactile sensory system: encoding from the periphery to the cortex." Wiley Interdisciplinary Reviews: Systems Biology and Medicine 6, no. 3 pp. 279-287, 2014.

[16] J. Fishel, V. J. Santos, and G. E. Loeb. "A robust micro-vibration sensor for biomimetic fingertips." in 2nd IEEE RAS & EMBS International Conference on, pp. 659-663. IEEE, 2008.

[17] D. Reshef, Y. Reshef, H. Finucane, S. Grossman, G. McVean, P. Turnbaugh, E. Lander, M. Mitzenmacher, P. Sabeti. Detecting novel associations in large datasets. Science 334, 6062 (2011).

[18] L. Festinger, A theory of cognitive dissonance, Evanston, IL: Row & Peterson, 1957.

[19] L. Festinger and J. M. Carlsmith, "Cognitive consequences of forced compliance. Journal of Abnormal and Social Psychology, 58, 203 – 210, 1959.

[20] A. Julio and E. Wästlund. "Exploring touch-screen biometrics for user identification on smart phones." In Privacy and Identity Management for Life, pp. 130-143. Springer Berlin Heidelberg, 2012.

[21] P. Rousseeuw, I. Ruts and J.W. Tukey, `The bagplot: A bivariate boxplot', The American Statistician Vol. 53(4), pp.382-387, 1999.

[22] R.J. Hyndman, and S. H. Lin, "Rainbow plots, bagplots, and boxplots for functional data." Journal of Computational and Graphical Statistics 19, no. 1 (2010).
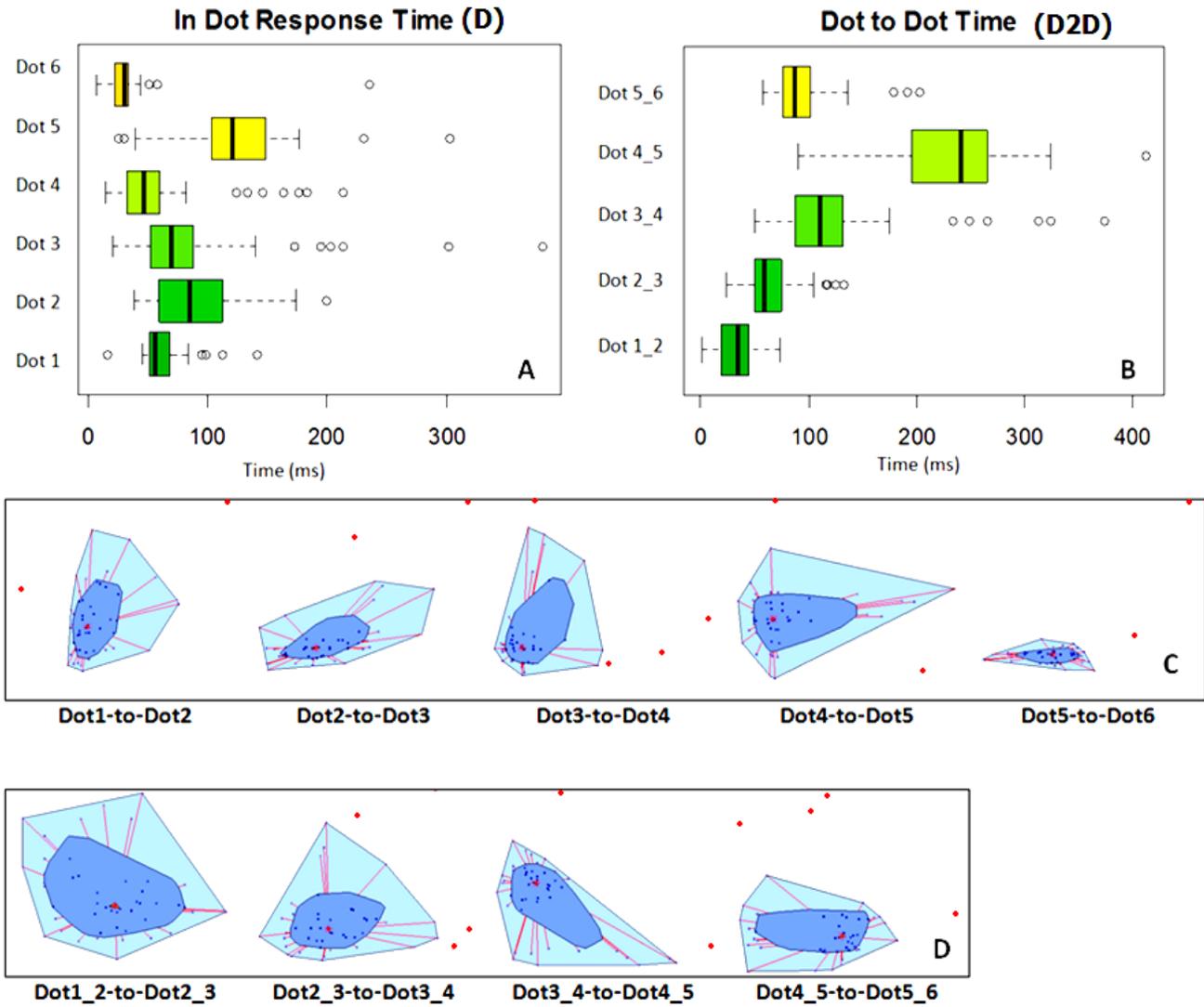
Fig. 8.   Trends in Cognitive Consistency Analysis (Lock Pattern data): (A) Box plot of in-dot (D) response time; (B) Box plot of Dot-to-Dot time (D2D) and (c) Median and Outlier distributions in tapping on consecutive dots and (d) Median and Outlier distributions in consecutive dot-to-dot transitions
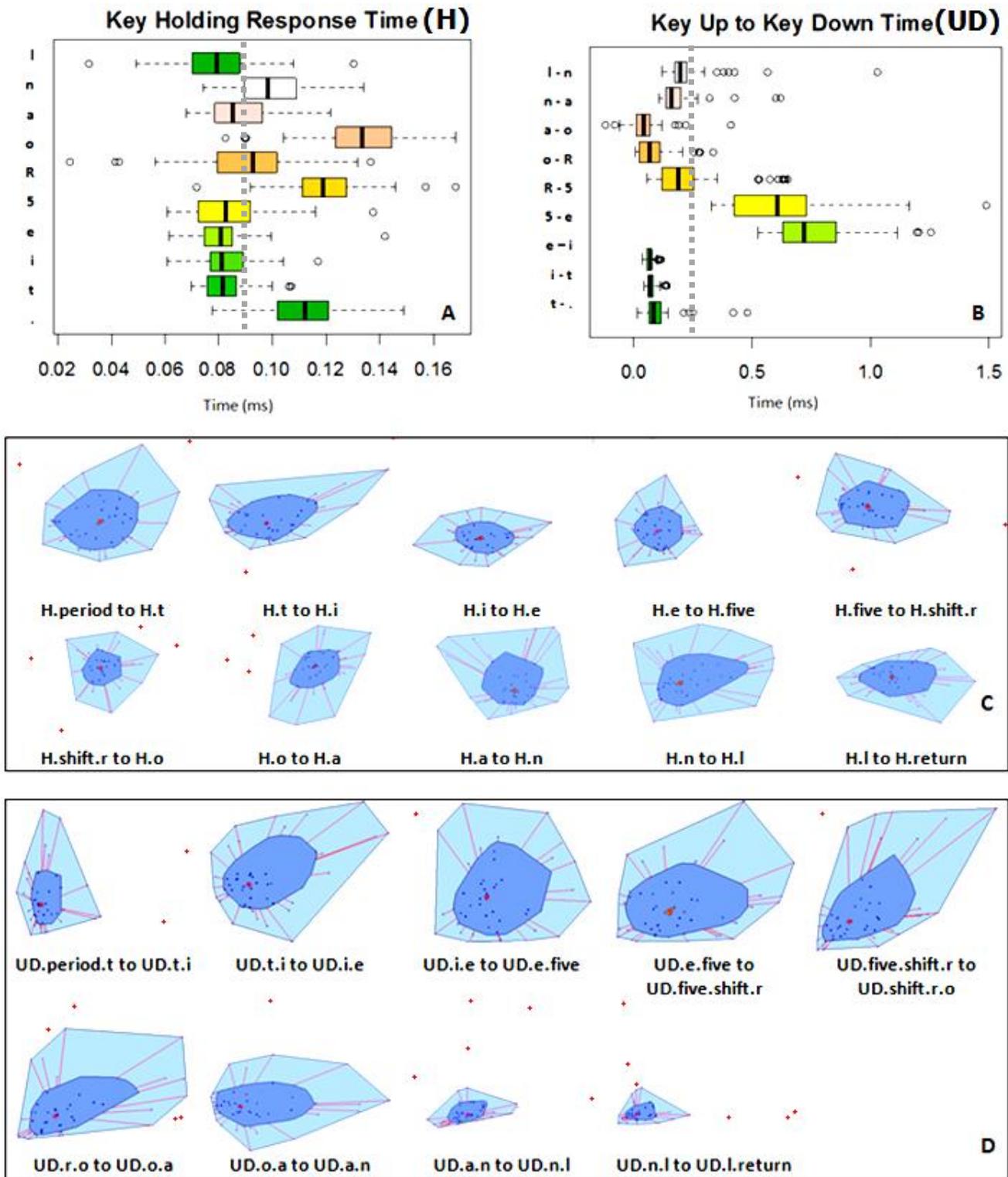
Fig. 9.   Trends in Cognitive Consistency Analysis (Keystroke data): (A) Box plot of key holding (H) response time; (B) Box plot of Key Up-to-Key Down time (UD) and (c) Median and Outlier distributions in consecutive key holding and (d) Median and Outlier distributions in consecutive key up to key down transitions